

Archived version from NCDOCKS Institutional Repository <http://libres.uncg.edu/ir/asu/>



Southeastern Geology: Volume 45, No. 3

April 2008

Editor in Chief: S. Duncan Heron, Jr.

Abstract

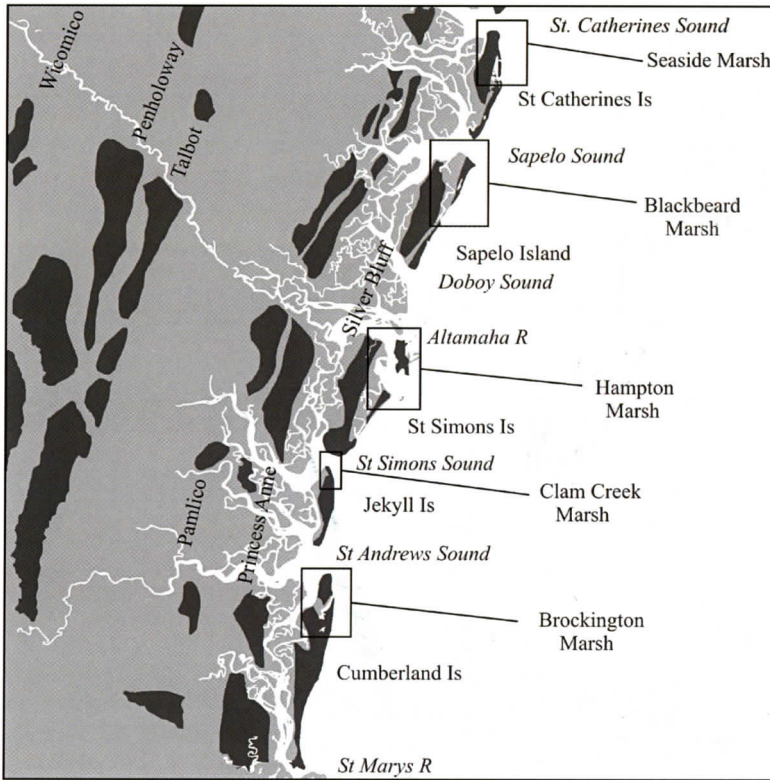
Academic journal published quarterly by the Department of Geology, Duke University.

Heron, Jr., S. (2008). Southeastern Geology, Vol. 45 No. 3, April 2008. Permission to re-print granted by Duncan Heron via Steve Hageman, Professor of Geology, Dept. of Geological & Environmental Sciences, Appalachian State University.

SOUTHEASTERN GEOLOGY



COASTAL AND MARINE GEOLOGY OF THE SOUTHEASTERN UNITED STATES



Vol. 45, No. 3

April 2008

SOUTHEASTERN GEOLOGY

PUBLISHED

at

DUKE UNIVERSITY

Duncan Heron

Editor in Chief

David M. Bush

Editor

This journal publishes the results of original research on all phases of geology, geophysics, geochemistry and environmental geology as related to the Southeast. Send manuscripts to **David Bush, Department of Geosciences, University of West Georgia, Carrollton, Georgia 30118, for Fed-X, etc. 1601 Maple St.,** Phone: 678-839-4057, Fax: 678-839-4071, Email: dbush@westga.edu. Please observe the following:

- 1) Type the manuscript with double space lines and submit in duplicate, or submit as an Acrobat file attached to an email.
- 2) Cite references and prepare bibliographic lists in accordance with the method found within the pages of this journal. Data citations examples can be found at <http://www.geoinfo.org/TFGeosciData.htm>
- 3) Submit line drawings and complex tables reduced to final publication size (no bigger than 8 x 5 3/8 inches).
- 4) Make certain that all photographs are sharp, clear, and of good contrast.
- 5) Stratigraphic terminology should abide by the North American Stratigraphic Code (American Association Petroleum Geologists Bulletin, v. 67, p. 841-875).
- 6) Email Acrobat (pdf) submissions are encouraged.

Subscriptions to *Southeastern Geology* for volume 45 are: individuals - \$24.00 (paid by personal check); corporations and libraries - \$36.00; foreign \$48. Inquires should be sent to: **SOUTHEASTERN GEOLOGY, DUKE UNIVERSITY, DIVISION OF EARTH & OCEAN SCIENCES, BOX 90233, DURHAM, NORTH CAROLINA 27708-0233.** Make checks payable to: *Southeastern Geology*.

Information about **SOUTHEASTERN GEOLOGY** is on the World Wide Web including a searchable author-title index 1958-2005 (Acrobat format). The URL for the Web site is: <http://www.southeasterngeology.org>

SOUTHEASTERN GEOLOGY is a peer review journal.

ISSN 0038-3678

SOUTHEASTERN GEOLOGY

Table of Contents

Volume 45, No. 3 April 2008

COASTAL AND MARINE GEOLOGY OF THE SOUTHEASTERN UNITED STATES

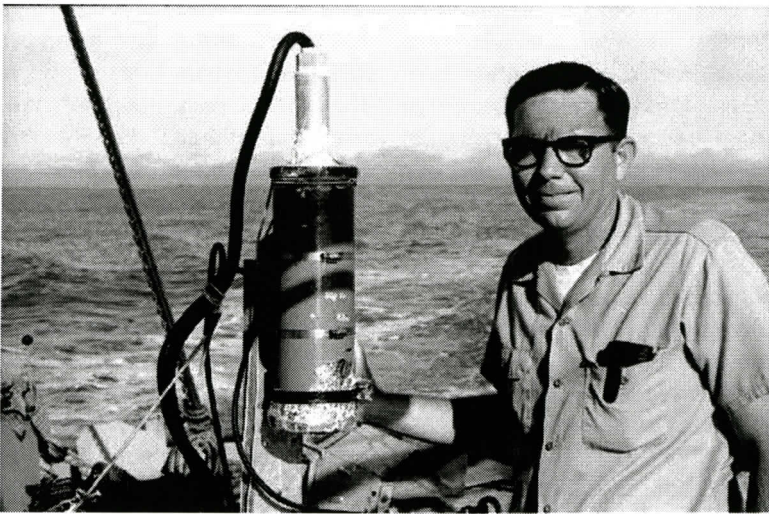
1. **HYDROGRAPHY AND BOTTOM BOUNDARY LAYER DYNAMICS:
INFLUENCE ON INNER SHELF SEDIMENT MOBILITY, LONG BAY,
NORTH CAROLINA**
LUKE A. DAVIS, LYNN A. LEONARD AND GREGG A. SNEDDEN 97
2. **THE EFFECTS OF HARDBOTTOM GEOMETRY ON SEDIMENT
TRANSPORT PROCESSES ON THE MID-CONTINENTAL SHELF IN
ONSLow BAY, NORTH CAROLINA**
P. ANSLEY WREN, JEFF A. MARSHALL, LYNN A. LEONARD, AND
MELODY VAN DER LINDE 111
3. **SHALLOW MARINE MARGIN SEDIMENTS, MODERN MARINE
EROSION AND THE FATE OF SEQUENCE BOUNDARIES GEORGIA
BIGHT (USA)**
ERVAN G. GARRISON, GREG MCFALL AND SCOTT E. NOAKES 127
4. **RELOCATION OF BRUNSWICK RIVER AND OTHER ESTUARIES
ON THE GEORGIA, USA COAST AS A CONSEQUENCE OF
HOLOCENE TRANSGRESSION**
TIMOTHY M. CHOWNS, BRYAN S. SCHULTZ, JAMES R. GRIFFIN, AND
MORGAN R. CROOK JR..... 143
5. **HIGH RESOLUTION SHALLOW GEOLOGIC CHARACTERIZATION
OF A LATE PLEISTOCENE EOLIAN ENVIRONMENT USING
GROUND PENETRATING RADAR AND OPTICALLY STIMULATED
LUMINESCENCE TECHNIQUES: NORTH CAROLINA, USA**
DAVID MALLINSON, SHANNON MAHAN, CHRISTOPHER MOORE 161
6. **THE INFLUENCE OF DRAINAGE HIERARCHY ON PATHWAYS OF
BARRIER RETREAT: AN EXAMPLE FROM CHINCOTEAGUE
BIGHT, VIRGINIA, U.S.A.**
G.F. OERTEL, T.R. ALLEN AND A.M. FOYLE..... 179

Serials Department
Appalachian State Univ. Library
Boone, NC

COASTAL AND MARINE GEOLOGY OF THE SOUTHEASTERN UNITED STATES

Vernon "Jim" Henry has had, up to this point, a distinguished 47-year career studying coastal and shelf geologic processes, determining the geological evolution of barrier islands, mapping shelf morphology and stratigraphy, and documenting coastline change in the southeastern US. Many of his studies and those of his students still stand as the only information we have on a variety of important geologic topics in Georgia. Jim started his career fresh out of graduate school from Texas A&M, where he received his Ph.D. in 1961. During his career, Jim has been a faculty member and the Director of the University of Georgia (UGA) Marine Institute on Sapelo Island (1961-1971), Program Manager of the Marine Geology and Geophysics Program at the National Science Foundation in Washington, D.C., (1968-1970), coordinator of the UGA Department of Geology marine geology program on Skidaway Island (1971-1982) and Chairman of the Georgia State University Department of Geology (1982-1992), from which he had his first retirement. Not yet ready to relax, Jim returned to academia as a part-time Professor in the Department of Geology and Geography at Georgia Southern University (1992-2003) until his second retirement in 2003. During this time, he directed and oversaw the renovation of the Applied Coastal Research Laboratory (ACRL), Georgia Southern's field facility on Skidaway Island. Throughout his career, Jim has provided guidance to local, State and Federal decision makers and the scientific community by his service on a number of advisory boards and professional panels, as the first chairman of the Grays Reef National Marine Sanctuary Advisory Council and was recognized for these efforts in 1996 when he was awarded one of the first NOAA Environmental Hero awards. Jim still maintains an office at the ACRL and is actively involved in barrier island research. When Jim finally decides to call it quits, a grand era of southeastern geology will come to a close. He has been a great researcher, mentor, teacher, and friend to more people than can be counted.

Clark Alexander
Skidaway Institute of Oceanography
Savannah, GA



Jim Henry in the field aboard the RV Kit Jones seaward of Sapelo Island, 1965.

HYDROGRAPHY AND BOTTOM BOUNDARY LAYER DYNAMICS: INFLUENCE ON INNER SHELF SEDIMENT MOBILITY, LONG BAY, NORTH CAROLINA

¹LUKE A. DAVIS, ²LYNN A. LEONARD AND ³GREGG A. SNEDDEN

¹*Kimley-Horn and Associates, Inc., Jacksonville, FL 32256-8634
luke.davis@kimley-horn.com*

²*Department of Geography and Geology
University of North Carolina Wilmington, Wilmington, NC 28403-3201
lynnl@uncw.edu*

³*National Wetlands Research Center, U.S. Geological Survey
Baton Rouge, LA 70803-0001
gsnedden@usgs.gov*

ABSTRACT

This study examined the hydrography and bottom boundary-layer dynamics of two typical storm events affecting coastal North Carolina (NC); a hurricane and the passages of two small consecutive extratropical storms during November 2005. Two upward-looking 1200-kHz Acoustic Doppler Current Profilers (ADCP) were deployed on the inner shelf in northern Long Bay, NC at water depths of less than 15 m. Both instruments profiled the overlying water column in 0.35 m bins beginning at a height of 1.35 m above the bottom (mab). Simultaneous measurements of wind speed and direction, wave and current parameters, and acoustic backscatter were coupled with output from a bottom boundary layer (bbl) model to describe the hydrography and boundary layer conditions during each event. The bbl model also was used to quantify sediment transport in the boundary layer during each storm. Both study sites exhibited similar temporal variations in wave and current magnitude, however, wave heights during the November event were higher than waves associated with the hurricane. Near-bottom mean and subtidal currents, however, were of greater magnitude during the hurricane. Peak depth-integrated suspended sediment transport during the November event exceeded transport associated with the hurricane by 25-70%. Substantial spatial variations in sediment transport existed throughout both events.

During both events, along-shelf sediment transport exceeded across-shelf transport and was related to the magnitude and direction of subtidal currents. Given the variations in sediment type across the bay, complex shoreline configuration, and local bathymetry, the sediment transport rates reported here are very site specific. However, the general hydrography associated with the two storms is representative of conditions across northern Long Bay. Since the beaches in the study area undergo frequent renourishment to counter the effects of beach erosion, the results of this study also are relevant to coastal management decision-making. Specifically, these issues include 1) identification of municipalities that should share the cost for renourishment given the likelihood for significant along-shelf sand movement and 2) appropriate timing of sand placement with respect to local climatology and sea-turtle nesting restrictions.

INTRODUCTION

Sediment transport events on inner shelf margins are driven largely by increased wave orbital velocities coupled with sustained wind-driven currents associated with meteorological forcing (Williams and Rose, 2001; Kim et al., 1997; Madsen et al., 1993; Xu and Wright, 1993). The North Carolina (NC) inner shelf is frequently affected by two types of storms; extratropical systems and hurricanes. Extratropical systems also referred to as nor'easters, occur

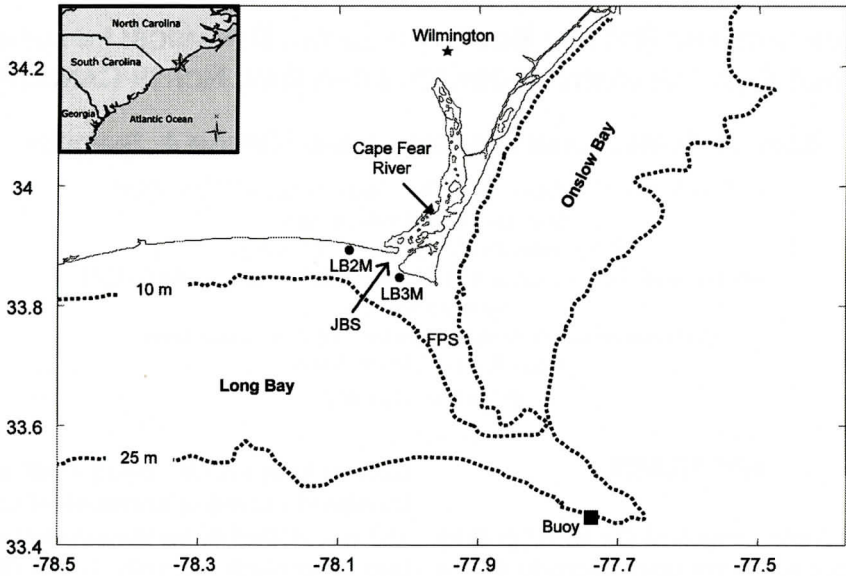


Figure 1. A study area map showing surrounding offshore waters and adjacent shoals (JBS: Jay Bird Shoals; FPS: Frying Pan Shoals). ADCPs were located at LB2M and LB3M.

every 3 to 12 days between October and April (Dolan et al. 1988). Most of these storms are low magnitude, short duration events, though some may produce large waves and high winds for several days (Dolan and Davis, 1992; Wright et al., 1994). Hurricanes usually develop in the tropical Atlantic between June and November and periodically impact the NC coast. From 1996 to 2005, nine hurricanes and four tropical storms made landfall or tracked through the region. An increase in category 2 and 3 hurricanes compared to previous decades has heightened managerial interest in understanding processes leading to beach erosion, the redistribution of “beach quality” sand, and the effects of sand movement on hardbottom habitat viability.

Previous studies have shown that inner shelf processes are dominated by storm-driven currents (Wright et al., 1994; Pepper and Stone, 2002). These currents have been postulated to provide the primary mechanism for across-shelf sediment transport (Trowbridge and Young, 1989; Wright et al., 1991). Other studies (e.g. Cacchione et al., 1994; Wren and Leonard, 2005) suggest that wave and current bottom stresses, particularly during storms, initiate sediment mobilization on the inner shelf and pro-

vide the mechanism that determines sediment availability for transport. In the southeast U.S., it has been proposed that extratropical storms might be more significant than hurricanes in terms of overall sediment movement on the inner shelf because they occur with greater frequency (Dolan et al. 1988). This assumption is consistent with Wright et al. (1994) who suggested that extratropical storms, regardless of their magnitude, are critical to sediment transport on many time scales due to their recurrence interval.

In Onslow Bay, NC (Figure 1), wave-current interactions and storm swell significantly influence sediment resuspension (Marshall 2004, Wren and Leonard 2005). Marshall (2004) noted sediment resuspension due to increased wave orbital velocity on the inner shelf during both tropical and extratropical storms. Wren and Leonard (2005) found that while increased storm swell orbital velocities are the primary mechanism for suspending material from the seabed, subtidal currents are responsible for transport of suspended material along or across the mid-continental shelf. Both of these studies largely focused on the effects of Hurricane Isabel in 2003, although Marshall (2004) also examined several small to moderate extratropical

storms.

Few studies have examined the effect of storms on sediment mobility in northern Long Bay, NC. This area lies within an area frequently affected by tropical and extratropical storms, but buffered from the full impact of some of these systems due to the presence of an east-west trending coastline as well as Frying Pan Shoals along its northern boundary (Figure 1). The primary study goal is to identify and describe the physical mechanisms and bottom boundary layer dynamics during two coastal storms that mobilized sediment on the sediment-starved inner shelf of northern Long Bay, NC. The objectives are: (1) compare the spatial and temporal variability of the hydrography and sediment response in Long Bay during autumn 2005 and (2) apply a bottom boundary layer model to quantify nearshore conditions and sediment mobility associated with the passage of Hurricane Ophelia (13-16 Sept 2005) and a period consisting of the passage of two back-to-back small nor'easters in November 2005 (henceforth referred to as the November event).

STUDY AREA

Long Bay is located off the southeastern coast of North Carolina (Figure 1). The study area is located on the inner shelf of northern Long Bay, adjacent to the mouth of the Cape Fear River, and bounded to the northeast by Cape Fear and Frying Pan Shoals. Two sites were established within the study area. The first, LB2M, was located 1.8 km offshore of Oak Island and 40 km southwest of Wilmington at a depth of 7 m. The second, LB3M, was located 0.9 km offshore of Bald Head Island at a depth of 5.8 m and approximately 5.7 km east of LB2M (Figure 1). In the study area, the mean tidal range is 1.3 m and tides are dominated by the M_2 constituent (NOAA, 2006a). Mean annual significant wave height is 0.6 m with a dominant period of 6.5 s.

The study area receives outflow from the Cape Fear River (CFR) which is characterized by relatively low (annual mean $\approx 275 \text{ m}^3 \text{ s}^{-1}$) but highly variable (stdev $\approx 300 \text{ m}^3 \text{ s}^{-1}$) discharge. The CFR mainstem originates in the NC

Piedmont physiographic province, but is fed by two major tributaries, the Northeast CFR and the Black River. These systems are black-water coastal plain rivers that drain vast floodplains and swamps and exhibit low suspended solid concentrations (usually $< 10 \text{ mg l}^{-1}$). The relatively low sediment load of the CFR is attributed to the influence of these tributaries (Mallin, 2006). Consequently, northern Long Bay is considered sediment-starved despite its proximity to the CFR.

The thin sediment veneer on the inner shelf near the mouth of the CFR consists of sediment types ranging from muddy fine sand to shell hash. The majority of sediment near the CFR mouth consists of poorly sorted sands that grade into fine sand and silt in the seaward direction (Battisto, 2000). In the study area, surface sediments consisted of medium sand ($\bar{x} = 0.0268 \text{ cm}$) at LB2M and fine sand ($\bar{x} = 0.017 \text{ cm}$) at LB3M.

METHODS AND INSTRUMENTATION

CFR discharge was obtained from www.cormp.org following the method described by Carpenter and Yonts (1979). Hourly wind data were obtained from NDBC buoy 41013 located on Frying Pan Shoals approximately 60 km southeast of the study area (Figure 1). Wave and current data were collected by two upward-looking 1200-kHz RDI Workhorse Sentinel ADCP's located at each site. Both instruments profiled the overlying water column in 0.35 m bins beginning at a height of 1.35 m above bottom (mab). Measurements were collected at a rate of 0.5 Hz over a 6-minute sampling burst. One burst was recorded every 10 minutes. Wave data were recorded every 4 hours at LB2M and every 3 hours at LB3M. For all mean and subtidal current data, the along-shelf axis was taken at 15° south of east for LB2M and 22° south of east for LB3M. Positive along-shelf was eastward towards Cape Fear and positive across-shelf was towards the coast. To measure relative changes in turbidity, the beam-averaged echo amplitude from the ADCP was used. This technique is useful for approxi-

mating relative changes in suspended particulate matter in the water column, overlying sandy substrates (Traykovski et al., 1999; Battisto, 2000; Williams and Rose, 2001). Using a methodology outlined by RD Instruments, a more accurate estimation of the absolute backscatter in units of decibels was calculated (Deines, 1999). A Lanczos cosine filter with a half-amplitude cutoff period of 40 hours was applied to all current and ABS data to minimize the tidal variability.

A bottom boundary layer (bbl) model (Styles and Glenn, 2002) was used to calculate bed shear stress (τ) and critical shear velocities (u_*) due to currents and the combined effects of wave-current interaction at the seabed. It also was used to compute critical shear velocity (u_{*crit}) based on an input grain size. Depth integrated sediment transport from 1.35 mab to the seabed was derived from model output based on burst averaged currents and grain size distributions as employed by (Wren and Leonard, 2005).

Input data used in the model included: (1) mean near-bottom currents U_r , measured at a 1.35 mab reference elevation (Z_r), (2) near-bottom orbital velocities U_b and excursion amplitudes A_b , and (3) wave and current incidence angle Φ_{cw} ; all of which were derived from the ADCP data prior to model implementation. Bottom r.m.s. orbital velocities, U_b , were calculated using:

$$U_b = \frac{\sqrt{2}\omega a}{\sinh\left(\frac{2\pi d}{L}\right)} \quad \text{Eq. 1.1}$$

where U_b = wave orbital velocity (cm s^{-1}), ω = angular frequency, $a = \frac{H_{rms}}{2}$ (m), d = water depth (m), and L = wavelength (m).

RESULTS

Autumn 2005 Hydrography and Sediment Response

During autumn 2005, the mean discharge of the Cape Fear River was $80 \text{ m}^3 \text{ s}^{-1}$. This was

about 40% of the 2005 annual mean ($196 \text{ m}^3 \text{ s}^{-1}$). The period of lowest discharge occurred just prior to H. Ophelia on 8 September ($28.4 \text{ m}^3 \text{ s}^{-1}$). The highest discharge, nearly $300 \text{ m}^3 \text{ s}^{-1}$, occurred in mid-October. Wind direction during the study period was variable, but southerly and southwesterly winds were dominant. Elevated winds ($> 8 \text{ m s}^{-1}$) occurred only during the passage of H. Ophelia and several extratropical systems in late October and late November (Figure 2a). Winds did not exceed 10 m s^{-1} except during H. Ophelia when maximum sustained easterly winds reached 14.3 m s^{-1} .

Hurricane Ophelia was a category 1 storm as it tracked northeastward parallel to the NC coast September 11-17 with maximum winds of 38.5 m s^{-1} . Wind direction was predominantly offshore as the storm approached, but switched to alongshore on 13 September as the storm passed the study area. The center of circulation never made landfall, but sections of the eyewall passed adjacent to NDBC buoy 41013 (Figure 1). The first system developed from a stationary warm front in the Gulf of Mexico and tracked northeastward toward the study area on 21-22 November. The second system originated as a Canadian cold front that converged with another low pressure system on 23-24 November. The event as a whole and the individual storm systems were class 1 storms (Dolan and Davis 1992) with sustained winds between 1.7 and 9.3 m s^{-1} and maximum winds directed onshore (Figure 2a).

Maximum near-bottom subtidal currents usually coincided with wind events. Subtidal currents reached 16.8 cm s^{-1} at LB2M and 38.6 cm s^{-1} at LB3M during a period of sustained along-shelf winds during H. Ophelia (Figure 2b, c). The rotating wind fields associated with both events led to increased along-shelf subtidal currents at both sites but particularly at LB3M. The response of along-shelf subtidal currents to the November event was more subdued than the response to Ophelia due to the weaker winds and shorter duration of the November event.

During fair-weather conditions, subtidal currents were predominantly eastward at LB2M and onshore at LB3M (Figure 2b,c). The subtidal current velocity at LB3M was approximately

HYDROGRAPHY AND SEDIMENT MOBILITY IN LONG BAY

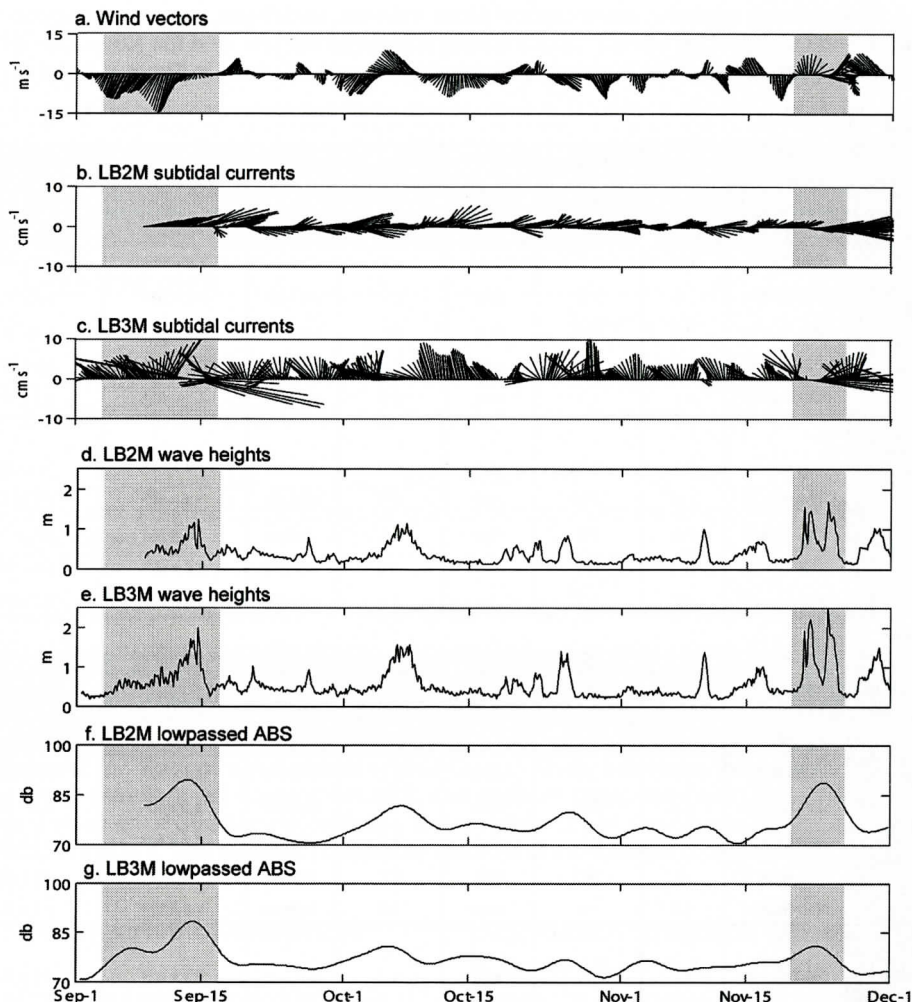


Figure 2. Autumn 2005 hydrography and acoustic backscatter signal (ABS); (a.) Lowpassed wind vectors; (b.) LB2M subtidal currents; (c.) LB3M subtidal currents; (d.) LB2M wave height; (e.) LB3M wave height; (f.) LB2M lowpassed ABS; (g.) LB3M lowpassed ABS. In panels a through c, the vectors were rotated so a line extending upward from the x-axis indicates winds blowing toward shore and a line extending to the right indicates wind blowing east toward Cape Fear. Hurricane Ophelia and the November event are identified with shadeboxes. Instrument failure occurred at LB2M from 1-8 September.

40% higher than the subtidal current velocity at LB2M for most of the deployment (Figure 2b, c). The across-shelf component was usually positive (onshore) at both sites but the along-shelf component varied; eastward and westward for LB2M and LB3M, respectively.

Significant wave height (H_s) was highly variable over the study period. Periodic increases in wave height were concurrent between sites suggesting that the entire study area responded

similarly to atmospheric forcing (Figure 2d, e). Site LB2M, however, consistently exhibited lower wave heights than LB3M. Most waves propagated northward and northeastward and these two directions comprised over 96% of the wave field during the study. Increased wave heights usually coincided with sustained onshore winds. The primary exception, a period of significant wave heights exceeding 1.2 and 1.7 m at LB2M and LB3M, respectively, occurred

Table 1. Near-bottom currents, wave-current shear velocity, and depth-integrated sediment concentration and transport for several bursts during Hurricane Ophelia and the November Event at both sites. The time of specific bursts are denoted by the shadeboxes in Figures 3 and 4.

LB2M								
2005 events	Burst Time UTC	U^{*cw} (cm s^{-1})	Along-shelf currents		Across-shelf currents		Depth-integrated sediment conc. (mg cm^{-2})	Depth-integrated sediment transport ($\text{mg cm}^{-1} \text{s}^{-1}$)
			Magnitude	Direction	Magnitude	Direction		
			(cm s^{-1})		(cm s^{-1})			
H. Ophelia	2200 Sept-8	6.5	6.4	east	2.3	onshore	1.8×10^{-2}	6.6×10^{-4}
	1800 Sept-13	7.8	7.5	east	3.8	onshore	1.6×10^{-1}	2.9×10^{-2}
	1800 Sept-14	9.5	15.8	east	4.8	onshore	7.2×10^{-1}	1.4×10^{-1}
	1400 Sept-15	5.2	7.1	east	5.5	onshore	9.6×10^{-3}	5.9×10^{-4}
	0200 Sept-16	4.1	4.2	east	-0.9	offshore	4.7×10^{-4}	3.0×10^{-6}
Nov. Event	0400 Nov-20	4.1	6.5	east	-0.1	offshore	6.2×10^{-5}	2×10^{-6}
	0800 Nov-22	11.2	10.4	east	-2.7	offshore	1.4×10^0	1.8×10^{-1}
	0800 Nov-23	5.3	7.8	east	2.1	onshore	1.6×10^{-2}	3.3×10^{-4}
	0800 Nov-24	12.1	13.7	east	-3.0	offshore	2.0×10^0	4.8×10^{-1}
	2000 Nov-25	4.7	8.7	east	3.5	onshore	1.5×10^{-3}	3.3×10^{-4}
LB3M								
2005 events	Burst Time (UTC)	U^{*cw} (cm s^{-1})	Along-shelf currents		Across-shelf currents		Depth-integrated sediment conc. (mg cm^{-2})	Depth-integrated sediment transport ($\text{mg cm}^{-1} \text{s}^{-1}$)
			Magnitude	Direction	Magnitude	Direction		
			(cm s^{-1})		(cm s^{-1})			
H. Ophelia	2300 Sept-8	5.6	2.0	west	5.5	onshore	2.4×10^{-1}	7.6×10^{-2}
	1700 Sept-13	9.6	25.9	west	5.6	onshore	2.3×10^0	3.8×10^0
	2000 Sept-14	11.3	21.0	east	2.0	offshore	5.2×10^0	1.8×10^1
	1400 Sept-15	5	10.1	east	3.7	onshore	2.0×10^{-1}	1.0×10^{-1}
	0200 Sept-16	3.5	7.1	west	6.9	onshore	1.2×10^{-3}	2.7×10^{-5}
Nov. Event	0300 Nov-20	4.6	0.6	west	4.2	onshore	6.2×10^{-2}	1.5×10^{-3}
	0900 Nov-22	13	15.3	east	2.7	offshore	8.6×10^0	6.7×10^0
	0900 Nov-23	6.6	1.9	east	2.7	onshore	6.1×10^{-1}	2.4×10^{-1}
	0600 Nov-24	14.7	19.1	east	3.7	offshore	1.1×10^1	2.4×10^1
	2100 Nov-25	4.1	1.0	west	7.6	onshore	2.0×10^{-2}	7.2×10^{-3}

as H. Ophelia passed offshore and strong offshore winds abated. For the November event, two peaks in H_s were separated by a 24-hour period of decreased H_s that coincided with a change in wind speed and direction between storm systems. Maximum H_s occurred on 24 November.

Elevated ABS intensity was usually coincident with increased H_s at both sites. The agreement between ABS and H_s , however, was slightly better at LB2M than at LB3M. When ABS was regressed against H_s , the relationship

was weak, but statistically significant. The R^2 values were 0.33 and 0.37 for LB2M and LB3M, respectively, with a $p < 0.05$ at both sites. The ABS signal magnitude was comparable between sites except during periods of increased H_s . During these events, the ABS at LB2M exceeded the LB3M signal despite lower wave heights. This pattern may be due to exposure of underlying muddy sands (25% mud) at LB2M once the thin veneer of coarser surface sediments (< 2% mud) had been mobilized.

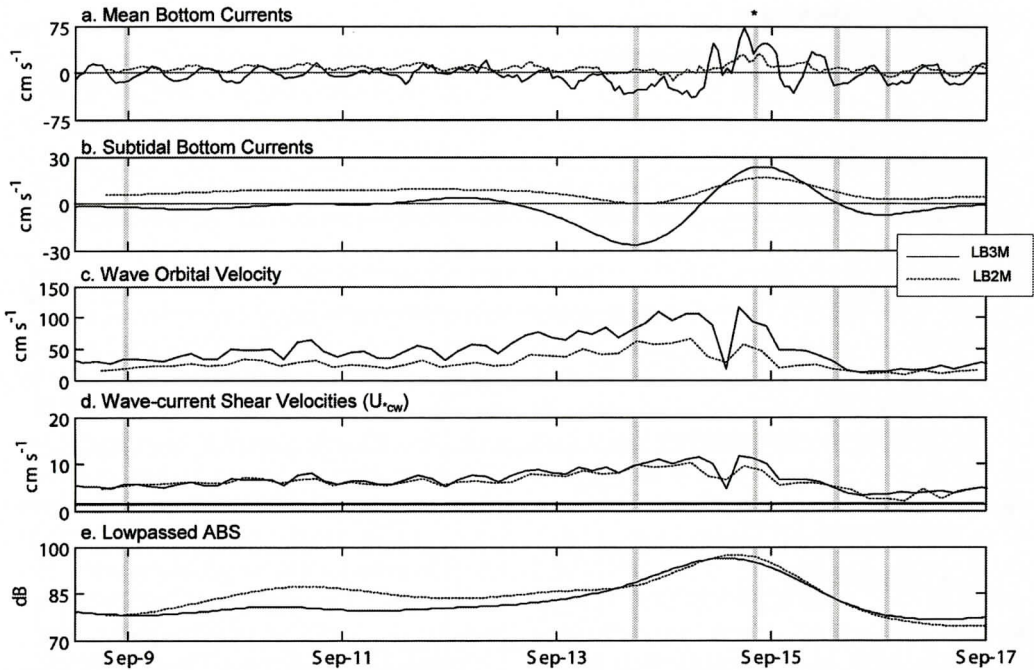


Figure 3. Bottom boundary layer parameters during Hurricane Ophelia at LB2M (dashed) and LB3M (solid). (a.) Hourly mean directional bottom currents; (b.) Hourly sub-tidal directional bottom currents; (c.) Bottom wave orbital velocities; (d.) Shear velocities (horizontal line denotes critical shear velocity); (e.) Lowpassed ABS. The positive along-shelf direction is eastward and positive across-shelf direction is onshore. The shadeboxes in the panels represent the bursts described in Table 1. The asterisk represents the time of peak storm conditions as referred to in the text.

Storm-driven Conditions

Mean near-bottom current magnitude (U_r) was comparable for both storm events at LB2M (Figure 3a, 4a) despite variations in both wind speed and direction between the events. Fair weather U_r values were $<10 \text{ cm s}^{-1}$ and exhibited a tidal component. During both events, mean bottom currents exceeded the mean pre-storm velocity of 10 cm s^{-1} . This increase, presumably due to subtidal currents, overwhelmed the tidal component. During H. Ophelia, bottom currents exceeded 10 cm s^{-1} from 14–18 September and reached a peak of 19.2 cm s^{-1} late on 14 September (Figure 3a). For the November event, bottom currents exceeded 10 cm s^{-1} for only 1 day (Figure 4a) and reached a maximum of 20 cm s^{-1} on 25 November. For both storms, along-shelf U_r was greater than across-shelf U_r at LB2M (Table 1).

During H. Ophelia, subtidal currents were

predominantly along-shelf reaching velocities of almost 16 cm s^{-1} toward the east (Table 1). During the November event, subtidal currents also were along-shelf and eastward, reaching a peak velocity (15 cm s^{-1}) comparable to H. Ophelia. One major factor influencing sediment transport between the two events was the duration of elevated ($>10 \text{ cm s}^{-1}$) subtidal velocities, which lasted approximately 1.5 days for the hurricane and almost 2.5 days for the November event (Figures 3, 4).

Maximum near-bottom wave orbital velocities (U_b) at LB2M were coincident with maximum U_r . For the hurricane, U_b gradually increased during storm approach and then subsided with storm passage. U_b values in excess of 40 cm s^{-1} were reached about one day prior to the elevation of the currents. These values persisted for approximately two days, reaching a maximum of 66 cm s^{-1} on 14 September (Figure 3) after the eye of the storm had passed

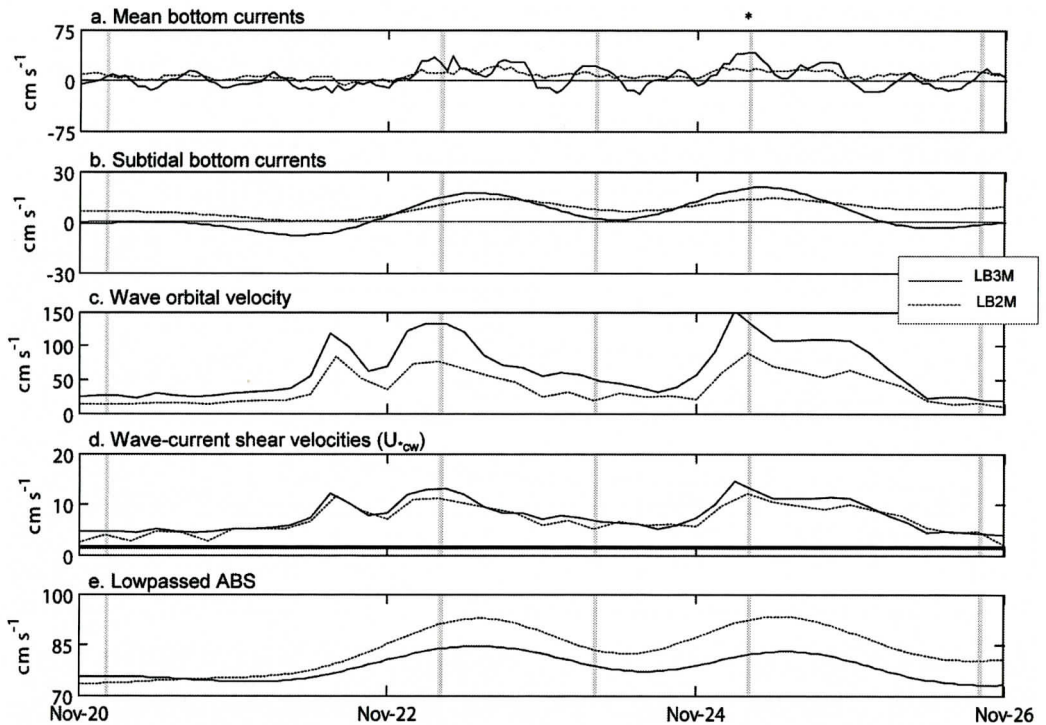


Figure 4. Bottom boundary layer parameters during the November event at LB2M (dashed) and LB3M (solid). (a.) Hourly mean directional bottom currents; (b.) Hourly sub-tidal directional bottom currents; (c.) Bottom wave orbital velocities; (d.) Shear velocities (horizontal line denotes critical shear velocity); (e.) Lowpassed ABS. The positive along-shelf direction is eastward and positive across-shelf direction is onshore. The shadeboxes in the panels represent the bursts described in Table 1. The asterisk represents the time of peak storm conditions as referred to in the text.

north of the study area. For the November event, U_b peaked twice; first on 21 November, approximately 12 hours prior to elevated U_r and likely indicates the onset of storm swell waves to the area. On 23 November a reversal in wind direction opposed the storm-induced water column momentum that resulted in the decrease of U_r and U_b to pre-storm levels (Figure 4b, c). Winds intensified and shifted towards the across-shelf direction on 25 November as the second storm approached and U_r and U_b reached maximum values of 20 and 89 cm s^{-1} , respectively. During both storms, elevated U_b coincided with increased ABS (Figures 3e, 4e).

At LB3M, mean U_r values rarely exceeded 15 cm s^{-1} (Figures 3a, 4a) and a tidal component was evident in the along-shelf component of U_r prior to each storm. During both events, mean

near-bottom current magnitudes (U_r) were comparable, although the maximum U_r during H. Ophelia was almost twice that observed for the November event. These results differ from LB2M where maximum U_r for each storm type was similar, $\sim 20 \text{ cm s}^{-1}$. Further, the tidal signal in the along-shelf component at LB3M was not dampened during storm passage as was observed at LB2M. U_r at LB3M began to exceed mean pre-storm velocities (15 m s^{-1}) on 14 September and 22 November, respectively (Figures 3a, 4a). Maximum U_r at LB3M was 2 to 3.5 times greater than the maximum at LB2M and reached 72 cm s^{-1} during H. Ophelia and 42 cm s^{-1} during the November event (Figures 3a, 4a). At the peak of each event, along-shelf U_r exceeded across-shelf U_r (Figure 2c).

During H. Ophelia, the along-shelf subtidal

current reversed from westward to eastward in response to the shifting wind field (Figure 2) reaching maxima of approximately 25 cm s^{-1} regardless of direction. This reversal of along-shelf currents was not observed at LB2M (Figure 2b, c; Table 1). During the November event, along-shelf velocity reached magnitudes ($\sim 20 \text{ cm s}^{-1}$) comparable to H. Ophelia. Similar to LB2M, the duration of elevated subtidal currents ($>15 \text{ m s}^{-1}$) during the November event exceeded the duration associated with H. Ophelia by at least 12 hours (Figures 3 and 4).

At LB3M, maximum near-bottom wave orbital velocities (U_b) again coincided with peak currents for both storm events (Figures 3 and 4). Prior to the hurricane, mean U_b values were 35 cm s^{-1} and rarely exceeded 60 cm s^{-1} . As the storm approached, U_b values in excess of 50 cm s^{-1} were reached approximately 1.5 days before U_r and subtidal currents increased. U_b values in excess of 70 cm s^{-1} were sustained for nearly 2 days beginning 13 September. U_b reached a maximum of 116 cm s^{-1} on 14 September (Figure 3c) after the storm center had passed north of the study area. Maximum U_b at LB3M during the hurricane was almost twice the maximum U_b at LB2M.

During the November event, U_r , subtidal currents, and U_b at LB3M also exhibited two distinct peaks. As the first frontal system passed through the study area (21 Nov), both currents and U_b intensified although the U_b response, presumably due to storm swell, preceded the currents by about 12 hours. Pre-storm wave orbital velocities of 30 cm s^{-1} increased to $>70 \text{ cm s}^{-1}$ on 21 November (Figure 4c). These U_b were sustained for 24 hours or about half of the maximum U_b duration associated with H. Ophelia. Similar to U_r , U_b also declined for about 24 hours when winds shifted between the two fronts. Currents and orbital velocities responded to an increase in onshore winds of the second system (25 Nov) and reached maximum values of 40 cm s^{-1} and 152 cm s^{-1} , respectively (Figure 4a, c). For both events and study sites, ABS increased in unison with U_b (Figures 3, 4), but ABS at LB3M was usually less than at LB2M.

Boundary Layer Response and Sediment Transport During the Storms

The velocity necessary to initiate movement of the median grain size, U_{*crit} was 1.4 cm s^{-1} for LB2M and 1.3 cm s^{-1} for LB3M. The mean shear velocity due solely to currents, U_{*c} , was usually less than or equal to U_{*crit} during both events at each site. U_{*c} values sporadically exceeded U_{*crit} but still never exceeded 5 cm s^{-1} . At both sites, shear velocity due to wave-current interaction, U_{*cw} , was several times greater than U_{*c} and exceeded U_{*crit} 100% of the time during both events (Figures 3, 4). At LB2M, maximum U_{*cw} was 10 cm s^{-1} during Ophelia and 12 cm s^{-1} during the November event. At LB3M maximum U_{*cw} was 11 cm s^{-1} during Ophelia and close to 15 cm s^{-1} during the November event (Table 1). Sediment resuspension at both sites, as indicated by ABS, closely followed U_b and U_{*cw} for both storms (Figures 3 and 4).

The bbl model was used to determine current velocity, suspended sediment concentration, and sediment transport in the boundary layer at each site for five sampling bursts from each event. Individual bursts were selected for the following storm phases: pre-storm, increasing currents, peak intensity, waning conditions, and post-storm. There was little difference in current velocity, suspended sediment concentration, and sediment transport between storm events for a given site, although LB3M values exceeded LB2M values.

As Hurricane Ophelia approached the study area, current velocities were relatively weak and suspended sediment concentration and transport within the boundary layer were low (Table 1). U_r , U_b , and suspended sediment transport (Figures 3, 4; Table 1) began to notably increase on 12 September. During peak storm conditions (14 Sept), boundary layer velocities at LB2M nearly doubled and sediment transport was three orders of magnitude above pre-storm levels. At LB3M, current velocities were 70 cm s^{-1} and sediment transport was two orders of magnitude greater than pre-storm conditions (Figure 3c). Boundary layer velocities

waned as the storm tracked northeastward, and sediment transport essentially ceased by 16 September.

As the first system of the November event approached (20 Nov), boundary layer currents were relatively weak and sediment transport was minimal (Table 1). Boundary layer current velocity and sediment transport reached their first maxima on 22 November with values at LB3M exceeding LB2M. As the first system tracked away from the study area (23 Nov), wind velocity decreased and switched directions and sediment transport in the boundary layer decreased by one and three orders of magnitude for LB3M and LB2M, respectively (Table 1). During the second and stronger peak in storm conditions (24 Nov), sediment transport at LB2M increased to more than four times the rate observed two days prior. At LB3M U_r exceeded 40 cm s^{-1} , but did not surpass U_r during associated with *H. Ophelia* ($>70 \text{ cm s}^{-1}$). Sediment transport at LB3M (24 Nov) was three times greater than peak sediment transport observed on 22 November (Figure 4, Table 1). By 25 November, sediment transport was returning to pre-storm levels. Based on peak values, sediment transport rates during the November event was 1.3 (LB3M) and 3.4 (LB2M) times greater than the peak transport rates of *H. Ophelia* even though near-bottom mean and subtidal currents associated with the hurricane surpassed those of the November event. Given that the total duration of the November event was longer, the total sediment transport flux in the bottom boundary layer during the November event should have exceeded the transport fluxes associated with *H. Ophelia*. In most cases, however, the peak sediment transport rates associated with each of the single frontal systems of the November event, exceeded those during *Ophelia*.

DISCUSSION AND SUMMARY

Influence of Storm Type and Location on Sediment Transport in Long Bay

The hydrography and bottom boundary layer

dynamics during the autumn of 2005 were dominated by the passage of *H. Ophelia* and several low magnitude extratropical events. Bottom boundary layer sediment transport was several orders of magnitude higher during events than during fair weather conditions. Due to spatial variations in wave height, current magnitude, and grain size, sediment transport at LB3M was roughly two orders of magnitude higher than sediment transport at LB2M. At both sites, sediment transport was dominated by the along-shelf component, which was consistent with current direction.

It has been proposed that extratropical storms may be more significant in terms of overall sediment movement on the inner continental shelf because they occur with greater frequency (Dolan et al., 1988). To examine the relative impact of site location and storm type on suspended sediment transport in northern Long Bay, along-/across-shelf current magnitudes and directions were compared to depth-integrated sediment transport fluxes during peak storm conditions in the bottom boundary layer (Table 1). Because sediment transport was calculated as the product of current velocity and sediment concentration, it was assumed that current direction dictated transport direction. Since along-shelf currents were predominantly eastward, suspended sediment transport was likely eastward as well. These results are consistent with previous studies conducted on the inner and mid-continental shelf of Onslow Bay, where the along-shelf component of sediment transport dominated the net transport direction during both hurricanes and extratropical storms (Marshall, 2004; Wren and Leonard, 2005).

As proposed by Lyne et al. (1990), Caccione et al. (1994), and Wren and Leonard (2005), the intensity of bottom stress resulting from the combination of waves and currents contributed to the spatial and temporal variations in sediment transport. For the events examined here, depth-integrated peak sediment transport during the November event was approximately 25-70% greater than the depth-integrated transport for *Ophelia* despite lower subtidal current magnitudes. The U_{*cw} during the November event exceeded U_{*crit} and was

sustained for long periods at both sites thereby resulting in higher suspended sediment concentrations than during *Ophelia*. As long as subtidal currents were of sufficient strength to maintain the resuspended material in the water column, sediments were transported along-/across-shelf depending on the prevailing current direction. Due to higher U_b coupled with sustained subtidal currents during the November event, net transport for the November event exceeded the hurricane.

During this study, a class 1 extratropical storm transported more sediment than a category 1 hurricane. In the literature, however, the effects of strong hurricanes (e.g. 3 and higher) are more commonly reported due to their substantial impact on sediment transport and, possibly, to scientists' affinity to study low frequency, catastrophic events. In the study region, the frequency of tropical system impact from 1950-2005 was 0.7 storms per year (NOAA, 2006b; NHC 2006). If tropical depressions are included, the rate increases to 0.9 per year. The frequency of extratropical storm impact over the same time period was 30 to 40 times greater than tropical systems. Thus, the higher frequency of smaller storms has the potential to drive the majority of sediment transport on the inner shelf of this area as previously suggested by Dolan et al. (1988).

Implications for Shoreline Sustainability

The beaches shoreward of LB2M and LB3M, Oak Island and Bald Head Island, respectively, undergo frequent renourishment to counter the effects of beach erosion (Cleary et al., 2000). However, the rate of beach erosion has maintained pace with renourishment projects, thus transferring large quantities of sediment from the beach onto the shoreface and inner shelf (Pearson and Riggs, 1981). The results of this study suggest that much of the offshore transport occurs during peak conditions of extratropical storms. The only exception was at LB2M during *Ophelia* when weak onshore currents (5 cm s^{-1}) existed during a period of low transport fluxes ($0.14 \text{ mg cm}^{-1} \text{ s}^{-1}$). The net

offshore transport documented here for the November event is consistent with the results of Wright et al. (1986) who showed that wind-driven, southerly currents produced by northeaster storms can produce secondary, but strong, downwelling on the inner shelf of the Middle Atlantic Bight. When an extratropical storm closely follows the completion a beach renourishment project, the potential exists for large volumes of sand to be transported offshore. This scenario is particularly likely in North Carolina where the sea turtle nesting season (May – Oct.) forces most renourishment projects to occur during the early spring, a period of elevated extratropical storm frequency (<4 per month; Dolan et al., 1988).

Our results also suggest that storm-driven subtidal currents may result in significant along-shelf movement of sand. This type of transport raises a myriad of political implications, particularly for renourished material paid for utilizing municipal funds via personal property taxes. Even if the sand remains within the littoral zone, the sediment transported across municipal boundaries may benefit a community that did not participate in the project's cost. The complexity of this scenario increases when 'hard structures', such as groins and jetties are constructed. In this study area, hard structures do not exist and the storm types examined here most likely result in substantial along-shelf transport of sands that are subsequently sequestered in Jay Bird and/or Frying Pan Shoals, located east of LB2M and LB3M, respectively. According to Cleary and others (2000), these shoals contain millions of m^3 of viable sand resources, but the environmental concerns associated with dredging and the economic issues associated with adjacent Cape Fear shipping channel must be addressed before the material can be extracted. The dominant along-shelf transport may be similar to results reported by Marshall (2004) who noted the convergence of along-shelf currents in southern Onslow Bay towards Cape Fear. McNinch and Leutlich (2000) similarly observed converging sediment transport directions on each side of Cape Lookout Shoals in northern Onslow Bay during fair weather conditions. Although these along-shelf

subtidal currents may significantly contribute to the maintenance of large shoal systems in this study area, as well as the regional shoals associated within the Carolina Capes, this process constitutes a loss of suitable material available to the beach. Therefore, quantifying the magnitude and direction of sediment transport events during different storm types is necessary to fully understand and predict sedimentological response in the nearshore environment and to optimize the effectiveness of these costly public projects.

ACKNOWLEDGEMENTS

We would like to acknowledge Ken Hathaway and the U.S. Army Corps of Engineers for providing ADCP data for this project. We also thank Dr. Ansley Wren and Jeff Marshall for assisting with the implementation of bottom boundary layer model used in this paper. We appreciate the assistance of Jay Souza, Dave Wells, and Steve Hall, who were essential in diving operations and general data collection and also the crews of the *R/V Cape Fear* and *R/V Seahawk*. This research was primarily funded by the National Oceanic & Atmospheric Administration, Award # NA16RP2675 to the Coastal Ocean Research and Monitoring Program at the University of North Carolina Wilmington.

REFERENCES

- Battisto, G.M., 2000. Field measurement of mixed grain size suspension in the nearshore under waves. Ph.D. Thesis, Virginia Institute of Marine Science, Gloucester Point, VA, unpublished.
- Cacchione, D.A., Drake, D.E., Ferreira, J.T., and Tate, G.B., 1994. Bottom stress estimates and sand transport on northern California inner continental shelf. *Continental Shelf Research*, 14(10-11): 1273-1289.
- Carpenter, J.H. and Yonts, W.L., 1979. Freshwater Inflow to the Cape Fear River Estuary, NC October 1951-September 1979 (Appendix A), Carolina Power and Light Company, Raleigh, NC.
- Cleary, W.J., McLeod, M.A., Rauscher, M.A., Johnston, M.K., and Riggs, S.R., 2000. Beach Renourishment on Hurricane Impacted Barriers in Southeastern North Carolina, USA: Targeting Shoreface and Tidal Inlet Sand Resources. *Journal of Coastal Research- Special Issue*, 34: 232-255.
- Deines, K.L., 1999. Backscatter estimation using broadband acoustic doppler current profilers. *Oceans' 99 MTS/IEEE Conference Proceedings*, 13-16.
- Dolan, R. and Davis, R.E., 1992. Rating Northeasters. *Mariners Weather Log*, 36: 4-16.
- Dolan, R., Lins, H., and Hayden, B., 1988. Mid-Atlantic coastal storms. *Journal of Coastal Research*, 4: 417-433.
- Kim, S.-C., Wright, L.D., and Kim, B.O., 1997. The combined effects of synoptic-scale and local scale meteorological events on bed stress and sediment transport on the inner shelf of the Middle Atlantic Bight. *Continental Shelf Research*, 17 (4): 407-433.
- Lyne, V.D., Butman, B., and Grant, W.D., 1990. Sediment movement along the U.S. east coast continental shelf. I. Estimates of bottom stress using the Grant-Madsen model and near-bottom wave and current measurements. *Continental Shelf Research*, 10(5): 397-428.
- Madsen, O.S., Wright, L.D., Boon, J.D., and Chisholm, T.A., 1993. Wind stress, bed roughness and sediment transport on the inner shelf during an extreme storm event. *Continental Shelf Research*, 13 (11): 1303-1324.
- Mallin, M.A., 2006. The Ecology of the Cape Fear River System. http://www.uncwil.edu/river/run/river_tutorial/CFRSystem.htm.
- Marshall, J.A., 2004. Event driven sediment mobility on the inner continental shelf of Onslow Bay, NC. Master's Thesis, University of North Carolina Wilmington, Wilmington, NC, unpublished.
- McNinch, J.E. and Luettich, Jr. R.A., 2000. Physical processes around a cusped foreland headland: implications to the evolution and long-term maintenance of a cape-associated shoal. *Continental Shelf Research*, 20 (17), 2367-2389.
- National Hurricane Center, 2006. National Hurricane Center- Archive of Hurricane Seasons. <http://www.nhc.noaa.gov/pastall.shtml>.
- National Oceanic and Atmospheric Administration, 2006a. Tide Tables: North Carolina-South Carolina. <http://tidesandcurrents.noaa.gov/tides04/tab2ec3a.html>.
- National Oceanic and Atmospheric Administration, 2006b. Historical Hurricane Tracks. <http://maps.csc.noaa.gov/hurricanes/viewer.html>.
- Pearson, D.R. and Riggs, S.R., 1981. Relationship of surface sediments on the lower forebeach and nearshore shelf to beach nourishment at Wrightsville Beach, North Carolina. *Shore and Beach*, 49: 26-31.
- Pepper, D.A. and Stone, G.W., 2002. Atmospheric forcing of fine-sand transport on a low-energy inner shelf: south-central Louisiana, USA. *Geo-Marine Letters*, 22: 33-41.
- Styles, R. and Glenn, S.M., 2002. Modeling bottom roughness in the presence of wave-generated ripples. *Journal of Geophysical Research*, 107: 1-15.
- Traykovski, P., Hay, A., Irish, J.D., Lynch, J.F., 1999. Geometry, migration, and evolution of wave orbital ripples at LEO-15. *Journal of Geophysical Research*, 104: 1505-1524.

HYDROGRAPHY AND SEDIMENT MOBILITY IN LONG BAY

- Trowbridge, J. and Young, D., 1989. Sand transport by unbroken water waves under sheet flow conditions. *Journal of Geophysical Research*, 94(C8): 10971-10991.
- Williams, J.J. and Rose, C.P., 2001. Measured and predicted rates of sediment transport in storm conditions. *Marine Geology*, 179: 121-133.
- Wren, P.A. and Leonard, L.A., 2005. Sediment transport on the mid-continental shelf in Onslow Bay, North Carolina during Hurricane Isabel. *Estuarine, Coastal and Shelf Science*, 63: 43-56.
- Wright, L.D., Boon, J.D., III, Green, M.O., and List, J.H., 1986. Response of the midshoreface of the southern Mid Atlantic Bight to a "Northeaster". *Geo-Marine Letters*, 6: 153-160.
- Wright, L.D., Boon, J.D., Kim, S.C. and List, J.H., 1991. Modes of cross-shore sediment transport on the shoreface of the Middle Atlantic Bight. *Marine Geology*, 96: 19-51.
- Wright, L.D., Xu, J.P., and Madsen, O.S., 1994. Across-shelf benthic transports on the inner shelf of the Middle Atlantic Bight during the "Halloween Storm" of 1991. *Marine Geology*, 118: 61-77.
- Xu, J.P. and Wright, L.D., 1998. Observations of wind generated currents of Duck, North Carolina. *Journal of Coastal Research*, 14: 610-619.



THE EFFECTS OF HARDBOTTOM GEOMETRY ON SEDIMENT TRANSPORT PROCESSES ON THE MID-CONTINENTAL SHELF IN ONSLOW BAY, NORTH CAROLINA

**¹P. ANSLEY WREN, ²JEFF A. MARSHALL, ³LYNN A. LEONARD, AND
⁴MELODY VAN DER LINDE**

*¹Department of Marine Science, Coastal Carolina University, Conway, SC 29528
awren@coastal.edu*

*²Center for Marine and Wetland Studies
Coastal Carolina University
Conway, SC 29523
jmarshal@coastal.edu*

*³Center for Marine Science, University of North Carolina Wilmington, Wilmington, NC 28409, USA
lynnl@uncw.edu*

*⁴Center for Marine and Wetland Studies, Coastal Carolina University, Conway, SC 29523
mvanderl@coastal.edu*

ABSTRACT

Onslow Bay is a high-energy, sediment-starved shelf characterized by extensive areas of exposed hardgrounds varying in lithology and relief. These hardgrounds have been shown to be of economic importance due to the productive marine habitats they support; however, annual variations in the thickness and distribution of sands on hardbottom surfaces have been shown to profoundly affect these ecological communities. The present study compares mid-shelf sediment dynamics around a productive marine hardbottom with vertical relief of ~1 m to a nearby area characterized by a broad flat bottom and consisting mainly of fine to coarse grained surficial sands. The effects of reef geometry on sediment transport processes around this hardbottom area are examined using two long-term data sets containing current velocity profiles from the sea surface to the seabed, acoustic backscatter profiles, and seabed elevation data at the two sites. Current velocity profiles measured above and below the elevation of the reef ledge were compared at both sites during sediment transport events that exhibited similar current magnitude and direction in order to elucidate any effects that the hardbottom reef

may exert on the hydrodynamics. In addition, shear velocities were calculated using a 1-D bottom boundary layer model. These analyses indicate that the hardbottom reef does affect the hydrodynamics and sediment transport processes within the bottom boundary layer at the site closest to the hardbottom ledge, particularly when the currents are from the north and passing over the hardbottom surface.

INTRODUCTION

Many high-energy shelves on passive margins, such as those along the east and west coast of the Atlantic Ocean, are sediment-starved with little to no fluvial sediment input accumulating on the shelf. Sediment-starved continental margins characterize much of the Middle and South Atlantic Bights of the U.S., and this type of shelf environment is thought to be typical of much of the U.S. Atlantic coast (Riggs et al., 1998). Margins of this type are relatively devoid of thick sediment cover, exposing hardbottom of significant aerial extent (Riggs et al., 1998; Ojeda, Gayes, and Sapp, 2001). Seafloor mapping studies conducted along shelves in the Middle and South Atlantic Bights have estimated that approximately 60 - 70% of the continental shelves in these areas are

covered by exposed hard-bottoms that are morphologically complex, and that vary in lithology and relief (Riggs et al., 1998; Ojeda et al., 2004). These marine hard-bottom areas provide attachment substrate, predator refugia and foraging grounds for a wide range of invertebrates and fish, including many important fishery species (Grimes et al., 1982; Wenner et al., 1983; Sedberry and Van Dolah 1984). Large annual variations in sediment thickness and distribution on the hardbottom surfaces, however, have been shown to profoundly affect the ecological communities supported by these hardbottom areas (Renaud et al., 1996, 1997).

Although numerous studies have demonstrated active reworking of the inner-shelf regions along the US east coast shelf (Madsen et al., 1993; Wright et al., 1994; Traykovski et al., 1999; Marshall, 2004; Harris et al., 2003; Gutierrez, et al., 2005; Styles, 2005) few have examined transport on the mid-shelf (Wren and Leonard 2005), particularly in the southeastern US where hardbottom outcrops comprise a significant percentage of the sea floor (Cleary and Pilkey, 1968; Blackwelder et al., 1982; Riggs et al., 1998). Sediment movement across living hardbottoms can affect ecological communities through several mechanisms. Sedimentation has been shown to decrease the growth rates, densities and recruitment success of many sessile invertebrates such as corals, sponges and ascidians and in more extreme cases completely smother living reef habitats (Hunt and Wittenberg, 1992; Miller et al., 2002; Golbuu et al., 2003; Fabricius, 2005; Dikou and Woessik 2006). In an observational study on hardbottom reefs in North Carolina, Renaud et al. (1997) reported that changes in sediment thickness and distribution on hardbottom surfaces had profound effects on the resident ecological communities. Although, Wren and Leonard (2005) demonstrated significant sediment mobilization adjacent to a marine hardbottom reef offshore of southeastern NC, the influence of reef geometry on the hydrodynamics and the resultant sediment transport processes around the reef remains unclear.

As part of the Coastal Ocean Research and Monitoring Program (CORMP) at the Universi-

ty of North Carolina Wilmington, a bottom mounted frame was deployed on the mid-shelf 27 nm offshore of Wrightsville Beach, NC at a depth of approximately 29 meters. Flow velocity measurements have been collected from the seabed to the sea surface using a downward-looking Pulse Coherent Acoustic Doppler Profiler (PC-ADP) and an upward-looking Acoustic Doppler Current Profiler (ADCP). The frame was deployed adjacent to an extensive marine hardbottom area with varying vertical relief of approximately 1 - 2 m from 2000 - 2003. Subsequently, the instrumentation was moved approximately 1 km away from the reef area in order to examine the effects that the hardbottom reef may have on the hydrodynamics and sediment transport processes. Two long-term data sets of simultaneous measurements of the bottom boundary layer (BBL) hydrodynamics, acoustic backscatter, and seabed elevation data from each site have been used to identify sediment transport events on the mid-shelf. Current magnitude and direction profiles were generated using the ADCP and PC-ADP data for two types of sediment transport events at each site. Events were chosen such that the atmospheric forcing and the hydrodynamic response were similar in magnitude at both sites. The current profiles from both sites were compared throughout similar events in order to elucidate any effects that the hardbottom reef may have on the hydrodynamics and sediment transport processes. The primary objective of this study is to examine what effects the hardbottom reef geometry exerted on the processes that occur during different types of sediment transport events.

FIELD EXPERIMENT

Study site - Physical and meteorological setting

Onslow Bay is located off the southeastern coast of North Carolina and is bounded to the north and south by Cape Lookout and Cape Fear, respectively, and at the shelf edge by the Gulf Stream (Fig. 1). The mean tidal range in Onslow Bay is approximately 1.0 m and mainly

HARDBOTTOM EFFECTS ON HYDRODYNAMICS AND SEDIMENT TRANSPORT

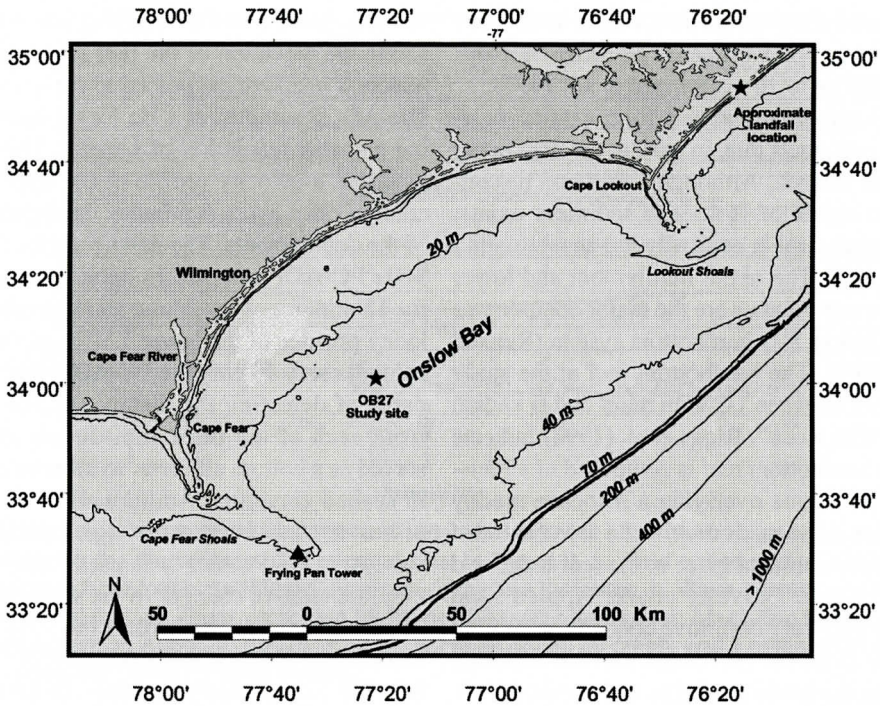


Figure 1. Map of Onslow Bay, North Carolina showing the mid-shelf study area (labeled OB27) which is locally known as “23 Mile Rock”. Meteorological data was measured at the NOAA C-Man station labeled Frying Pan Tower and an adjacent buoy.

consists of M2 frequency oscillations (Pietrafesa et al., 1985). Average significant wave heights are 1.5 m with an average dominant period of 8.0 seconds (NOAA, FPSN7 station). During the summer months, winds are generally out of the southwest and mild. Waves consist of longer period (9-10 second) fair weather swells moving across the shelf. The effects of extratropical low pressure systems (noreasters) and pressure gradients between upper level air masses influence the mid-shelf study area frequently throughout the fall and spring months. These northerly winds create steeper, smaller period waves with moderately high significant wave heights (> 2.0 m). During these common wind events, north to northeasterly winds typically persist for greater than 36 hours and the energy within the water column is typically elevated for 48 hours or longer, providing sufficient energy to the mid-shelf depths for sediment suspension. During the winter months, the dominant winds are associated with

frontal systems passing through the area on a 4-10 day period (Pietrafesa et al., 1985). The passage of the frontal systems are associated with elevated energy within the water column due to strong southeasterly to southwesterly winds as cold fronts approach the coast. Wind velocities and wave energy are generally higher during the winter frontal systems that pass over the area, however, these events are generally short lived (~24 hours).

Study site - Geological setting

Onslow Bay is considered to be sediment-starved given the negligible inputs of new sediment by fluvial inputs and minimal sediment exchange between adjacent shelf embayments (Blackwelder et al., 1982). The major sources of sediment for the inner and mid-shelf are shoreface bypassing of unconsolidated ancient sediment and bio-erosion of the marine hard grounds (Milliman, 1972). The inner to middle

continental shelf of Onslow Bay is characterized by a complex sequence of rocky outcrops with relief up to 10 m (Renaud et al., 1997).

The hardbottom habitats form extensive, irregular reef tracts due, in part, to the area being sediment starved. Although a thin and discontinuous veneer of Holocene sediment exists, surface sediment is generally not accumulating on the shelf. The upper hardbottom and lower sand flat sub-habitats are the major components of the Onslow Bay hardbottom system (Renaud et al., 1997). The hardbottom reef at the study site varies between 1-2 m in relief and is known as "23 Mile Rock". Riggs et al. (1998) indicate that the hardbottom reef is composed of a Pleistocene limestone overlying a Miocene muddy sandstone. Fine sands overlie the top of the reef and are predominant close to the reef ledge and erosion ramp. Gravelly coarse rippled sand patches with very definitive contacts occur with distance from the reef ledge and are typically found on the lower sand flats and not on the upper hardbottom surfaces. Major differences in distribution and thickness of the fine sands on the upper hardbottom have been observed (Renaud et al., 1996) which suggests that these fine sands are mobile and readily suspended during sediment transport events.

Instrumentation and data

Data were collected between 2000 to 2006 at two mid-shelf locations, 25 m and 1 km from the reef ledge at "23 Mile Rock" (Fig. 1). Data were first collected from May through November 2000, and December 2001 through February 2002, when an instrumented frame was located on the fine sand apron located approximately 25 m from the hardbottom reef ledge. In June 2003, the instrumented frame was moved 1 km east of the hardbottom reef ledge and additional data were collected through May of 2006. At each location, a downward looking Sontek Pulse-Coherent Acoustic Doppler Profiler (PC-ADP) and an upward looking Acoustic Doppler Current Profiler (ADCP) were deployed on an aluminum frame secured to the bottom. The upward-looking 600 kHz RDI Workhorse Sentinel ADCP was used to collect

velocity profiles in the overlying water column above the elevation of the reef ledge, approximately 4 m above the seabed to the sea surface. The ADCP sampled at 1 Hz for 60 seconds using a spatial resolution of 1 meter. The ADCP recorded a velocity profile of the upper water column once every 5 minutes throughout each of the deployments. The downward looking 1.5 MHz PC-ADP sampled in burst mode at 1 Hz for 17 minutes every 2 hours and measured velocity profiles of the lower 1.30 m of the water column every 10 cm. The PC-ADP was also capable of detecting the distance to the seabed from each of the three transducers and thus served as a bottom altimeter to monitor changes in seabed elevation. Additionally, the uncalibrated acoustic backscatter signal (ABS) from the 1500 kHz PCADP was used as a proxy to measure relative changes in the suspended sediment concentrations within the BBL (Sherwood et al., 2006). The acoustic signal from the PCADP is especially sensitive to sand-sized particles and works similarly to the Acoustic Backscatter Sensor which has been shown to be especially successful with sands in sediment transport studies in the U.S. and the U.K. (Battisto, 2000; Williams and Rose, 2001, Traykovski et al., 1999). Throughout the study, the ABS data were corrected for the effects of geometric spreading and absorption of the acoustic signal to normalize data from different elevations within the profile following:

$$\text{DECAY} = -20 * \log_{10}(Z/\cos(15^\circ)) - 2 * \alpha * (Z/\cos(15^\circ))$$

where, $\alpha = 0.68$ and is the sound absorption coefficient for 1.5 MHz and 35 ppt salinity, (Z) is the range bin in cm above the bed, and 15° is the slant angle of the acoustic signal (Deines, 1999).

In order to quantitatively compare the sediment transport magnitude during each event, a bottom boundary layer model (BBL model) was used to estimate bottom shear stresses (Styles and Glenn, 2000; 2002). Input data used to run the BBL model included (1) PC-ADP burst-averaged mean currents measured at a reference elevation of 1 mab, (2) near-bottom orbital velocities and near bottom wave excursion amplitudes, and (3) wave and current incidence

HARDBOTTOM EFFECTS ON HYDRODYNAMICS AND SEDIMENT TRANSPORT

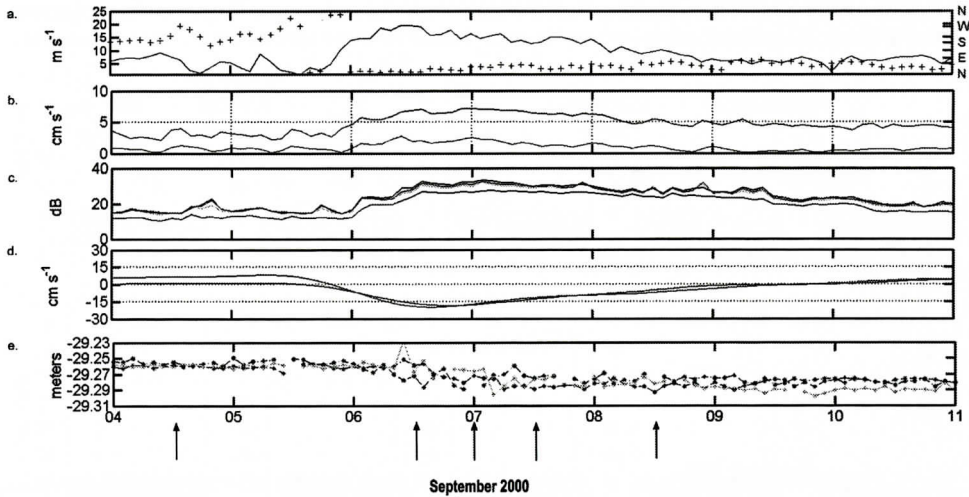


Figure 2. Data from the September 2000 Northerly wind event at site 1. Arrows correspond to profile data during the September 2000 event shown in Figure 3. **a.** Wind speed and wind direction. **d.** Thirty-three hour low-pass filtered currents – gray line indicates. **b.** Wave-current shear velocities (dark) and current shear velocities (light) north/south component; black line indicates east/west component. **c.** Acoustic Backscatter Signal at 30 cmab, 50 cmab, and 1 mab. PC-ADP seabed elevation data from all three beams.

angle. Bottom r.m.s wave velocities, u_b , were determined using the instantaneous velocity record, $u(t)$, for each burst after the mean current, had been removed. Following Madsen et al. (1995), the variance for each horizontal direction was determined and the near-bottom orbital velocity amplitude of the equivalent periodic wave was taken as:

$$u_b^2 = 2(\sigma_u^2 + \sigma_v^2)$$

Average wave periods at the sites were calculated from the near-bottom velocity data using the equation: $T = m(0)/m(1)$ where $m(0)$ is the zeroth moment of the velocity energy spectra and $m(1)$ is the first moment of the velocity energy spectra. Wave direction was calculated as the direction of maximum variance for each burst:

$$\theta = \frac{1}{2} \tan^{-1} \left(\frac{2\sigma_{uv}^2}{\sigma_{uu}^2 - \sigma_{vv}^2} \right)$$

where θ = direction (rad), σ_{uu}^2 and σ_{vv}^2 = variances of the respective eastward and northward

velocity components (u and v), and σ_{uv}^2 = covariance of the velocities.

Time series of the shear velocities due to currents and wave-current interactions were generated for each event. The median grain size (d_{50}) determined from surface sediment samples was input into the BBL model in order to predict the roughness of the seabed by determining the height and wavelength of the ripples on the seabed. Fine sands were dominant at both Sites 1 and 2, and the median grain size was 0.270 mm. Wind velocities, shear velocities, ABS values, wind-driven currents, and seabed elevation data were plotted for one southerly and one northerly wind event at each site in order to quantify the magnitude of the hydrodynamic and sediment transport processes. Current profiles were also generated for the entire water column and current magnitude and direction profiles were compared between sites to elucidate any effects that the hardbottom reef may have on the overall water column hydrodynamics under different current directions.

Table 1. Two types of commonly occurring meteorological events resulting in sediment transport on the mid-shelf. All current measurements reported here were from 1 meter above the bed.

	Event Date	Duration (hrs)	Winds (m s ⁻¹)	Significant wave height (m)	Maximum current (cm s ⁻¹)	Max u _{cw} (cm s ⁻¹)
Northerly wind events	09/06/00 - 09/08/00	72	10 - 21 NE	2.0 - 3.0	35	7.0
	05/05/06 - 05/07/06	60	5 - 15 N	2.0 - 3.2	34	8.2
Southerly wind events	01/06/02 - 01/08/02	36	10 - 25 SE-SW-W	3.0 - 5.0	20	9.0
	01/17/06 - 01/19/06	36	8 - 17 S-SW-W	2.0 - 4.0	24	6.1

RESULTS

Northerly wind events

The northerly wind event that occurred at Site 1 from September 6-8, 2000 resulted in a sediment response that was rapid and substantial. Wave heights were 2.0 - 2.5 m for 48 hours and dominant wave periods ranged from 5 - 8 seconds during this time. Model derived wave-current shear velocities reached 7 cm s⁻¹ over the 72 hour duration (Fig. 2b, Table 1). Current induced shear velocities helped to increase the total wave-current bed stress, as mean currents produced shear velocities of approximately 2 cm s⁻¹. Strong wind-driven currents of over 15 cm s⁻¹ were generated towards the south and west directions within the lower boundary layer (Fig. 2). The ABS increased immediately at all elevations above the seabed in response to surface wind and wave conditions, indicating suspended sediments were vertically mixed throughout the BBL (Fig. 2b). ABS values ranged from 28-35 dB and remained elevated throughout the event. Peak values occurred during the peak storm conditions between 0000 UTC on the September 6th through 0000 UTC on the September 8th exhibiting zero lag with surface wind conditions (Fig 2 a, c). The seabed elevation record from each of the three beams indicated that the seabed was actively being re-worked during this time (Fig. 2e). Fluctuations from each of the three beams showed a variation from 1 - 4 cm during the event. Additional-

ly, all three beams indicate that the elevation of the seabed was lowered by approximately 3cm from pre-storm to post-storm conditions resulting in net erosion at the site. Fluctuations of 1cm in relief were observed in the time series over the subsequent two days suggesting continued ripple activity on the seabed (Fig. 2e).

The current magnitude and direction profiles from the sea surface to seabed are shown during different stages of the event in Figure 3 (times denoted by arrows in Fig. 2). The first profile on September 4th was during the fair-weather conditions (winds < 10 cm s⁻¹) that were prevalent before the winds switched to a north-northeasterly direction at the start of the event. Mean current speeds measured by the ADCP throughout the upper water column (above the hardbottom reef) are similar to the measurements from the PCADP within the BBL. The magnitudes typically ranged from 15-20 cm s⁻¹, excluding the top two surface bins, and the vertical structure of the BBL profile exhibited a logarithmic shape. At this time, flows were generally tidal, with a small sub-tidal component at 1 mab towards the north at 7 cm s⁻¹ due to southerly winds that persisted before the event (Fig. 2a). As the winds wrapped around to northerly on September 5th and increased in speed, mean currents responded and began to flow towards the southwest (Fig. 2). By 1200 on September 6th the upper water column was flowing towards the southwest at approximately 40 cm s⁻¹ and currents within the BBL were flowing in the same direction; however, the magnitude of

HARDBOTTOM EFFECTS ON HYDRODYNAMICS AND SEDIMENT TRANSPORT

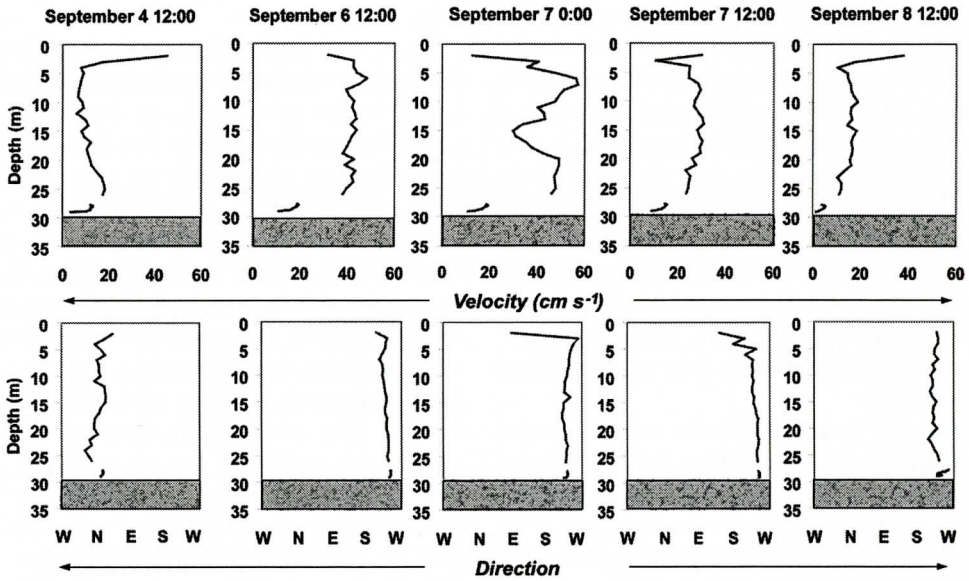


Figure 3. Current magnitude and direction profiles throughout the September 2000 Northerly wind event at Site 1. Velocities above 4 mab were measured by the ADCP and velocities within the bottom boundary layer were measured by the PC-ADP. Profiles appear to be discontinuous during the event when currents are flowing over the hardbottom located north of the instrument frame. Times denoted by arrows in Figure 2.

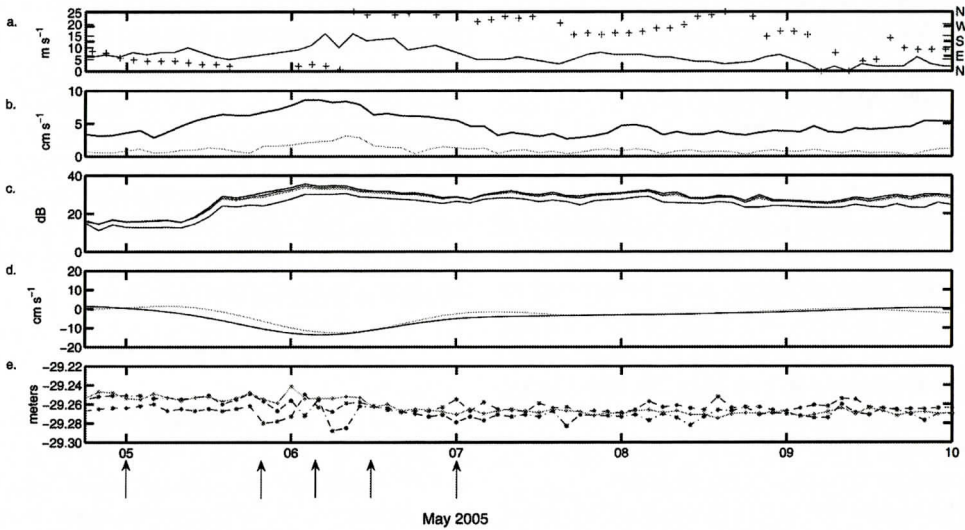


Figure 4. Data from the May 2005 Northerly wind event at Site 2. Arrows correspond to profile data during the May 2005 Northerly event shown in Figure 5. a. Wind speed and wind direction d. Thirty-three hour low-pass filtered currents – gray line indicates. b. Wave-current shear velocities (dark) and current shear velocities (light) north/south component; black line indicates east/west component. c. Acoustic Backscatter Signal at 30 cmab, 50 cmab, and 1 mab. PC-ADP seabed elevation data from all three beams

the flow in BBL did not increase as much as the upper water column (Fig 3). This type of separation between the flows within the upper water column and the BBL was typical in a majority of the profiles during this event at Site 1, and the discontinuity appears to be associated with strong currents greater than $\sim 40 \text{ cm s}^{-1}$ flowing from the northeast across the hardbottom area (Fig 3). The observed disconnect between the upper water column above the hardbottom reef and the BBL may be due to a "sheltering effect" from the hardbottom area located northeast of the study site.

During a similar northerly wind event that occurred at Site 2 from May 5-7, 2005, wave height and period data were not available at the FNS7 station; however, wave heights at the buoy on the mid-shelf in neighboring Long Bay measured wave heights between 2.0 to over 4.0 m for 36 hours with dominant wave periods between 5 and 8 seconds. The shear velocities increased simultaneously with the measured ABS as the wind switched around from easterly to northerly on May 5th (Fig. 4). As winds remained from the north and increased to 15 m s^{-1} on May 6th, shear velocities reached a maximum of over 8 cm s^{-1} (Fig. 4b, Table 1) and the measured ABS increased to 35 - 40 dB (Fig. 4c). Subtidal flows of between $5\text{-}10 \text{ cm s}^{-1}$ were generated towards the southwest within the BBL (Fig. 4d). High ABS values at all elevations indicated that a relatively large amount of suspended sediment was mixed throughout the BBL and these sediments were transported towards the southwest by the low-frequency wind-driven flow (Fig. 4 c, d). As northerly winds decreased early on May 7th, shear velocities and wind-driven currents decreased simultaneously, although ABS levels remained elevated for the subsequent 48 hours.

The seabed was active throughout this event, as fluctuations of 2-3 cm were measured throughout peak storm conditions. This response was similar to the Sept 2000 event at Site 1; however, the altimetry data indicate that the seabed was not as active during this event despite the higher shear velocities (Fig. 4e). Additionally, there was no net change in elevation between the pre-storm and post-storm condi-

tions.

The current profiles during this event (Fig 5) indicate that current velocities were weak ($< 10 \text{ cm s}^{-1}$) before the event. As the wind speed began to increase late on May 5th, the water column began to respond to the northeasterly winds as wind-driven currents were generated within the BBL (Fig 4d). During the set-up of the wind-driven flows, current speeds increased flowing towards the west on the surface and spiraling down to northwesterly and southwesterly within the BBL. By 0400 on May 6th, as wind-driven flows were reaching a maximum within the BBL (Fig. 4d, Table 2), the water column was flowing uniformly towards the southwest (Fig. 5). By 1200 on May 6th, flows reached 40 cm s^{-1} throughout the overlying water column (Fig. 5). The shape of profile at this time was typical of the profiles measured by the ADCP throughout this event. During this time, currents continued to be wind-driven at 1 mab, although it appears that the flows within the lower 5 meters of the water column did not increase simultaneously with the upper water column during this event (Fig. 5). Current directions at this time remained the same between the lower and upper water column and continued to flow towards the southwest. By early on May 7th, the northerly winds were waning down rapidly and currents responded throughout the water column. Wind-driven currents had diminished within the BBL (Fig. 4d) and the flows had slowed to approximately $10\text{-}15 \text{ cm s}^{-1}$ within the upper the water column (Fig. 5).

Southerly wind events

Two similar southerly wind events occurred at Site 1 and Site 2 during January 2002 and 2006, respectively. The event that occurred from January 6 - 8, 2002 resulted in winds from the southeast at 23 m s^{-1} , switching to southwesterly up to 20 m s^{-1} (Fig. 6a). Wave heights were between 3 - 5 m for approximately 36 hours and dominant periods ranged from 8 - 11 seconds. As winds increased in speed out of the southeast, shear velocities did not increase immediately; however, as the wind direction switched to southwesterly the shear velocities

HARDBOTTOM EFFECTS ON HYDRODYNAMICS AND SEDIMENT TRANSPORT

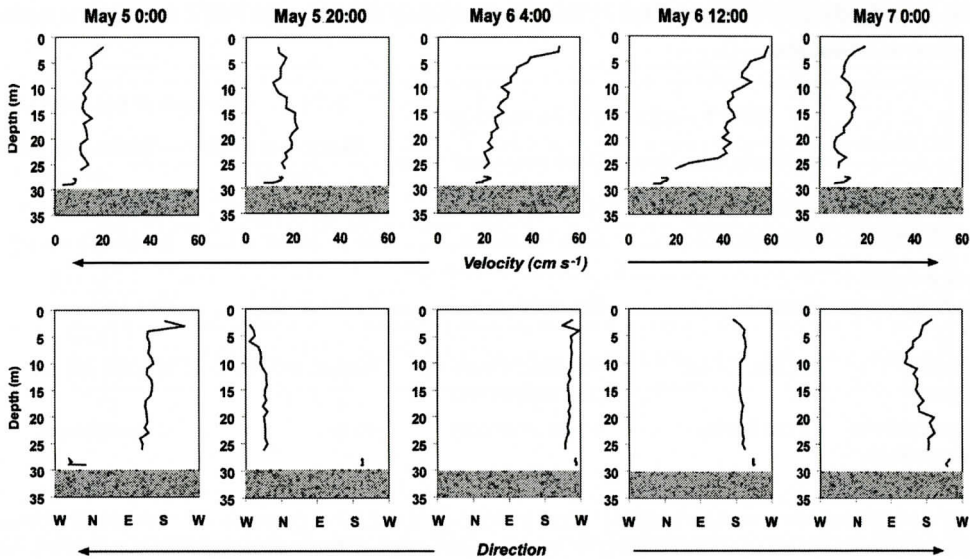


Figure 5. Current magnitude and direction profiles throughout the May 2005 Northerly wind event at Site 2. Velocities above 4 mab were measured by the ADCP and velocities within the bottom boundary layer were measured by the PC-ADP. Profiles appear to be more continuous between the upper and lower water column when the instrument frame was 1 km away from the hardbottom reef. Times denoted by arrows in Figure 4.

increased rapidly (Figure 6a,b) from less than 2 cm s^{-1} to upwards of 8 cm s^{-1} within a few hours due to the high wave energy. The acoustic backscatter signal increased to 28-40 dB and peaked early on January 7th (Fig. 6c). The model calculated shear velocities and measured ABS increased simultaneously indicating a good agreement between the BBL model and the measured sediment transport processes (Fig. 6b, c). Wind-driven currents peaked late on January 6th flowing towards the north at 8 cm s^{-1} and east at 9.5 cm s^{-1} within the BBL (Fig. 6d; Table 2). The shear velocities during this event were the highest of the four events (Table 1), however, due to the short duration of the event the transport of the large amount of suspended sediment within the BBL was limited.

The seabed response shows a gradual increase in the seabed elevation as the storm intensified on January 6th (Figure 6e). Furthermore, during the highest wave energy of the event at 0200 on January 7th, the three seabed altimetry beams show a variation in elevation of up to 6 cm, with one of the beams measuring a decrease in seabed elevation below

pre-storm conditions. The most likely explanation is that the acoustic signal was becoming saturated as wave energy was increasing on January 6th. The seabed was most likely being locally eroded as these sediments were being suspended within the BBL as evident in the high ABS values (Fig. 6c,e). The large fluctuations during peak storm conditions were a result of one of the beams detecting the seabed while the other two beam signals remained saturated. This type of beam saturation has been reported previously by Wren and Leonard (2005) when the ABS from this PCADP reached similar values, and in another recent study on the Washington coast (Sherwood et al., 2006). After the storm conditions waned, the seabed elevation indicates that there is very little ripple activity and ripple structure than the pre-storm conditions. This is another indication that the sediments were locally eroded from the bed and suspended during the event, creating a storm layer on the seafloor as shear velocities decreased rapidly on January 7th and sediments settled (Fig 6). After the event, the average seabed altimetry data also indicate that there was a

Table 2. Hydrodynamic and sediment transport response at Site 1 and Site 2 during two types of common wind events.

	SITE 1 – adjacent to hardbottom		SITE 2 – 1 km east of hardbottom	
	Northerly wind event	Southerly wind event	Northerly wind event	Southerly wind event
Max wind-driven current velocity	South 20 cm s ⁻¹ West 18 cm s ⁻¹	North 8.5 cm s ⁻¹ East 9.2 cm s ⁻¹	South: 13 cm s ⁻¹ West: 14 cm s ⁻¹	North: 13 cm s ⁻¹ East: 11.5 cm s ⁻¹
Current magnitude profile structure	Discontinuous	Discontinuous	Continuous	Continuous
Sediment response	Ripples 1-4 cm	Full suspension, ripples washed out	Ripples 2-3 cm	Ripples 1-2 cm
Net seabed elevation change	- 3 cm erosion	+1 cm accretion	none	-1 cm erosion

small positive change in the seabed elevation from pre- to post-storm conditions.

During this southerly wind event the current magnitude and direction profiles indicate that prior to the event winds were from the southwest resulting in currents of 8 - 20 cm s⁻¹ towards the north (Fig. 7). Current magnitudes were weaker within the BBL at this time, flowing towards the N-NE at 5 - 7 cm s⁻¹ (Fig. 7). Late on January 6th as winds shifted direction from southeasterly to southwesterly, the upper profile current velocities increased to approximately 25 cm s⁻¹ towards the east (Figs. 6, 7). During this time of maximum wind-driven currents within the BBL, the current magnitude profile appears to be fairly continuous between the upper water column and the BBL. The profile appears to be a logarithmic shape if the upper water column profile were extrapolated down logarithmically throughout the gap in the data (Fig. 7). Velocities within the upper water column continued to increase towards the northeast and reached a maximum on January 7th at 0300; however, currents within the BBL did not increase during this time and remained below 20 cm s⁻¹(Fig 7). The upper water column and BBL profiles were not continuous due to the slower current magnitudes within the BBL. There was a slight difference in direction between the overlying water column and the BBL at this time as well, which may be due to the frictional steering towards the left in the

BBL due to the high shear stresses. As the storm waned on January 8th, magnitude and directional profiles were more continuous throughout the entire water column (Fig. 7). Currents decreased throughout the water column and wrapped around from northward early on January 8th, to southwesterly by 1300 as winds switched to northwesterly. The overlying water column and the BBL appeared to be continuous throughout this time.

A similar southerly wind event occurred at Site 2 from January 17 - 21, 2006. Winds wrapped around to southerly at 15 m s⁻¹ on January 17th and then switched to southwesterly on January 18th and increased to over 15 cm s⁻¹. These strong southwesterly winds persisted for approximately 12 hours before backing around to the north on the 19th (Fig. 8a). Wave heights were 2.0 - 4.6 m for approximately 36 hours and dominant wave periods ranged from 5 - 10 seconds (Table 1). Shear velocities due to wave-current interactions increased late on January 17th, peaking on January 18th at over 6 cm s⁻¹ as the southerly wind speed increased (Fig. 8b). The measured acoustic backscatter signal and the model calculated shear velocities increased simultaneously and showed good agreement throughout the event. The ABS values indicate that a large amount of suspended sediment was well-mixed throughout the BBL throughout the event, and sediment continued to be sus-

HARDBOTTOM EFFECTS ON HYDRODYNAMICS AND SEDIMENT TRANSPORT

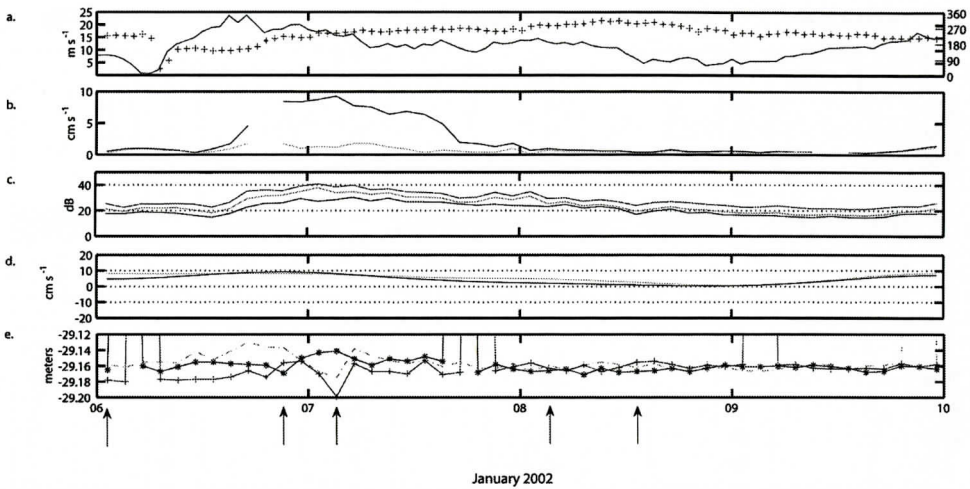


Figure 6. Data from the January 2002 Southerly wind event at Site 1. Arrows correspond to profile data during the January 2002 Southerly event shown in Figure 7. a. Wind speed and wind direction. d. Thirty-three hour low-pass filtered currents – gray line indicates b. Wave-current shear velocities (dark) and current shear velocities (light) north/south component; black line indicates east/west component. c. Acoustic Backscatter Signal at 30 cmab, 50 cmab, and 1 mab. PC-ADP seabed elevation data from all three beams.

pended up to 24 hours after shear velocities decreased on the 19th (Fig. 8). Wind-driven currents at 1 mab were directed towards the northeast at speeds of approximately 15 cm s^{-1} for approximately 24 hours during peak wind conditions on January 18th (Fig. 8d). The seabed elevation data shows less ripple activity during this event than the southerly wind event at Site 1, as fluctuations of only 1-2 cm are evident (Fig. 8e). The average seabed elevation was slightly lower after this southerly wind event occurred, in contrast to the increase in seabed elevation at Site 1 under similar conditions.

The current magnitude profiles throughout this southerly wind event at Site 2 show that magnitudes in the BBL were higher during this event than the southerly wind event at Site 1 (Fig. 9). The profile shape shown for January 18th at 1000 was typical during the building of the storm, with the highest currents at the surface and a gradual decrease in magnitude with depth (Fig 9). The profile shape became continuous throughout water column approximately 5 hours later as wind-driven currents within the BBL approached a maximum (Fig. 8d). Currents of 20 cm s^{-1} towards the NNE extended

from the surface through the BBL as shown for January 18th at 2000 (Fig. 9). As the storm waned on January 19th, the current magnitudes remained fairly continuous throughout the entire water column and the BBL. There is, however, a slight discontinuity in the profiles before and during the waning of the event that are in contrast with what occurred during the southerly wind event at Site 1, due to the fact that the discontinuities occur under very low flow conditions and not occur under high flow conditions during the peak of the storm. It appears the flows at Site 2 were being steered by the tidal flow components at this time, as the wind-driven currents were diminished in the BBL (Fig. 9).

DISCUSSION AND CONCLUSIONS

Two long-term data sets of simultaneous measurements of the bottom boundary layer (BBL) hydrodynamics, acoustic backscatter, and seabed elevation data have been used to identify similar types of sediment transport events at two study sites on the mid-shelf. A comparison of two common types of moderate wind events with similar physical forcing

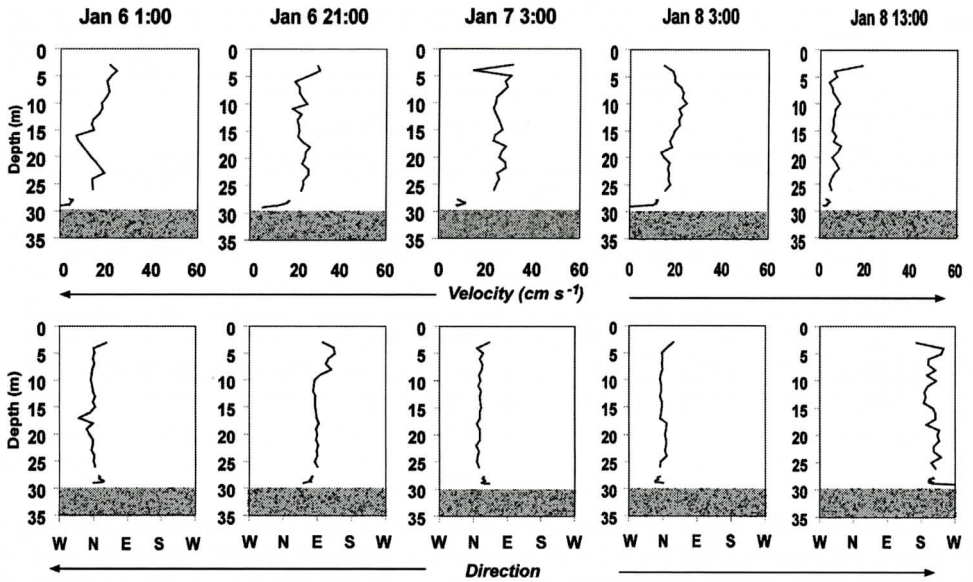


Figure 7. Current magnitude and direction profiles throughout the January 2002 Southerly wind event at Site 1. Velocities above 4 mab were measured by the ADCP and velocities within the bottom boundary layer were measured by the PC-ADP. Magnitude and direction profiles appear to be less continuous between the upper and lower water column when currents are flowing from south to north, towards the hardbottom reef. Times denoted by arrows in Figure 6.

mechanisms was conducted between Site 1, which was adjacent to a hardbottom reef, and Site 2, 1 km east of the hardbottom reef. The results of this study suggest that flows within the bottom boundary layer may be affected by the presence of the hardbottom. Flow velocities were measured throughout the water column at Sites 1 and Site 2 during two types of events with opposing current velocities. Similar current magnitudes at both sites were measured during the northerly wind events as currents were flowing from the north and northeast towards the southwest. At both sites, when currents were less than 20 cm s^{-1} throughout the water column, the current magnitude profiles appeared continuous from seabed to sea surface. During the event at Site 1 when currents were flowing from the north over the hardbottom surface, the data indicate that there was more potential for the current magnitudes throughout the entire water column to be continuous if the wind-driven currents within the BBL were fully developed. However, when currents throughout the overlying water column exceeded 30 cm s^{-1} , flows within the BBL were

slower and did not exceed 20 cm s^{-1} , resulting in a non-continuous profile shape.

Current profiles during the two southerly wind events suggest that the currents are less impeded at Site 2, away from the hardbottom reef, as continuity throughout the water column was observed throughout the event. It appears that the flows are still being impeded within the BBL at Site 1 adjacent to the hardbottom, even when currents are from the south flowing over the sands flats towards the reef area.

This study was of an exploratory nature and the conclusions are preliminary. Only one type of event was examined at each site and more work is needed to fully understand the effects that the hardbottom reef may have on the hydrodynamics and sediment transport processes around the reef. However, these in-situ data provide evidence that the current velocities around hardbottom reefs may be affected by the hardbottom geometry. Measured current profiles show that hydrodynamic and sediment transport studies focused around hardbottom reefs will require in-situ measurements within the BBL. If currents are measured at a higher el-

HARDBOTTOM EFFECTS ON HYDRODYNAMICS AND SEDIMENT TRANSPORT

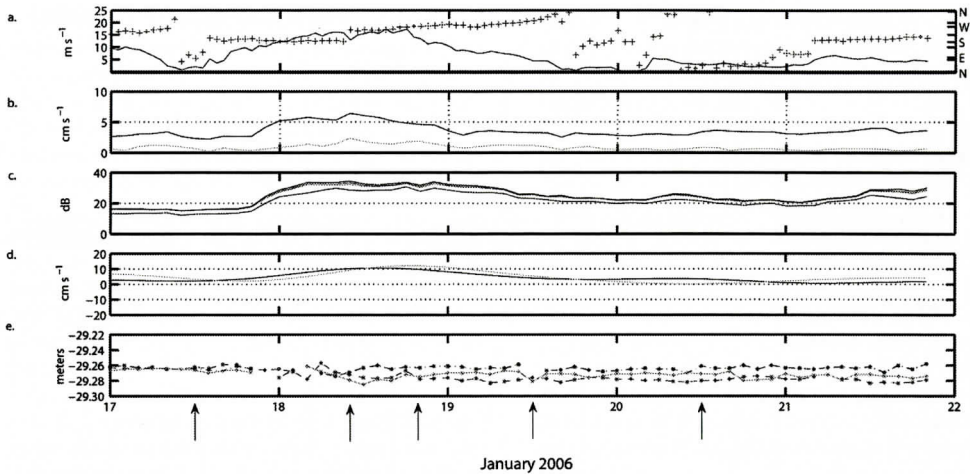


Figure 8. Data from the January 2006 Southerly wind event at site 2. Arrows correspond to profile data during the January 2006 Southerly event shown in Figure 9. a. Wind speed and wind direction. d. Thirty-three hour low-pass filtered currents – gray line indicates. b. Wave-current shear velocities (dark) and current shear velocities (light) north/south component; black line indicates east/west component. c. Acoustic Backscatter Signal at 30 cmab, 50 cmab, and 1 mab. PC-ADP seabed elevation data from all three beams.

evaluation within the water column and extrapolated logarithmically to the seabed, current velocities and suspended sediment transport within the BBL may be overestimated.

Additionally, the results from this study show that the seabed at the site adjacent to the hardbottom (Site 1) was more active during the sediment transport events than the site away from the hardbottom (Site 2). The seabed close to the hardbottom reef was reworked approximately 2-3 cm during the northerly wind event in September 2000, while up to 4 cm of reworking occurred during in the southerly event in January 2002. During both the northerly and southerly wind events at Site 2, the seabed elevation data indicated less ripple activity throughout the events and very little change in the average seabed elevation from pre- to post-storm. The implications of more reworking of the sediment close to the hardbottom may be connected with areas termed “infaunal halos” that have been observed within the fine sand aprons around the hardbottom reef ledges in Onslow Bay (Dahlgren et al., 1999). These “infaunal halos” have greatly reduced densities of infaunal species and have been documented to occur within the fine sand aprons extending out

to 25 m from the reef ledge. It has been hypothesized that the physical processes around these hardbottom areas may play a role in the infaunal distribution around these hardbottom ledges (Dahlgren et al., 1999). The results shown here indicate that the fine sands adjacent to the hardbottom are being re-worked more frequently, which could be a contributing factor to the lower densities of infauna found around the reef ledges.

Additionally, the general results of this study show that sediment transport does occur frequently on the mid-shelf during common frontal passages that affect the study area throughout most of the year. The two types of sediment transport events discussed here are examples of the events that occur commonly within this region and have been used as an example to demonstrate the potential for sediment transport. Although previous studies on the inner-shelf of the South Atlantic Bight have demonstrated the potential for sediment transport during commonly occurring frontal passages (Davis et al., 2008; Sullivan et al., 2006), to the authors’ knowledge, there have been no studies that have reported in-situ measurements of sediment transport during frontal passages on the

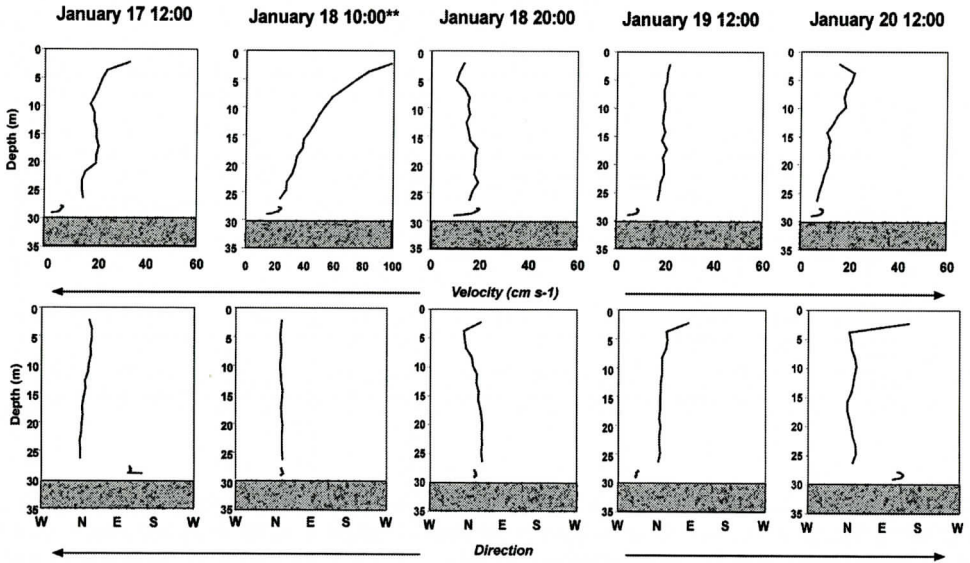


Figure 9. Current magnitude and direction profiles throughout the January 2006 southerly wind event at Site 2. Velocities above 4 mab were measured by the ADCP and velocities within the bottom boundary layer were measured by the PC-ADP. Profiles appear to be more continuous between the upper and lower water column when the instrument frame was 1 km away from the hardbottom reef. Times denoted by arrows in Figure 8. ** Note change in scale.

mid-shelf. These data indicate that the mid-shelf of Onslow Bay is an active region for sediment transport which may have important biological and ecological implications. The mid-shelf region of Onslow Bay forms the framework for the highly productive “livebottom communities” that are important to commercial and recreational fisheries and thus are of major economic importance (Riggs et. al, 1998). Renaud et al., 1997 indicated that the observed changes in distribution and thickness of the fine sand bodies during storms altered the population, distribution, and type of benthic infauna and flora on the hardbottom and have profound effects on the entire ecological communities that these mid-shelf hardbottoms in Onslow Bay support. It has been shown here that the shear stresses occurring on and around the mid-shelf hardbottom areas frequently exceed the critical shear stress for fine sands. The preliminary data shown here indicate that these mid-shelf reefs may be frequently disturbed, and the temporal scale for covering and uncovering these ecological communities may be as short as days to weeks. More work is needed to deter-

mine the frequency, magnitude, and duration of sediment transport around these hardbottom reef communities; however, defining the sediment transport processes that cover and uncover these hard bottom habitats on the mid-shelf is vital to understanding the effects that these mobile sand bodies have on proximal living reef habitats.

ACKNOWLEDGEMENTS

We would like to thank the CORMP technicians Jay Souza, Dave Wells, and Steve Hall, who were essential in diving operations and general data collection. Further thanks go to the Captains and crew of the *R/V Cape Fear* and *R/V Seahawk*. This research was primarily funded by the National Oceanic and Atmospheric Administration, Award #NA16RP2675 to the Coastal Ocean Research and Monitoring Program at the University of North Carolina at Wilmington.

REFERENCES

Battisto, G.M., 2000. Field measurement of mixed grain size

HARDBOTTOM EFFECTS ON HYDRODYNAMICS AND SEDIMENT TRANSPORT

- suspension in the nearshore under waves. M.S. Thesis, Virginia Institute of Marine Science, Gloucester Point, VA, unpublished.
- Blackwelder, B.W., Macintyre, I.G., Pilkey, O.H., 1982. Geology of the continental shelf, Onslow Bay. North Carolina, as revealed by submarine outcrops. American Association of Petroleum Geologists Bulletin, 66, 44-56.
- Cleary, W. J., Pilkey, O. H., 1968. Sedimentation in Onslow Bay: guidebook for field excursions. Southeastern Geologists Special Publications 1, 1-17.
- Dahlgren, C.P., M.H. Posey, and A.W. Hulbert, The effects of bioturbation on the infaunal community adjacent to an offshore hardbottom reef, Bulletin of Marine Science, 64(1): 21-34, 1999.
- Davis, L. A., Leonard, L. A., Snedden, G. A., 2008. Hydrography and bottom boundary layer hydrodynamics: influence on inner-shelf sediment mobility, Long Bay, North Carolina. Southeastern Geology, vol. 43 (this volume).
- Deines, K.L., 1999. Backscatter estimation using broadband acoustic doppler current profilers. Oceans '99 MTS/IEEE Conference Proceedings, 13-16.
- Dikou, A., R. van Woesik. 2006. Survival under chronic stress from sediment load: spatial patterns of hard coral communities in the southern islands of Singapore. Marine Pollution Bulletin 52:7-21.
- Fabricius, K.E. 2005. Effects of terrestrial runoff on the ecology of corals and coral reefs: review and synthesis. Marine Pollution Bulletin 50:125-146.
- Golbuu, Y., S. Victor, E Wolanski, RH Richmond. 2003. Trapping of fine sediment in a semi-enclosed bay, Palau, Micronesia. Estuarine, Coastal and Shelf Science 57:941-949.
- Grimes, C.B., C.S. Mannoeh, G.R. Huntsman. 1982. Reef and outcropping fishes of the outer continental shelf of North Carolina and South Carolina, and ecological notes on the red porgy and vermillion snapper. Bulletin of Marine Science 32:277-289.
- Gutierrez, B.T., Voulgaris, G., Thieler, E.R., 2005. Exploring the persistence of sorted bedforms on the inner-shelf of Wrightsville Beach, North Carolina. Continental Shelf Research, 25: 65-90.
- Harris, C. K., Butman, B., Traykovski, P. 2003. Winter-time circulation and sediment transport in the Hudson Shelf Valley. Continental Shelf Research 23 (2003) 801-820.
- Hunt, W., M. Wittenberg. 1992. Effects of eutrophication and sedimentation on juvenile corals: II. Settlement. Marine Biology 114:625-631.
- Madsen, O.S., Wright, L.D., Boon, J.D., Chisholm, T.A., 1993. Wind stress, bed roughness and sediment suspension on the inner shelf during an extreme storm event. Continental Shelf Research 13, 1303-1324.
- Madsen, O.S. 1995. Spectral wave-current bottom boundary layer flows, Proc. 24th ICCE. ASCE, 1:384-398
- Marshall, J.A., 2004. Event driven sediment mobility on the inner continental shelf of Onslow Bay, NC. M.S. Thesis, University of North Carolina at Wilmington.
- Miller, D.C., C.L. Muir, O.A. Hauser. 2002. Detrimental effects of sedimentation on marine benthos: what can be learned from natural processes and rates? Ecological Engineering 19:211-232.
- Milliman, J.D., 1972. Atlantic continental shelf and slope of the United States; petrology of the sand fraction of sediments, northern New Jersey to southern Florida. Geological Survey professional paper 529-J.
- Ogston, A.S., Sternberg, R.W., 1999. Sediment-transport events on the northern California continental shelf. Marine Geology 154, 69-82.
- Ojeda, G.Y., Gayes, P.T., Sapp, A.L., 2001. Habitat mapping and sea bottom change detection on the shoreface and inner shelf adjacent to the Grand Strand Beach Nourishment Project, Final report prepared for the U.S. Army Corps of Engineers, Charleston District, Center for Marine and Wetland Studies, Coastal Carolina University, 95 pp.
- Ojeda, German Y., Paul T. Gayes, Robert F. Van Dolah, William C. Schwab, 2004. Spatially quantitative seafloor habitat mapping: example from the northern South Carolina inner continental shelf. Estuarine, Coastal, and Shelf Science, 59, 399-416.
- Pietrafesa, L.J., Janowitz, G.S., Wittman, P.A., 1985. Physical oceanographic processes in the Carolina Capes, In: Oceanography of the Southeastern U.S. Continental Shelf, 23-32.
- Renaud, P.E., Ambrose Jr., W.G., Riggs, S.R., Syster, D.A., 1996. Multi-level effects of severe storms on an offshore temperate reef system: benthic sediments, macroalgae and implications for fisheries. Marine Ecology 17, 383-389.
- Renaud, P.E., Riggs, S.R., Ambrose Jr., W.G., Schmid, K., Snyder, S.W., 1997. Biological-geological interactions: storm effects on macroalgal communities mediated by sediment characteristics and distribution. Continental Shelf Research 17 (1), 37-56.
- Riggs, S.R., Ambrose, W.G., Jr., Cook, J.W., and Snyder, S.W., 1998. Sediment Production on Sediment-starved Continental Margins: The Interrelationship between Hardbottoms, Sedimentological and Benthic Community Processes, and Storm Dynamics. Journal of Sedimentary Research Section A: Sedimentary Petrology and Processes 68(1), 135-148.
- Sedberry, G.R., R.F. Van Dolah 1984. Demersal fish assemblages associated with hardbottom habitat in the South Atlantic Bight of the USA. Envir. Biol. Fish. 4:241-258.
- Sherwood, C.R, Lacy, J. R., an Voulgaris, G., 2006. Shear velocity estimates on the inner shelf off Grays Harbor, Washington, USA. Continental Shelf Research 26 1995-2018.
- Styles, R. and Glenn, S.M., 2005. Long-term sediment mobilization at a sandy inner shelf site, LEO-15. Journal of Geophysical Research, 110, 1-20.
- Styles, R. and Glenn, S.M., 2002. Modeling bottom roughness in the presence of wave-generated ripples. Journal of Geophysical Research, 107, 1-15.
- Styles, R. and Glenn, S.M., 2000. Modeling stratified wave

- and current bottom boundary layers on the continental shelf. *Journal of Geophysical Research*, 105, 24,119 - 24,139.
- Sullivan, C.M., Warner, J.C., Voulgaris, G., 2006. Influence of storms on circulation and sediment transport in Long Bay, South Carolina. 2006 Ocean Sciences Meeting, Honolulu, HI.
- Traykovski, P., A. Hay, J.D. Irish, and J.F. Lynch, 1999. Geometry, migration, and evolution of wave orbital ripples at LEO-15. *Journal of Geophysical Research*, 104, 1505-1524.
- Wenner, E.L., D.M. Knott, R.F. Van Dolah, V.G. Burrell Jr. 1983. Invertebrate communities associated with hard bottom habitats in the South Atlantic Bight. *Estuarine, Coastal and Shelf Science* 17:143-158.
- Williams, J.J., Rose, C.P., 2001. Measured and predicted rates of sediment transport in storm conditions. *Marine Geology* 179, 121-133.
- Wren, P. A. and L. A. Leonard, 2005. Sediment transport on the mid-continental shelf in Onslow Bay, North Carolina during Hurricane Isabel. *Estuarine, Coastal, and Shelf Science*, 63, 43-59.
- Wright, L.D., Xu, J.P., and Madsen, O.S., 1994. Across-shelf benthic transports on the inner-shelf of the Middle Atlantic Bight During the Halloween storm of 1991. *Marine Geology*, 118 (1-2): 61-77.
- Xie, L., Pietrafesa, L.J., Raman, S., 1997. Interaction between Surface Wind and Ocean Circulation in the Carolina Capes in a Coupled Low-order Model. *Continental Shelf Research* 17, 1483-1511.

SHALLOW MARINE MARGIN SEDIMENTS, MODERN MARINE EROSION AND THE FATE OF SEQUENCE BOUNDARIES, GEORGIA BIGHT (USA)

¹ERVAN G. GARRISON, ²GREG MCFALL AND ¹SCOTT E. NOAKES

¹*Department of Geology, The University of Georgia, Athens, GA 30602.* ²*National Oceanic and Atmospheric Administration (NOAA), Grays Reef National Marine Sanctuary, 10 Ocean Science Circle, Savannah, GA 31411.*

ABSTRACT

Our studies of shallow shelf lithofacies have yielded a clearer understanding of the relationship of lithification, sequence and relative sea level (RSL) just prior - and post - Last Glacial Maximum (LGM) for the Georgia Bight. Data from vibracores and hand samples have been taken from two offshore sites - Gray's Reef National Marine Sanctuary and J-Reef. Both sites are shallow (-20 mbsl) outcrops of Pliocene - Pleistocene age. Direct age determination using AMS-radiocarbon; Uranium Series and Optical Stimulated Luminescence (OSL) methods confirm this. Using analyses of sediments and inclusions, together with the geological mapping of outcrops/exposures, we have identified at least two new provisional members of the late Pleistocene marine sequence. Our results indicate a subaerial exposure from MIS 3 through late MIS 2 with the subsequent, post-LGM transgression. Our study indicates that survival of sedimentologically observed markers for both relative sea level and at least one sequence boundary. Shell beds, observed at both reefs, are discussed as proxies for sea level and stratigraphy. Modern sediment supply has been reduced by anthropogenic activities and erosion now dominates the shallow, low accommodation space, marine margins of the inner-to-mid shelf of the Georgia Bight.

INTRODUCTION

Ten glacio-eustatic events have been identified (Foyle et al. 2004:73). The record of these 10 events, paleoshorelines, submerged or stranded barriers, is extremely incomplete on

the shelf of the Georgia Bight (ibid, 73). These glacio-eustatic events are preserved on the North Carolina shelf in paleochannels (ibid; Duane et al. 1972) as well as further north on the New Jersey shelf as submerged ridges and scour features (Goff et al. 2005). Recent studies (Stubbs et al, 2007) off South Carolina have identified a relic meandering river channel on the inner-mid shelf. Glacio-eustatic events are embedded within stratigraphic sequences of shelf sedimentary lithology that occur on the inner-to-mid shelf. Further, it is observed that these shallow (< 20 m mean sea level or -20 msl) shelf sediments are undergoing modern erosion from both geostrophic and seasonal storm-related bottom currents. Coupled with erosion processes associated with cyclical changes in relative sea level (RSL) in the Pleistocene, the net result of this Quaternary erosion, coupled with lower modern sediment budgets, is the less than 20 m sedimentary section observed in the Georgia Bight. These sediments consist of fine-to-coarse grained sandstones that range from cemented or weakly-cemented rock strata (Gray's Reef and J-Reef) to a non-consolidated sediment prism observed across the inner-to-mid shelf.

In this study we characterize, lithologically and chronologically, as well as map, Quaternary sediments at two locations in the Georgia Bight: Gray's Reef, a National Marine Sanctuary and J-Reef a low exposure of shell beds about 16 km north of the Gray's Reef (fig. 1). By so doing, we develop a geologically-based scenario for RSL and examine its implication for the preservation of sediment sequences on a shallow marine shelf such as the Georgia Bight. Foyle, et al (2004), in noting the incomplete nature of the sequence record, on the Georgia shelf, indirectly allude to a larger issue in the

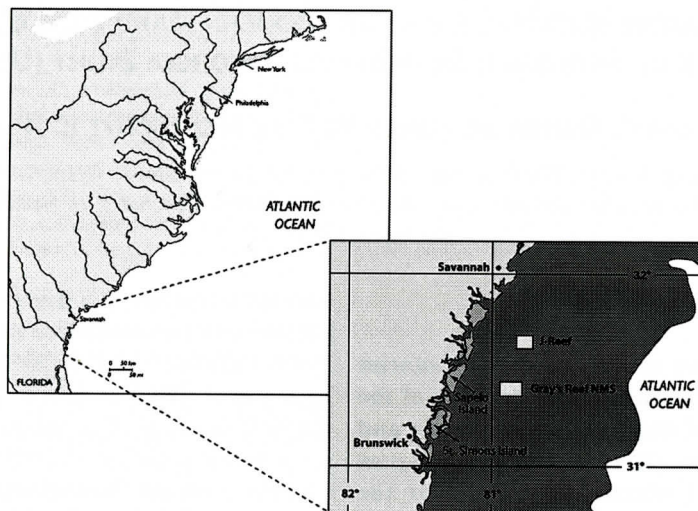


Figure 1. The Georgia Bight highlighting the study area of Gray's Reef National Marine Sanctuary and J-Reef.

nature of sediment sequences along shallow marine margins – how, if at all, may we reconstruct these sequences or, at least, how may we use their fragmentary nature to discuss sea level (and climate) cyclicity?

One helpful aspect of the stratigraphic record discovered at both Gray's and J-Reef, that allows us to speculate on changes in sea level and basin edge environments, is the well-preserved shell beds in both these locations. These unique sediments contain both paleobiological and lithological proxies for sea level and climate in the form of the taphocenose and its burial matrix of coastal sediments. First observed in 2002, the shell beds opened up a productive line of inquiry into both paleobiology and depositional environments - sedimentological and climatological - that constrained that biology. Numerous authors (Kidwell, 1986, 1988; Meldahl and Cutler, 1992; Kidwell, et al, 1993; del Rio, et al, 2001, Brett, 1998; Holland, 1993; 1995), have emphasized the importance as clues to sea level change. In this study we shall use these deposits to discuss sea level change and its preservation - or lack of preservation - in shallow marine sediments of the inner-to-mid shelf of the Georgia Bight.

STUDY LOCATION AND CENOZOIC GEOLOGIC SETTING

The Coastal Plain province offshore of Georgia, USA (Milliman et al. 1972) (fig. 1) is characterized by a gradual regional dip (0.4 - 1.0 m / km) and is composed of Jurassic, Cretaceous, Tertiary and Quaternary sediments that thicken seaward (ibid). Although relatively uniform in a geomorphic sense, a flattish coastal plain, this continental shelf is marked by various topographic features such as outcrops/live bottoms like Gray's Reef and J-reef, canyons (north of Cape Hatteras), and shoal complexes (Sexton et al. 1992) as well as drowned coastal stream valleys. The former subaerial, or emerged component of this Coastal Plain decreases from 300 km in northern Florida to less than 50 km in northern New Jersey, while in the Quaternary its emergent width increased by 100 km in the south and by over 50 km in the north (cf. Kraft 1977; Miller 1998:43). The inner shelf of the study area can be described as an accommodation dominated shelf with a significant amount of thin, transgressive lag deposits (Johnson and Baldwin 1996:238). The inner shelf can be characterized as a passive continental margin with little or no tectonism or eustasy. The dom-

inant water mass (and current) in the Georgia Bight is the Gulf Stream. The west wall of the Gulf Stream is typically 15-20 or more km seaward of Gray's Reef.

Antoine and Henry (1965) described Quaternary sediments of the Outer Continental Shelf of the Southeastern U.S. as a thin veneer overlying Tertiary bedrock. The Georgia Bight stratigraphic sequence compresses 2 million years of Quaternary basin-margin evolution into deposits no more than 20 m thick across its breadth (Woolsey and Henry 1974; Woolsey 1977; Harding and Henry 1994). This is a reasonable characterization of the Outer Shelf as well. Seaward of the modern shoreline, Cretaceous-Cenozoic age rocks underlie the Continental Shelf and Slope (Buffler et al. 1978). Adesida (2000) reviews this stratigraphic framework for the Eocene through Miocene sequences in her shallow seismic reflection study of Sapelo Island, Georgia.

METHODS

Sediment Coring

A total of nine vibracores, five taken in 1996 and four in 2000, utilizing the NOAA ship *Ferrel* for both collection cruises, these cores were collected in two locales along or near the -20m isobath, Gray's Reef and J-Reef (Table 1). Sediment cores taken in 1996 were retrieved using a 3 inch (7.6 cm) diameter core barrel pneumatic and the 2000 cruise used a 3 inch diameter core barrel hydraulic vibracorer. Data sediment cores were analyzed first lithologically and geochemically (Littman 2000), and then for pollen (Weaver 2002) in their respective theses.

In both 1996 and 2000, all vibracores were split into working and archival halves. Hand cores were extruded into core trays. The 1996 and 2000 sediment cores were logged and photographed along their length. Sediment samples were taken at natural stratigraphic breaks, 5 cm on either side of any obvious contact. Cores were sampled for shells and botanical (wood) remains suitable for radiometric dating. In contrast to 1996, due in part to a focus on her palynological study reported on elsewhere

(Weaver 2002), two 2000 cores, #3 and #5, were sampled at 10 cm intervals along their length. In both cores, every other sample from top-to-bottom was eliminated, yielding a total of 17 sediment samples of 15 cc each (eight from core #3, nine from core #5). Cores #1 and #2 from 2000 were left unopened. Core #4 was sampled exclusively for chronostratigraphy purposes.

In addition to the vibracores, sediments were retrieved by use of diver-deployed, hand-and-hydraulic corers with 1 inch (2.54 cm) to 2 inch (5.08 cm) diameter barrels. These devices, plus simple hand excavation, were utilized in areas too close to the outcrops for the use of the larger, vessel deployed coring systems. Along with use of diver-deployed corers, surface surveys and limited excavations examined the sediment near the reef fronts.

Geochronology

Chronology of the cores are based on conventional/accelerator mass spectrometry (AMS) radio-carbon dates (16); optical stimulated luminescence (OSL) dates (3); and one uranium-thorium (U/Th) age. The AMS ages were determined from a variety of material found in the cores or in excavation - bone, shell, carbonate and wood.

The OSL dating was carried out under controlled red-light conditions in the laboratory. Samples were treated with 10% HCl and 30% H₂O₂ to remove carbonates and organic material, and sieved to obtain the 120-150µm size fraction which was dated. The SAR protocol (Murray and Wintle 2000) was used to determine the paleodose. Data were analyzed using Duller's (1999) ANALYST program.

The U/Th age was determined by gamma counting the reef sediment with inductively coupled plasma - mass spectrometry (ICP-MS). Uranium activity/amount was determined using the isotope Pa-234m while thorium was estimated using the isotopes Bi-214 and Pb-214.

Paleobiology

Beginning in 2002, our attention turned to

Table 1. 1996 and 2000 vibracore locations at Gray's Reef and J-Reef.

Site Date	Date	Latitude (N)	Longitude (W)	Water Depth (m)	Core length (m)
J-Reef	1966	31° 35.89'	80° 47.93'	19.2	1.98
J-Reef	1966	31° 35.89'	80° 47.93'	19.2	2.74
Gray's Reef	1966	31° 24.62'	80° 051.2'	19.5	3.66
J-Reef	1966	31° 35.56'	80° 47.03'	21.	<2
J-Reef	1966	31° 35.9'	80° 47.75'	20.4	4.57
Gray's Reef Station 16	1966	31° 23.833'	80° 53.473'	18	Rock, no core
GR1a (4)	2000	31° 24.616'	80° 47.100'	17.6	-2.4
GR-NE (3)	2000	31° 24.7'	80° 50.8'	19.5	2.15
GR2a	2000	31° 24.62'	80° 51.2'	19.4	Rock, no core
GR-NW:	2000	31° 24.381'	80° 54.267'	16	<1
GR-SW: (3)	2000	31° 22.30'	80° 55.00'	17.3	1.58

the invertebrate paleontology of, first, Gray's Reef and later in 2005, J-Reef. At Gray's Reef, there are two stations, 16 and 20, which have the focus of our investigations. Station 16 had the largest number of vertebrate fossil finds. Station 20 was first identified for study because of the discovery of a thick (>1 m) sea scallop stratum or shell bed adjacent to the Gray's Reef outcrops. We later identified the shell beds at station 16 and at J-Reef, at a location called Research Ledge, as Pleistocene-aged shell beds.

RESULTS

Inner-to-Mid Shelf Sediments of the Georgia Bight

Paleobiology

Any paleoenvironmental interpretation of the recovered sediments, would include the lithology and morphology of grains – sands to muds; inclusions such as shell, vertebrate and botanical inclusions, separating them, chronologically, into Pleistocene and Holocene facies. We identify the bulk of sediments observed, in this study, as Pleistocene aged with

very little evidence of Holocene aged facies. We have detected fluvial and estuarine facies in paleochannels and, as expected, fewer shell species, with less diversity within the assemblages (Kidwell *et al.*, 2005).

The mollusk assemblage, found in the various sediments, is representative of several depositional environments. In the unconsolidated sediments, at both Gray's Reef and J-Reef, together with cores of the more consolidated facies, we have identified the following species: *Mellita* (Sand Dollar); *Crassostrea virginica* (Eastern Oyster); *Olivella floralia* (Common Rice Olive); *Luncina nassula* (Woven Lucina); *Plicatula gibbosa* (Kitten's Paw); *Linga sombrosi* (Sombrero Lucina) and *Macona tenata* a tellina-like species). Also present were *Mercenaria mercenaria* (Surf clam); *Mulina lateralis* (Dwarf surf clam) and *Astarte nana* (Dwarf Astarte). In the shell beds, the dominant species is *Placopecten magellanicus* (Sea Scallop). Within these various species, together with the lithofacies, we can more readily identify a near-shore and open marine depositional environment with some back barrier species. Because the shell assemblage is mixed, both in uncon-

SHALLOW MARINE MARGIN SEDIMENTS

Table 2. Georgia Bight Sediments – Gray’s Reef and J-Reef Localities

Facies	Shelly Sand	Brown Sand	Gray Mud	Gray Mud Laminated	Cemented Shelly-Sand	“Reef rock” (Raysor)
Location	Gray’s Reef J-Reef	Gray’s Reef J-Reef	J-Reef	J-Reef	Gray’s Reef J-Reef	Gray’s Reef
Lithology	M-C-S ₁ Sand Shell Frag- ments	M-F-S ₂ No shells	C-R-S-S ₃	S-S ₄ M-F-S ₂	M-C-S ₁ Shell	C-sandstone ₅ D-Sandstone ₆ S-Biomicrite ₇
Structures	None	Blocky peds	None	Laminations	Weakly Cemented	Cemented
Color (Mun- sell, wet)	2.5Y6/1- 2.5Y7/1 10Y5/1-6/1	5Y3/2- 2.5Y 5/3 (dry)	5GY5/4-4/1	5GY5/5-4/1	5Y6/1-2.5Y7/1	5Y6/1
Sand (wt.%)	94-98	90	10-12	10-12	94-98	80-98
Clay (wt.%)	0-2	2-4	10-14	10-14	0	<1
CO ₃ (wt.%)	0-11	<1	<1	<1	11-13	<20
Heavy Min- erals (%)	11	<1	<1	<1	<1	<1
Magnetic Susceptibil- ity (SI units)	0.73-6.43 x 10 ⁻⁵	-----	-----	-----	0.6-0.7 x 10 ⁻⁵	-----
₁ Medium-Coarse Sand; ₂ Medium-Fine Sand; ₃ Clay-Rich-Silty Sand; ₄ Silty-Sand; ₅ Calcareous Sandstone; ₆ Dolomitic Sandstone; ₇ Sandy Biomicrite						

solidated and consolidated facies, the most obvious conclusion is that this is the result of erosional and diagenetic processes. Erosion is indicated by abrasion, fragmentation, color and luster loss, as well as shell edge damage. Diagenesis is inferred from shell thinning (although erosion can produce the same result), color and luster loss. Shell thinning, and concomitant loss of shell architecture, is common where shell dissolution, through chemical diagenesis, is prevalent.

Lithostratigraphy

Sediments recovered from the analyzed sediment cores were divided into two principal sediment facies: those associated with the well-described Pleistocene-aged Satilla Formation, and that of the Raysor (Duplin) Formation dated to the Pliocene (Huddleston 1988; Harding and Henry 1994). The Satilla and Raysor For-

mations are two members of a suite of nineteen unconformably bound Oligocene and Miocene, three Pliocene, and two Pleistocene stratigraphic units (Weems and Edwards 2001:7-15) (Fig. 2). Of the two formations, we have been able to directly date the Satilla Formation to the late Pleistocene (Table 3). In both locations the upper Satilla Formation sediments are capped by the exposed shell beds of significant thicknesses (> 3 m or more). Based on the results from vibracores; hand cores and samples, we can define, within the Satilla Formation, the following provisional members: (a) a Brown Sand Member, (b) a Cemented Shelly Sand Member and (c) a unconsolidated Shelly Sand. Taking the Raysor and Satilla Formation, together, we describe the following lithostratigraphy for the Gray’s Reef area of the Georgia Bight:

1. Unconsolidated shelly sand - Holocene
2. Brown sand – Pleistocene

ERVAN G. GARRISON, GREG MCFALL AND SCOTT E. NOAKES

Table 3. Chronology of Sediments at Gray's Reef and J-Reef^a

Method	Sediment	Material	Location	Laboratory	Age ¹⁴ C Yr BP ^b	Age cal yr BP ^c	Age OSL / U/Th Yr BP
AMS	Reworked Shelly Sand	Bone	Surface ^d	Beta-103683	6090+/-60	7160-6790	
AMS	Reworked Shelly Sand	Shell	Surfacet ^d	UGA-11688	8950+/-70		
AMS	Reworked Shelly Sand	Carbonate	Surface, (<i>Ophiomorpha</i>) ^d	Beta-92356	18970+/-140	22479-20571	
OSL	Shelly Sand	Quartz Sand	Core 4, -30/cm ^d				24023+/-4954
AMS	Shelly Sand	Shell	Core 4, -30/cm ^d	Beta-172381	29120+/-690		
AMS	Shelly Sand	Shell	Core 4, -170/cm ^d	Beta-172380	24640+/-460		
OSL	Shelly Sand	Quartz Sand	Core 4, -170/cm ^d				23702+/-5411
AMS	Shelly Sand	Shell	Core 1, -170/cm ^d	UGA-11689	43770+/-470		
OSL	Brown Sand	Quartz Sand	Core 1, -220/cm ^d				39265+/-5692
U/TH	Brown Sand	Sediment	Core 1, -220/cm ^d				37481+/-1372
AMS	Reworked Shelly Sand	Shell	Ledge, -15/cm ^d	UGA-11690	45170+/-1530		
AMS	Gray Mud	Wood (<i>Taxodium</i> ?)	Core 1, -220/cm ^e	Beta-103780	>50290		
AMS	Gray Mud	Wood	Core 4, -220/cm ^e	Beta-105507	>48020		
AMS	Brown Sand	Oyster Shell	Ledge, ~10 cm ^e	UGA-00887	31082+/-180		
AMS	Brown Sand	Scallop Shell	Ledge, ~10 cm ^e	UGA-00888	35055+/-248		
AMS	Cemented Shelly Sand	Wood	Ledge, ~10 cm ^e	UGA-01045	35767+/-264		
AMS	Cemented Shelly Sand	Wood	Ledge, ~10 cm ^e	UGA-01046	39316+/-316		
AMS	Cemented Shelly Sand	Scallop Shell	Ledge, ~10 cm ^e	UGA-00889	42146+/-396		
AMS	Reworked Shelly Sand	Wood (<i>Licaria</i> sp.)	Ledge, ~10 cm ^e	UGA-00782	41326+/-455		
AMS	Reworked Shelly Sand	Wood (<i>Juniper</i> sp.)	Ledge, ~10 cm ^e	UGA-00890	40488+/-350		

SHALLOW MARINE MARGIN SEDIMENTS

3. Cemented shelly sand - Pleistocene
4. Dolomitic sandstone - Pliocene

Two facies B a "Brown Sand" (Unit 2) and a "Cemented Shelly Sand" - (unit 3) have been identified by this study as provisional/informal members of the Satilla Formation, while the Gray's Reef outcrops of dolomitic sandstone (unit 4) were identified as Raysor Formation. As one of the two lithified facies, it is the oldest such material in the study area. It is well studied and described by Harding and Henry (1994); Henry and Van Sant (1982); Hunt (1974); and Littman (2000). At Gray's Reef, it forms a northeast - southwest trending (strike) set of low ridges (1-2 m) and overhangs along the - 20 m isobath. The shell beds occur within the cemented sand facies. This sediment was not directly described in Harding and Henry's evaluation of the geology of Gray's Reef (1994). Neither its unique lithology, paleontology nor stratigraphic position was appreciated in this study until 2004. Hand operated coring methods - hand-driven and hydraulic - together with collection of hand samples at outcrops and exposures - were used to examine this facies. Attempts to penetrate these strata were general-

ly unsuccessful using vibracorers in both 1996 and 2000. It is believed, because of its similar lithology to that of the unconsolidated shelf sediments, to be the parent material of the latter (Table 2). At Gray's Reef, the older Pliocene-aged Raysor Formation outcrops were exhumed from these cemented sand and shell beds. At J-Reef, the outcrops are formed entirely from this younger Satilla facies and the older Raysor lithology is not seen. Two-plus meter exposures of the concreted shell beds, at nearby artificial reefs, have been observed to have been created by storm surge and erosion, without exhumation of the Raysor Formation.

The discovery of large numbers (> 100 shells/m²) of fossil *Placopecten magellanicus* (scallops) in imbricated shell beds at J-Reef and at Gray's Reef led to the direct dating of this sediment using those shell. The scallops, observed as an assemblage in the cemented matrix, are identified at both Gray's Reef and J-Reef in the consolidated beds at the former location and in outcrops at the latter. Mapping of this stratum across Gray's Reef leads to the conclusion that the Pliocene reef facies has been exhumed from the cemented scallop-rich shell

Table 3. Notes

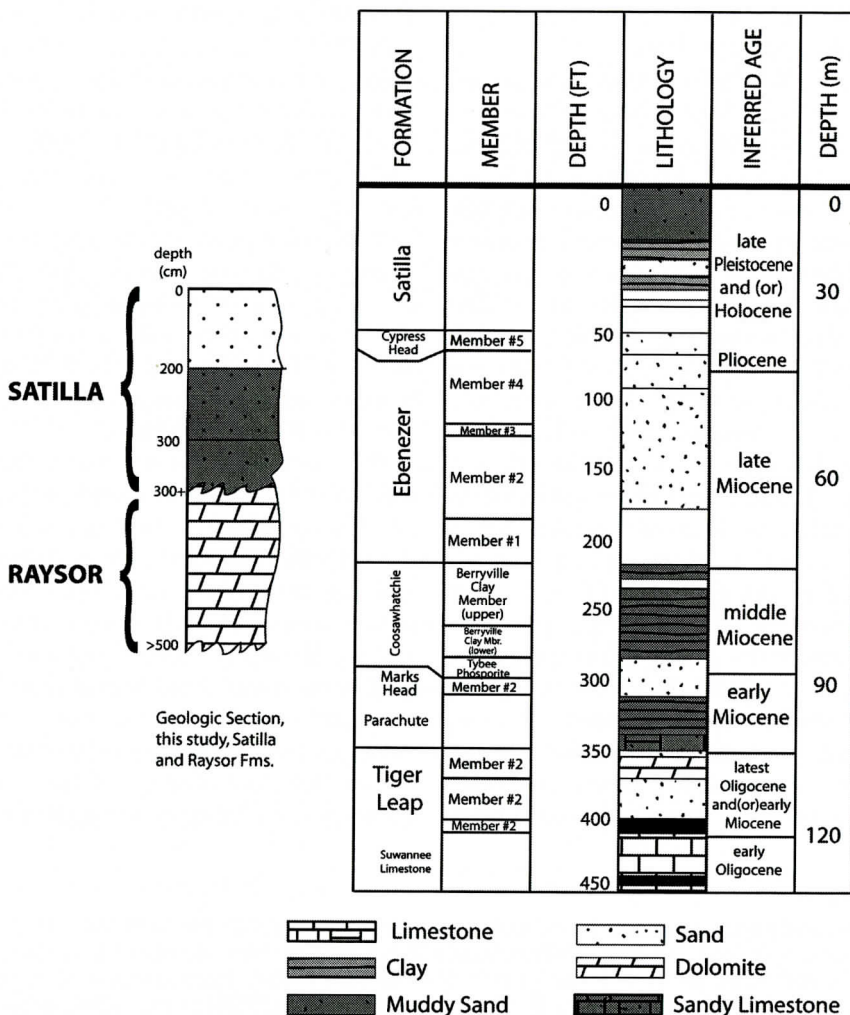
^aThe chronostratigraphic zones correspond to lithostratigraphic levels: 6 000 YBP to 18 000 YBP, reworked surface sediment, Shelly-Sand; 23 000 YBP to 28 000 YBP, Cemented Shelly-Sand and Gray laminated mud; 39 000 YBP to >50 000 YBP, Brown Sand 31 000 YBP 38 000 YBP. The dates for wood inclusions found in the reworked Shelly-Sand are assignable to the Cemented Shelly-Sand which is their place of origin.

^bConventional radiocarbon age, ¹³C corrected using the Libby14 (half-life 5568 years). Errors represent 1 standard deviation.

^cCalibrated radiocarbon age in years before A.D. 1950. Based on INTCAL98 calibration data using CALIB 5.01 (Stuiver, et al 1998). Calibration done only for ages <20,26514 C yr. B.P. Range represents 1 standard deviation.

^dSample located at Grays Reef, the *Ophiomorpha* is considered a minimum date only and not direct date of the sediment

^eSample located at J-Reef, Cores 1 & 4 were taken in a paleochannel, all other dates are from the so-called "Research Ledge" outcrop. The OSL and U/Th ages were derived from sediments taken from cores. Radiocarbon laboratories used in this study were Beta Analytic Incorporated (BETA), Miami, Florida; The University of Georgia Center for Applied Isotope Studies (UGA). All samples were thoroughly pre-treated with standard acid-alkali-acid washes prior to isotopic analysis by accelerator mass spectrometry (AMS). The radiocarbon ages are conventional ages, corrected to the ¹³C/¹²C ratio, and use the Libby ¹⁴C half-life of 5568 years. Calibrated ages are given in years before A.D. 1950 while those of OSL are reported as years before A.D. 2003 when the OSL paleodoses were determined. The U/Th age is reported as years before A.D. 1950. Because of large fluctuations in atmospheric ¹⁴C content in the >30 ka time range, mainly as a result of variation in the geomagnetic field and the North American thermohaline circulation, AMS age estimates can be as much as 7 ka too young (Beck et al. 2001; Laj et al. 2002). For AMS dates greater than 42 ka the age offset may be somewhat less, possibly in the 3-4 ka range. Reliable calibration curves for this time range remain elusive (O'Connell and Allen 2004).



Generalized Geologic Section for coastal Georgia from Oligocene through Pleistocene (After Weeds and Edwards, 2001)

Figure 2. Generalized geologic section for coastal Georgia based on Weems and Edwards (2001). The inset geologic section for this study corresponds to the upper portion of the general geologic section. In the upper portion of the Georgia Bight, the Raysor Formation occurs seaward of the Cypresshead Formation in the Pliocene portion of the geologic section. The muddy sand in the general geologic section appears in our study's section as Unit 2, the Brown Sand.

beds. Our sediment descriptions are keyed to the cores taken at Gray's Reef and J-Reef (figs. 3,4). Excavation of the shell beds at the reef outcrops yielded two immediate facts: (1) the density of scallop valves per meter is high (over 100 shells per meter), and (2) the scallop stratum is unconformable with the older Gray's

Reef rock at that site. That unconformity excludes the bulk of the Pleistocene era or more (>1.6 m.y.). At J-Reef the shell beds are in a conformable relationship with the finer grained sediment, which we informally name the Brown Sand facies. No exposure of earlier than the late Pleistocene was observed at J-Reef.

SHALLOW MARINE MARGIN SEDIMENTS

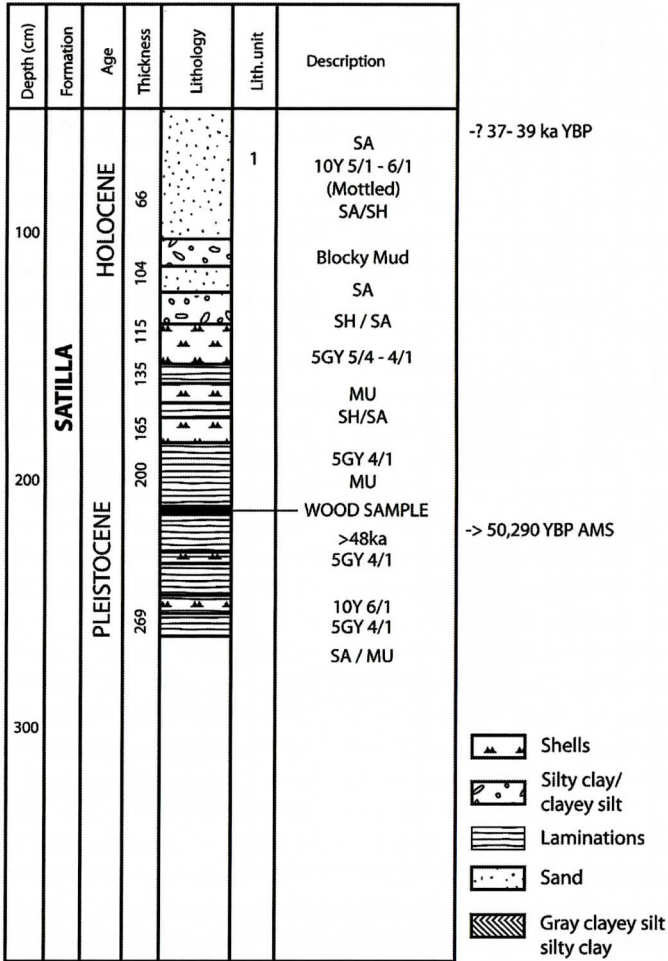


Figure 3. Vibracore from the J-Reef paleochannel's estuarine-fluvial depositional regime of laminated sand-mud and clay Satilla Formation strata with a Unit 1 sand cover. Munsell colors and absolute date ranges are shown.

Ages for Georgia Bight Sediments

Table 3 summarizes our chronometric results. One principal objective of this study was to obtain and analyze Georgia Bight sediments using high resolution radiometric dating methods. Dating of the Raysor Formation is based on lithology and stratigraphy Huddleston (1988). The reef facies, at Gray's Reef, unit 4, is both materially and time-equivalent to the Raysor (also referred to as the Duplin Formation). Woolsey (1977) identified this unit at Sapelo Island, 32 km landward today of Gray's Reef. At Sapelo, it is - 18 m MSL beneath this barrier island. Using a reasonable value for dip, the unit

would outcrop at - 22 m MSL or the mean average of the reef substrate. Based on planktonic foraminifera found in the Raysor, (Huddleston 1988) assigns an age of early late Pliocene or 2-3Ma. Dowsett and Cronin (1990) estimate an age of 3.5 - 3.0 Ma for the Duplin and Raysor Formations, again, based on planktonic foraminifera, as well as calcareous nannofossils and marine ostracodes.

Using OSL as a correlative tool, the AMS dates we report are less suspect with regard to well known calibration issues for ages > 30 ka (Van der Plicht 2002). The first of the two consolidated shell beds, the Brown Sand, unit 2,

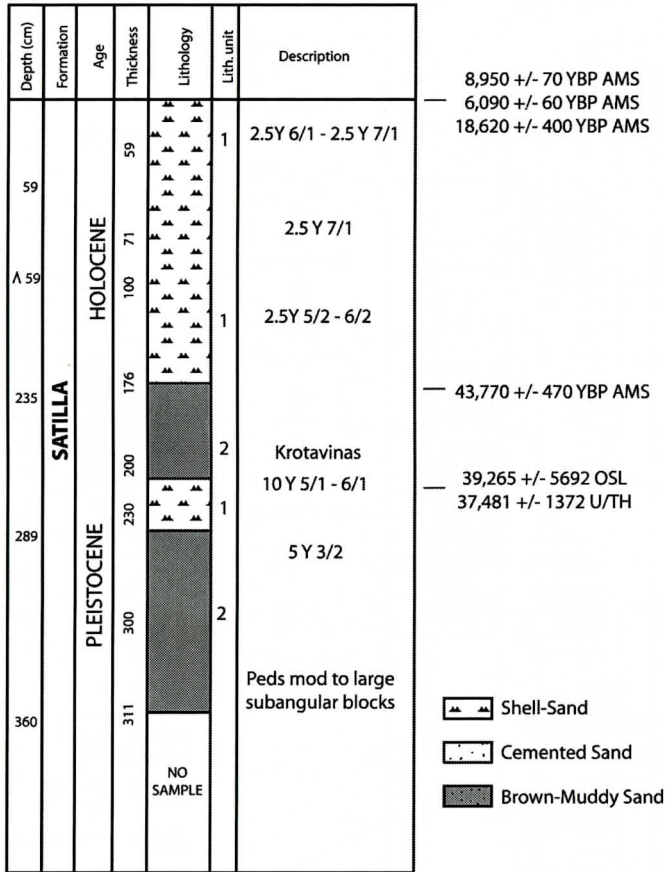


Figure 4. Well dated vibracore from Gray's Reef (GRNMS1). All sedimentological units described in this study are indicated along with Munsell colors. *Krotavinas* indicate burrows that transect Unit 2. Brown Sand pedology is shown suggesting its possible origin as a subaerial, humate rich soil.

sediment dates to at least the early glacial, e.g., late M.I.S. 3/early M.I.S. 2. The lower, conformable cemented shell beds, unit 3, observed below the Brown Sand member at J Reef is the older of these two sediments 31 to 39 ka for the former and 35 to 45 ka for the latter (Table 3).

Littman's studies of a paleochannel at J Reef, found unconsolidated shelf sediments in a un-conformable position over a Gray mud (Tables 1, 2), fluvial/estuarine sediment of a ravinement surface. Two AMS dates obtained on wood samples from these sediments were A dead carbon or infinite ages, e.g > 48 ka (Littman, 2000). The age range for the overlying, unconsolidated sediments, unit 1, is 23 - 29 ka, compared to older ages of the paleochannel's muds,

leaves a temporal lacuna of unknown magnitude between the two. The chronological picture is much clearer for the shell beds of Gray's and J Reefs with one radiocarbon date for a scallop shell of 45,170 +/- 1530 BP for the former and a range of four radiocarbon dates on wood inclusions of 35 - 41 ka (Table 3) for the latter.

In addition to these dates for J-Reef, a radiocarbon age for a scallop falls within this range as well, at 42,146 +/-396 BP. Based on these ages we conclude the shell beds are correlative at both locations.

DISCUSSION

Depositional Environments

The various sediments observed in the cores and outcrops, while, in many cases, allogenic in nature, can be correlated, with some degree of confidence, to defined depositional environments. The shell beds, principally within unit 3 of the Satilla Formation, are the result of near-shore, shelf depositional environments, probably, best characterized as highly reworked. This reworking, in all probability, took place during transgression when the shelf would be sediment-starved. The overlying, unconsolidated sediments of unit 1 are completely erosional deposits resulting from transgression and ravinement. These coarse, shelly sands are characteristic of shallow marine shelf environments.

The Brown sand unit (2) is our best evidence for a lowstand exposure. This unit is humate-rich, and represents remnant sediments of a barrier system since such humates are characteristic of spodic soil profiles found on barrier islands (Buol, et al, 1997; Hoyt and Hails, 1974). Pedogenic characteristics are listed in Table 2. The sedimentary character of this silty-sand suggests a fluvial origin for it. Generally speaking, alluvial sediments are poorly-sorted because finer, silt-clay-sized particles, in suspension, are trapped between sand grains or deposited with them when discharge diminishes (Blatt, et al., 1980). The Brown Sand could be back-barrier sediment where finer grained sediments can build up in estuaries (Milliman, et al, 1972). Whichever the case, the Brown Sand unit is most indicative of a barrier-back-barrier depositional environment "stranded" by a falling-to-lowstand systems tract, directly dated to the 39-31 Ka range (Table 3).

Taphonomy of shell beds and implications for RSL and shelf sequences for shallow shelves like the Georgia Bight

Kidwell (1988) in her paper "Taphonomic Comparison of Active and Passive Margins", identifies two types of shell beds and their rele-

vance to sea level fluctuations.

Complex shell beds are thick (1.5 to >10 m) deposits and rest on unconformities. Identified at Gray's Reef, minor or simple shell beds are single event concentrations representing discrete episodes of erosion. Del Rio, et al (2001) in a study of marine Miocene shell beds in Patagonia, recognized Transgressive (TSST), High Stand (HSST), and Regressive (RSST/FSST) phases in these spectacular deposits.

Meldahl and Cutler (1992) examined Pleistocene shell beds in the Northern Gulf of California identifying 3 types of beds that form on Continental margins - beach berm; tidal channel lags and subtidal beds. The latter they identified as unconformity beds. Their study identified unconformity beds as due to neotectonics rather than sea level. Meldahl and Cutler point to these unconformity shell beds as significant stratigraphic markers on active margins. We will argue that the shell beds at both Gray's and J-Reefs are similar but here the isostatic sea level processes are involved in their formation. We argue that these late Quaternary shell deposits denote and calibrate RSL in the shallow Georgia Embayment.

Flessa et al (1993) posit that long-term survival of shells requires frequent, shallow burial which retards bioerosion as well a mechanical erosion. The taphonomy of Georgia shelf shell assemblages, offshore Sapelo Island, was studied by Frey (1973), Frey and Howard (1972, 1986) and Dörjes, et al (1986). The shell assemblages (not shell beds) contained both nearshore and shelf species. In the latter the authors report 44% "relict" shells from 18 genera (*Arcinella*, *Pectin*, *Tellina*, *Argopectin*, *Chione*, etc.). By their, nature relict and modern, they are time averaged. We expect the same of the shelf shell beds. Valves observed in the beds at Gray's and J-Reef share a common convex-up orientation, which corresponds to a shallow, marine current-dominated environment. Sediments, that form the fine-to-medium sand burial matrix, were provided by coastal streams through M.I.S. 3 into M.I.S. 2.

With the M.I.S. 2 regression, all the shell beds were subaerial until the Holocene transgression, ca. 8,000 BP for the reefs. During this

subaerial phase, shell within the Brown Sand underwent diagenesis associated with groundwater, in spodosols, resulting in both shell thinning and complete dissolution of valves. This is observed with almost all shells recovered at Gray's and J-Reef. Transgression removed significant portions of the shell beds at Gray's Reef exposing the unconformity between the Pleistocene and Pliocene deposits. Erosion is ongoing at J-Reef through a process that involves modern bioturbation of the Brown Sand Member. Infauna have extensively burrowed this sediment in its upper portion (~ 30 cm). This disturbance, in turn, facilitates its erosion by bottom currents. The erosion exposes older, conformable facies but no Pliocene exposure was observed at J-Reef, only that of earlier Pleistocene sediments such as the shell beds.

Shell beds as stratigraphic markers

We agree with Kidwell and others in the use of shell beds as stratigraphic markers.

We identify the shell beds at Gray's and J-Reefs as unconformity beds formed during late Pleistocene (M.I.S. 3) highstand(s). The Sea Scallops function as limiting species in that they constrain the depositional environment to the lowest intertidal to shallow subtidal. These shell beds represent condensed sections of depositional sequences (Holland, 1993; 1995). They are predictably "severe" in their concentration and "biasing" of species during highstands and maximum flooding surfaces (*ibid*). Based on our dating, deposition occurred from 44 to 31 Ka.

A "sequence stratigraphy" for Georgia Bight Pleistocene Sediments

The Quaternary and Pliocene units of the Georgia Bight are both unconsolidated and consolidated clastic shallow-neritic sediments B mainly composed of fine-to-medium-grained quartz arenites overlying a so-called R2 seismic reflector, Miocene aged, described by Foyle, *et al* 2001; Hoyt and Henry 1967; Milliman, *et al*. 1972; Huddleston 1988; Idris and Henry 1995; Henry and Idris 1992; Swift *et al*. 1972; Swift and Niedorada 1985; Gayer *et al*. 1992; Foyle *et*

al. 2004. This sand cover is 10-15 m thick and rarely extends beyond 15-20 km offshore, pinching out in water depths of 10-15 m (Pilkey and Frankenberg 1964; Henry and Idris *ibid*) and becoming more coarse-grained. Sexton *et al*. (1992) and other workers (Milliman *et al. ibid*; Howard and Reineck 1973) describe the observed change in shelf sediments as the seaward extension of the modern marine accommodation space for the Bight. Most fine grained-clay/silt/fine sand - sediment occur in drowned stream valleys, such as seen in the J-Reef paleochannel (Pilkey *et al*. 1981; Littman 2000; this study). Their preservation is enhanced because ravinement, by the low-energy wave-field, of the Georgia Bight (less than 3 m), is relatively minor (Foyle, *et al*, 2004.).

Direct dating the younger Pleistocene sediments made it possible to address issues of RSL and sequence architecture. At Gray's Reef and nearby J-Reef (16 km north) represent Pliocene-Pleistocene lithologies, the latter being exhumed by sea level rise (transgression) post- Last Glacial Maximum (LGM) ca. 21 KYBP. Gray's Reef and J-Reef were overstepped by the modern transgression ca. 8 KYBP. At Gray's Reef the transgression exhumed a Pliocene exposure; at J-Reef it exhumed the Pleistocene. At both sites Pleistocene age shell beds are present. In addition, at both sites we map, and date, a slightly younger sand facies (Brown Sand, Unit 2) 39 KYBP vs. 43-44 KYBP for the shell beds. This is interpreted as a shoreward subaerial component of a lowstand. Chronology has these two Satilla fm elements in a conformable sequence.

According to Mitchum, *et al* (1977) the general sequence model of a depositional sequence with a lowstand systems tract (LSST); a transgressive systems tract (TSST) and a highstand systems tract (HSST). The sequence picture painted by our observations is "simple" in that it fits the classic S-sequence model: HSST - SB - LSST - TSST - HSST. The sequence boundary (SB) is the HSST exposure surface through the falling systems tract (FSST). If the Brown Sand, that overlies the lower shell beds, is truly a shell depauperate subaerial surface then it would have been exposed from after 32

KYBP until ca. 8 KYP. Foyle, *et al* (2001) observes that the Quaternary, Pliocene, Miocene and Upper Floridian Aquifer (UFA) units are separated from each other by subaerial erosional surfaces – sequence boundaries. This being the case, then the Brown Sand, as the best candidate for a subaerial, erosional surface, is, also, the best candidate for a Quaternary-aged sequence boundary, dated to late MIS 3, 39 – 31 Ka.

One other candidate for an earlier sequence boundary is that of the unconformity between units 3 and 4. There is some justification for this as a recent revision of Plio-Pleistocene eustatic cycles by Wornardt and Vail (1991) indicates that cycle 3.6, for the Florida Neogene, contains one major transgressive-regressive cycle dated to 3.0 to 3.8 Ma. Seen in the fossiliferous shell beds of the Pinecrest Formation, in Florida, a large unconformity, separates strata dated to cycle 3.7 dated to 3.0 - 1.9 Ma. This unconformity may be correlative to the unconformity observed between the Raysor Formation unit and the overlying Pleistocene units seen in this study.

CONCLUSIONS

Our studies of the shallow inner-to-mid shelf Quaternary and Pliocene sediments at both Gray's Reef and J-Reef have provided a clearer understanding of these deposits as proxies for relative sea level (RSL). The uppermost Satilla Formation is interpreted as reworked clastic deposits originating from Pleistocene sources located in the Piedmont and Blue Ridge Provinces. Based on the sediment coring, survey of exposed outcrops, and absolute dating of sediments and inclusions, a clearer understanding of late Pleistocene-to-Holocene depositional and erosional processes in the Georgia Bight is now possible.

The lithostratigraphic nomenclature for this Quaternary section is the Satilla Formation. It is composed of at least two provisional members, and in paleovalleys, such as that of Medway drainage, perhaps more. The consolidated facies observed below the palimpsest sand sheet are: (1) a weakly cemented Brown Sand and (2)

weak-to-moderately Cemented Shelly-Sand. These facies are observed in both cores and at outcrops at or near the -20 m isobath. A facies equivalent to the Brown Sand has been reported off South Carolina's Santee River (Sexton, *et al*. 1992:169). The Cemented Shelly-Sand is observed at Gray's Reef and J-Reef in bedded form (Gray's Reef) and outcrops (J-Reef). Within this member are assemblages of marine shell species, most notably *Placoepecten magellanicus*. Direct dating of both inclusions (AMS) and sediment grains (OSL) has constrained the ages of these two facies to 31-43 KYBP (Brown Sand) and >42-44 KYBP, or M.I.S. 3 for the Cemented Shelly-Sand. The Cemented Shelly-Sand is unconformable, at Gray's Reef, with the arenite of the Raysor Formation (Pliocene). At J-Reef a similar situation is suggested, but not directly observed. What is certain, is this weakly cemented facies is undergoing erosion at the present time and the exhumation of the Raysor Formation, at Gray's Reef, is the result of both transgression and ravinement, after LGM.

The invertebrate (and vertebrate assemblages) observed at Gray's Reef and J-Reef represent both marine (*Placoepecten*) and brackish-to-freshwater (*Crassostrea*; clam species - various). The Satilla aged shell beds date to M.I.S. 4 - M.I.S. 3 with subaerial exposure beginning in the late phases of the latter marine isotope stage (< 40 KYBP). From that time on, through M.I.S. 2, until the Holocene transgression, both Gray's Reef and J-Reef were alternately fluvial-estuarine systems. Both locations were, at some time, in both regression and transgression, progradational barrier-island complexes backed by estuaries similar to those seen on the modern coast.

Overstep of the -20 m isobath was post - 10 KYBP. This is attested to by vertebrate fossils of bison, mammoth, and horse, all late Pleistocene in age, and in the case of bison, Holocene in age (Table 3). Because of the observed, ongoing erosion of the Satilla Formation and its members, preservation of the LGM low-stand on the inner-to-mid shelf is difficult to observe. It may be better preserved on the outer shelf. The Cemented Shelly-Sand facies/

member is of high stand - falling systems tract origin. Its cementation occurred in the subaerial period, from late M.I.S. 3 through M.I.S. 2. Since transgression, its erosion has continued through the present. Better evidence of a lowstand in the Quaternary may be found in the paleovalleys such as at the Medway paleochannel just north of J reef and others recently observed near Gray's Reef as well as on the South Carolina shelf (Paul Gayes, personal communication, 2007; Stubbs, *et al.*, 2007). Our radiocarbon ages for wood samples, taken from the J-Reef paleochannel sediments, indicate "dead carbon" or "infinite" ages for the mud-sand facies found there in sediment cores (Littman, 2001). Overall, this study, provides a better understanding of the late Quaternary stratigraphy, its sedimentology, absolute ages and processes involved in preservation (or loss) of these facies on shallow, marine margins like the Georgia Bight.

ACKNOWLEDGMENTS

The authors were provided with extensive material, and in the case of the National Oceanic and Atmospheric Administration (NOAA), both personnel and financial support of the research. Both S. Littman and W. Weaver, University of Georgia students, were generously supported by graduate stipends from NOAA. The agency provided vessel support for all the offshore research for the 1996, 1998, and 2000 sediment coring and geophysical cruises: NOAA's ship FERREL was used. For diving operations, the Gray's Reef National Marine Sanctuary provided vessel support. Our key supporter throughout the research was Reed Bohne, Manager, Gray's Reef National Marine Sanctuary. Other key NOAA personnel were Alex and David Score, Ralph Rodgers, Bruce Cowden, Cathy Sakas, Keith Golden, Marcie Lee, and Pete Fischel. The crew of FERREL was invaluable during in our sediment coring operations. Two universities provided critical material and personnel support. For the 1996 coring operations, Dr. John Anderson and the Department of Geosciences, at Rice University, provided a vibracoring system. In 1998, and

again in 2000, Dr. Paul Gayes and the Center for Marine and Wetland Studies, Coastal Carolina University, provided their vibracoring system, along with Mr. Neil Giestra, to operate it. We benefited from taxonomic identification services provided by Professor David Webb, Florida Museum of Natural History, and Dr. Jason Geisler, Georgia Southern University. Dr. George Brook, Department of Geography, the University of Georgia (UGA), mentored students who wrote theses on their Gray's reef research (Littman and Weaver) in palynology and reviewed earlier versions of this paper. Dr. David Leigh, Department of Geography (UGA), provided laboratory space and advice to Littman and Weaver during sediment analyses. Ms. Jocie Graham, Department of Anthropology (UGA) formatted the final version of this manuscript.

REFERENCES

- Adesida, A.O. 2000. The stratigraphic framework of Eocene through Miocene sequences beneath Sapelo Island, Georgia: A shallow seismic reflection study. Masters Thesis. University of Georgia. Athens. 140 p.
- Allmon, W.D. 1993. Age, environment and mode of deposition of the densely fossiliferous Pinecrest Sand (Pliocene of Florida): implications for the role of biological productivity in shell bed formation. *Palaios*, 8(2): 183-201.
- Antoine, J.W., and V.J. Henry, 1965, Seismic refraction study of shallow part of continental shelf off Georgia coast: American Association of Petroleum Geologists Bulletin, Memoir 49, p. 601-609.
- Beck, W.J., B.W. Ward, and L.W. Ward, 2001, Extremely large variations of atmospheric ^{14}C during the last glacial period. *Science*, v. 292, p. 2453-2458.
- Blatt, H.G. Middleton, and R. Murray. 1980. *Origin of Sedimentary Rocks*. Prentice-Hall. Englewood Cliffs, NJ. 634 p.
- Brett, C.E. 1998. Sequence stratigraphy, paleoecology, and evolution: Biotic clues and responses to sea level fluctuations. *Palaios*, 13(3): 241-262.
- Buffler, R.T., J.S. Watkins, and W.P. Dillon, 1978, Geology of the Southeastern Georgia Embayment, U.S. Atlantic Continental Margin, based on Multichannel Seismic Reflection Profiles: American Association of Petroleum Geologists Bulletin, Memoir 29, p. 11-25.
- Buol, S.W., F.D. Hole, K.W. Weiler, J.A. Ewen, J. Dalparthy, S.F. Herbert and T.S. Steenhuis. 1997. *Soil Genesis and Classification*. Iowa State University Press. Ames.
- Del Rio, C. J., S.A. Martinez and R.A. Scasso. 2001. Nature and origin of the spectacular marine Miocene shell beds of northern Patagonia (Argentina): Paleocological and

SHALLOW MARINE MARGIN SEDIMENTS

- bathymetric significance. *Palaios*, 16(1):3-25.
- Döerjes, J., R.W. Frey and J. Howard. 1986. Origins of, and mechanisms for, mollusk shell accumulations on Georgia beaches. *Senckenbergiana Maritima*, 18(1-2):1-43.
- Dowsett, H.J. and T.M. Cronin, 1990. High eustatic sea level during the middle Pliocene: Evidence from the southeastern Atlantic coastal plain. *Geology*, 18:435-438.
- Duane, D.B., M.E. Field, E.P. Meisburger, D.J. Swift, and S.J. Williams, 1972. Linear shoals on the Atlantic continental shelf, Florida to Long Island, in D.J. Swift, D.B. Duane, D.B., O.H. Pilkey, eds., Shelf Sediment Transport - Process and Patterns: Stroudsburg, Pennsylvania, Dowden, Hutchinson and Ross, Inc., p. 447-498.
- Duller, G.A.T. 1999. *Analyst Version 2.12*, Luminescence Laboratory, University of Wales, Aberystwyth.
- Flessa, K.W., A.H. Cutler and K.H. Meldahl. 1993. Time and taphonomy: quantitative estimates of time-averaging and stratigraphic disorder in shallow marine habitat. *Paleobiology*, 19:226-286.
- Foyle, A.M., V.J. Henry, and C.R. Alexander, 2001 The Miocene aquitard and the Floridan Aquifer of the Georgia/South Carolina coast: Geophysical mapping of potential seawater intrusion sites. *Georgia Geologic Survey Bulletin 132*, Georgia Department of Natural Resources, Atlanta, 78 p.
- Foyle, A.M., V.J. Henry, and C.R. Alexander, 2004, Georgia-South Carolina Coastal Erosion Study: Phase 2 Southern Study Region State of Knowledge Report & Semi-Annotated Bibliography: Savannah, Georgia, Skidaway Institute of Oceanography, 251 p.
- Frey, R.W. (Ed.), 1973. *The Neogene of the Georgia Coast*. Department of Geology, University of Georgia, Athens.
- Frey, R.W. and J. Howard. 1986. Taphonomic characteristics of the offshore mollusk shells, Sapleo Island, Georgia. *Tulane Studies in Geology and Paleontology*, 19:51-61.
- Gayes, P.T., Scott, D.B., Collins, E.S., and Nelson, D.G., 1992, Quaternary coasts of the United States: marine and estuarine systems. SEPM publication No. 48, p. 155-160.
- Goff, J.A., J.A. Austin, Jr., S. Gulick, S. Nordjord, B. Christensen, C. Sommerfield, H. Olson and C. Alexander, 2005, Recent and modern erosion on the New Jersey outer shelf, *Marine Geology*, 216(4): 275-296.
- Harding J. L. and V. J. Henry, 1994 Geological history of Gray's Reef National Marine Sanctuary. (Report to the National Oceanic and Atmospheric Administration, 10 Ocean Science Circle, Savannah, GA.)
- Henry, V.J. and F.M. Idris, 1992, Offshore minerals assessment studies on the Georgia continental shelf B Phase 2: Seismic stratigraphy of the TACTS area and evaluation of selected sites for economic hard minerals potential: Georgia Department of Natural Resources Project Report 18, Atlanta, Georgia, 143 pp.
- Henry, V.J., and S.B. Van Sant, 1982. Results of reconnaissance mapping of the Gray's Reef National marine Sanctuary, Georgia Dept. of Natural Resources, Brunswick.
- Holland, S. M. 1993. Sequence stratigraphy of a carbonate-clastic ramp: the Cincinnati Series (upper Ordovician in its type area). *Geol. Soc. Bull.*, 105:306-322.
- Holland, S. M. 1995. The stratigraphic distribution of fossils. *Paleobiology*, 21:92-109.
- Howard, J.D., R.W. Frey, and H.E. Reineck, 1973. Holocene sediments in the Georgia coastal area. In Frey, R.W. (Ed) 1973. *The Neogene of the Georgia Coast*. Department of Geology, University of Georgia, Athens.
- Hoyt, J.H., and V.J. Henry, 1967, Influence of island migration on barrier island sedimentation. *Geological Society of America Bulletin*, v. 78, 86 p.
- Huddleston, P.F., 1988. A revision of the lithostratigraphic units of the coastal plain of Georgia - Miocene through Holocene. *Georgia Geological Survey Bulletin*, 104.
- Hunt, J.L., Jr., 1974. The geology and origin of Gray's Reef, Georgia Continental Shelf, M.S. Thesis, University of Georgia, Athens.
- Idris, F.M., and V.J. Henry Jr., 1995, Shallow Cenozoic stratigraphy and structure: South Carolina lower coastal plain and continental shelf: *Bulletin of the Georgia Geological Survey*, v. 107, p. 762-778.
- Johnson, H.D., and C.T. Baldwin, 1996, Shallow clastic seas, in: H.G. Reading, ed., *Sedimentary Environments: Processes, Facies and Stratigraphy*, 2nd Ed. Blackwell Science. Oxford. Pp. 233-280.
- Kidwell, S.M. 1986. Models for fossil concentrations: Paleobiologic implications: *Paleobiology*, 12:6-24.
- Kidwell, S.M. 1988. Taphonomic comparison of passive and active continental margin: Neogene shell beds of the Atlantic coastal plain and the northern Gulf of California. *Paleogeography, Paleoclimatology, Paleocology*, 63:201-223.
- Kidwell, S.M. and A.K. Behrensmeier, eds. 1993. Taphonomic Approaches to Time Resolution in Fossil Assemblages: Paleontological Society Short Course No. 6, Knoxville, 302 p.
- Kraft, J.C., 1977, Late Quaternary paleogeographic changes in the coastal environments of Delaware, Middle Atlantic Bight, related to archaeological settings: *Transactions of the New York Academy of Science*, v. 288, p. 35-69.
- Kidwell, S. M., M.M.R. Best, and D.S. Kaufman. 2005. Taphonomic tradeoffs in tropical marine death assemblages: differential time averaging, shell loss, and probable bias in siliclastic vs. carbonate facies. *Geology*, 33: 729-732.
- Krantz, D.E., D.S. Jones and D.F. Williams. 1984. Growth rates of the Sea Scallop, *Plactopecten magellanicus*, determined by 18O/16O record in shell carbonates. *Bio. Bull.*, 176:186-199.
- Laj, C., Kissel, C., Mazaud, A., Michel, E., Mascheler, R., and Beer, J., 2002, Geomagnetic field intensity, North American deep water circulation and 14C during the last 50 Kyr: *Earth and Planetary Science Letters*, v. 200, p. 177-190.
- Littman, S., 2000. Pleistocene/Holocene sea level change in

- the Georgia Bight: a paleoenvironmental reconstruction of Gray's Reef National marine Sanctuary and J. Reef. Unpublished Master's thesis, University of Georgia, Athens.
- Meldahl, K.H. and A.H. Cutler. 1992. Neotectonics and taphonomy: Pleistocene molluscan shell accumulated in the northern Gulf of California. *Palaios*, 7(2):187-197.
- Miller, J.J., 1998, An Environmental History of Northeast Florida. The University of Florida Press, Gainesville. 223 p.
- Milliman, J.D., O.H. Pilkey, and D.A. Ross, 1972, Sediments of the continental margin off the eastern United States: Geological Society of America Bulletin, no. 83, p. 1315-1334.
- Mitchum, R.M., Jr., P.R. Vail, and S. Thompson, III. 1977. The depositional sequence as a basic unit for stratigraphic analysis: in C.E. Payton, ed., Seismic stratigraphy B Applications to hydrocarbon exploration: American Association of Petroleum Geologists Memoir No. 26: 53-62.
- Murray A.S., and A.G. Wintle, 2000, Dating quartz using an improved single-aliquot regenerative dose (SAR) protocol: Radiation Measurements, v. 32, p. 57-73.
- Connell, J.F., and J. Allen, 2004, Dating the colonization of Sahul (Pleistocene Australia-New Guinea): a review of recent research: Journal of Archaeological Science v. 31, p. 835-853.
- Pilkey, O.H., B.W. Blackwelder, H.I. Knebel, and M.W. Myers, 1981, The Georgia Embayment continental shelf: stratigraphy of a submergence: Geological Society of America Bulletin, no. 92, p. 52-63.
- Pilkey, O.H., and D. Frankenberg, 1964, The relict-recent sediment boundary on the Georgia Continental Shelf: Bulletin of the Georgia Academy of Sciences, v. 22, p. 37-40.
- Sexton, W.J., M.O. Hayes, and D.J. Colquhoun, 1992, Evolution of Quaternary shoal complexes of the south central South Carolina coast. Quaternary Coasts of the United States: marine and Lacustrine Systems: SEPM Special Publication No. 48. SEPM Tulsa, OK, p. 160-172.
- Stubbs, C.C.A., L. Sautter and H.M. Scott. 2007. The Transect River channel: sonar and scuba exploration of an ancient river. Poster presentation, Southeastern Section Meeting of the Geological Society of America, Savannah, Georgia, March 29th.
- Swift, D.J., J.W. Kofoed, F.P. Saulberg, and P. Sears, 1972, Holocene evolution of the shelf surface, central and south Atlantic shelf of North America, in: D.J. Swift, D.B. Duane, O.H. Pilkey, eds., Shelf Sediment, Transport, Process and Pattern. Dowden, Hutchison and Ross, Stroudsburg, Pennsylvania, p. 499-574.
- Swift, D.J., and A.W. Neidorada, 1985, Fluid and sediment dynamics on continental shelves, in: R.W. Tillman, D.J. Swift, R.G. Walker, eds., Shelf Sands and Sandstone Reservoirs: Society of Economic Paleontologists and Mineralogists Short Course No. 13., p. 47-133.
- Van der Plicht, J., 2002, Calibration of the 14C time scale; towards the complete dating range, Hooghiemstra, *Geologie en Mijnbouw*: Netherlands Journal of Geosciences, v. 81, p. 85-96.
- Weaver, W., 2002. Paleoecology and Prehistory: Fossil Pollen at Gray's Reef National Marine Sanctuary. Masters thesis. University of Georgia, Athens.
- Weems, R.E. and L.E. Edwards, 2001. Geology of the Oligocene, Miocene, and Younger Deposits in the Coastal Area of Georgia. *Bull. Ga. Geol. Surv.* 124 pp.
- Woolsey, J.R., 1977, Neogene stratigraphy of the Georgia coast and inner continental shelf. Unpublished. University of Georgia, Athens, GA, 251 pp.
- Woolsey, J.R., and V.J. Henry, 1974, Shallow, high-resolution investigations of the Georgia coast and inner continental shelf, in Symposium of the Petroleum Geology of the Georgia Coastal Plain: Bulletin of the Georgia Geological Survey, v. 87, p. 167-187.
- Wornardt, W.W. and P.R. Vail. 1991. Revision of the Plio-Pleistocene cycles and their application to sequence stratigraphy and shelf and slope sediments in the Gulf of Mexico. *Gulf Coast Association of Geological Societies, Transactions*, 41:719-744.

RELOCATION OF BRUNSWICK RIVER AND OTHER ESTUARIES ON THE GEORGIA, USA COAST AS A CONSEQUENCE OF HOLOCENE TRANSGRESSION

¹TIMOTHY M. CHOWNS, ²BRYAN S. SCHULTZ, ³JAMES R. GRIFFIN,
AND ⁴MORGAN R. CROOK JR.

¹*Department of Geosciences, University of West Georgia, Carrollton, GA 30118*

²*Department of Earth & Atmospheric Sciences, University of Tennessee, Knoxville, TN 37996-1410*

³*Geosyntec Consultants, 225 Riverside Avenue, Jacksonville, FL 32204*

⁴*Department of Anthropology, University of West Georgia, Carrollton, GA 30118*

ABSTRACT

Prior to about 1480 BP Brunswick River entered the Atlantic south of Jekyll Island. Subsequently, rising sea level encouraged the river to follow a more direct route and to empty north of the island. Satellite imagery suggests that many inlets along the Georgia coast have adjusted in a similar fashion. Circumstantial evidence suggests that the Ogeechee may have relocated from St. Catherines Sound and that Blackbeard Island may be a dissected spit formed by the relocation of Sapelo Sound. Partially abandoned inlets have narrowed due to the progradation of spits while expanded inlets are pinned between eroded banks of the Silver Bluff Formation and markedly crosscut Holocene features. On the Georgia coast marine transgression tends to favor tidal processes and inlet straightening, while stillstand and regression favor wave processes, spit-building and inlet diversion.

INTRODUCTION

Barrier islands are among the most dynamic environments on the planet, constantly adjusting equilibrium in response to changing wave and tidal regimes as well as to Holocene transgression (Hoyt, 1967). Georgia's Sea Islands (figure 1), including Jekyll Island, lie at the head of the Georgia Bight where coastal dynamics are controlled by a mixture of wave and tidal processes (Davis, 1994a, 1994b; Hayes 1994; Oertel and others, 1991). As a consequence of low wave energy (mean height, < 1.0

m; Kuroda in Howard and others, 1972), and moderate tidal range (2-3m range at spring tide) islands are relatively short and separated by deep tidal inlets. It was within this setting that Hoyt and Henry (1967) described the process by which islands and inlets migrate due to longshore transport and the characteristic stratigraphic response. Because of wave approach, barrier islands are eroded at the north end and have well developed spits on the southern ends. Over the years, longshore transport and spit building should be expected to displace river estuaries further and further down the longshore transport system. Indeed, Baldwin and others (2006) have demonstrated that in South Carolina the estuary of the Pee Dee River, has been displaced by about 25 miles (40 km) southwest since the Late Pleistocene (more than 50 miles [85 km] since the late Pliocene) due to this process.

However, although all the barrier islands on the Georgia coast demonstrate the same pattern of migration, surprisingly the estuaries show no sign of displacement; all follow the most direct course to the sea and intersect the modern shoreline close to a right angle (Oertel, 1975). The writers first became aware of this anomaly while working on St. Simons Sound between St. Simons and Jekyll islands (Chowns and others, 2002; 2006), but this situation persists from Santee Point, South Carolina to the St. Johns River near Jacksonville, Florida (Hayes, 1994). It is evidently related to tidal range and corresponds to the transition from mesotidal (2-4 m range) at the head of the Georgia Bight to microtidal (<2 m range) conditions along the Grand Strand in South Carolina and south of St

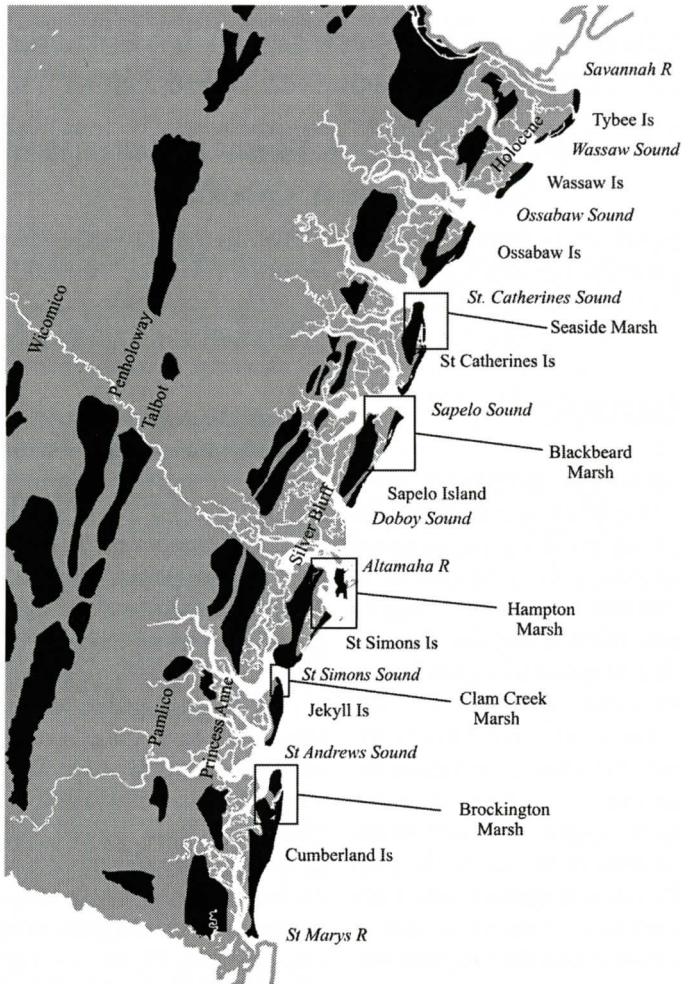


Figure 1. Georgia coast, barrier islands and inlets. Despite longshore transport to the south, notice that most inlets are not deflected but flow directly to the sea. This is a recent phenomenon dependent on rising sea level and has led to a series of abandoned inlets south of the modern inlets (shown in boxes). Holocene and Pleistocene barrier islands identified by darker shading.

Johns River in Florida (Davis & Hayes, 1984; Davis, 1994a). This paper addresses the causes of this tide dominated, inlet straightening and the possibility of an earlier wave dominated system.

STRATIGRAPHY

Jekyll Island consists of a nucleus of Pleistocene sands modified by Holocene erosion and accretion (figures 2 & 3). Pleistocene deposits belong to the Silver Bluff Formation deposited during a highstand 1-2m above modern sea lev-

el, dated between about 25-50,000 years ago (Hails & Hoyt, 1969; Hoyt & Hails, 1974). The age of this highstand is controversial because it falls within the Wisconsin glacial stage (Shackleton & Opdyke, 1973; Gibbard & van Kolfshoten, 2005). It may correspond to an interstadial within isotope stage 3 or is possibly much older (even Sangamon, stage 5). These Late Pleistocene deposits are now being reworked by the Holocene transgression (Henry & Fritz, 1985; Henry, 2005). The island may be conveniently divided into four parts as illustrated in figure 2.

Holocene Transgression and Relocation of Estuaries

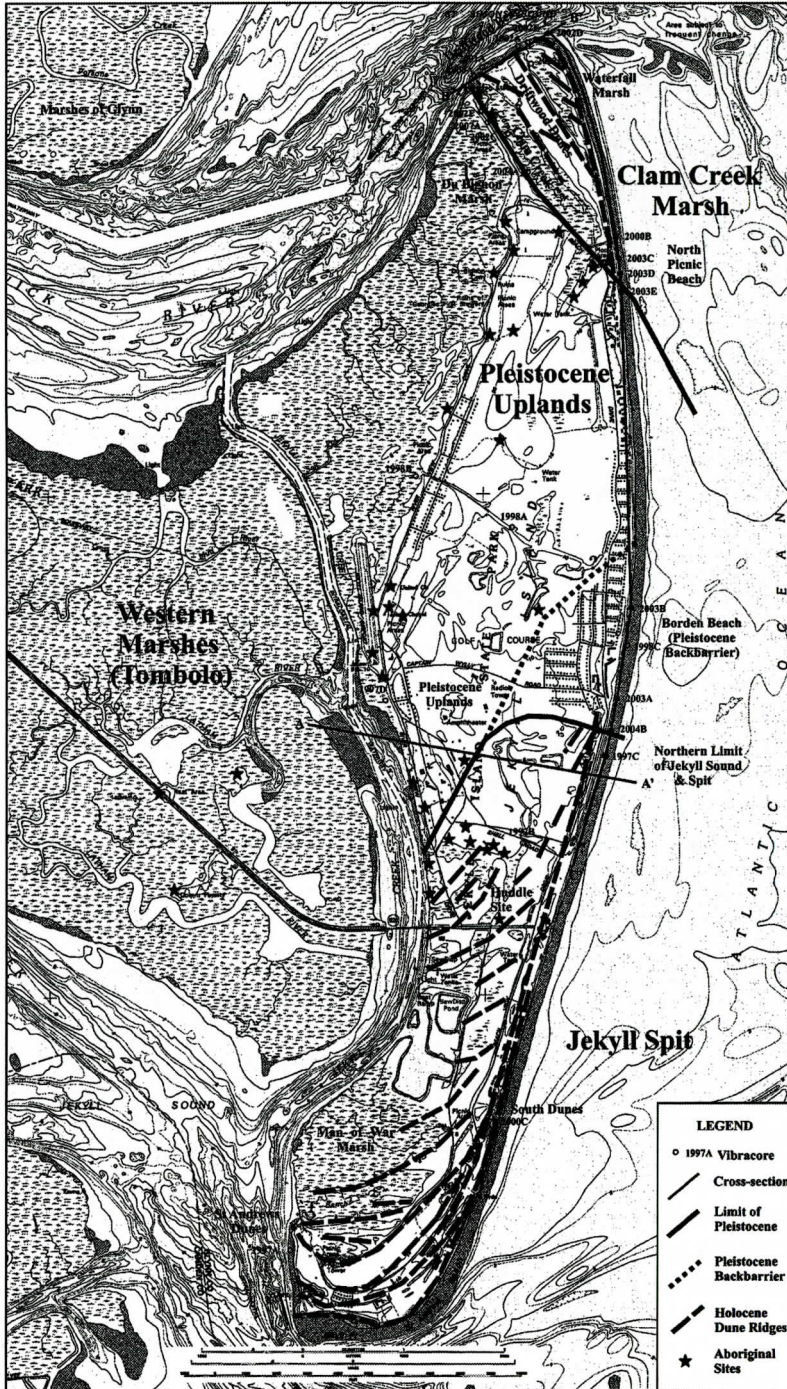


Figure 2. Simplified geologic map of Jekyll Island showing the distribution of Pleistocene and Holocene deposits and location of vibracores and cross-sections. Note the trend of recurved spits extending almost as far north as Captain Wyllly Road.

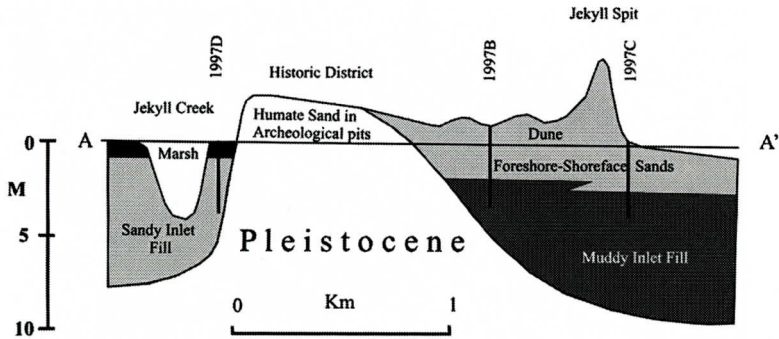


Figure 3. Cross-section across the middle of Jekyll Island (see figure 2) interpreted from vibrocores.

1. Pleistocene Uplands

Pleistocene sands are fine to coarse grained and indurated by dark gray humate or rusty brown iron oxide; in distinct contrast to fine grained Holocene sands with only minor humate (Henry & Fritz, 1985). Although aragonitic shell debris is sometimes present, most shells have been leached by meteoric groundwater and are represented as molds. Based on vibrocores, archeological test pits and topography, Pleistocene sands underlie most of the northern part of Jekyll Island between Captain Wyllie Road in the south, Clam Creek in the northeast and DuBignon Marsh in the northwest. Henry and Fritz (1985) show the Silver Bluff sands extending south of the causeway but we interpret Millionaire's Village to mark the southernmost extent of these uplands. The area consists of a series of north-north-easterly trending ridges that appear to be truncated by erosion in the east and partially inundated and buried under marsh in the west. The eastward bulge in the shoreline is perhaps due to the greater induration of these deposits. A radiometric date of 45,820 \pm 3300 BP (Beta, 220145) was obtained from fossil wood derived from this section (see table 2, 2003C, 13.7'; figures 4 & 6).

Along the modern shoreline the Pleistocene substrate is mantled by Holocene dune sands and immediately north of Captain Wyllie Road by a retrogressive sequence of back barrier facies below the dunes. The contact between back barrier facies and overlying dune sands is marked in several cores by a paleosol at a depth

of about -2.5 m. In places tree stumps (including bald cypress) associated with this paleosol may be visible on the foreshore after erosion. Freshwater cypress swamps are common beneath modern salt marsh at several places along the Georgia coast and clearly developed in advance of the modern highstand, perhaps during a minor regression between about 3000-2400 BP (DePratter & Howard, 1981). Lacking radiometric dates, the back barrier facies were at first thought to be Holocene (Chowns and others, 2006), but from the occurrence of shell molds and abundant mica are now judged to be more likely Pleistocene.

2. Jekyll Spit

Based on topography the entire southern part of Jekyll Island, extending from Captain Wyllie Road in the east and the southern end of Millionaires Village in the west, consists of recurved beach ridges and intervening swales, formed by Holocene accretion of Jekyll spit. Old dune ridges are pronounced at the south end of the island but become more subdued with age. Unfortunately, topography has been disrupted by landscaping of the golf course which straddles and obscures much of the contact with the Pleistocene nucleus. However, along the coast vibrocores show an abrupt transition from retrogradational to progradational facies just south of Captain Wyllie Road (between cores 2004B and 1997C) that is interpreted to mark the vicinity where the spit is attached. North of this point Holocene deposits rest on Pleistocene

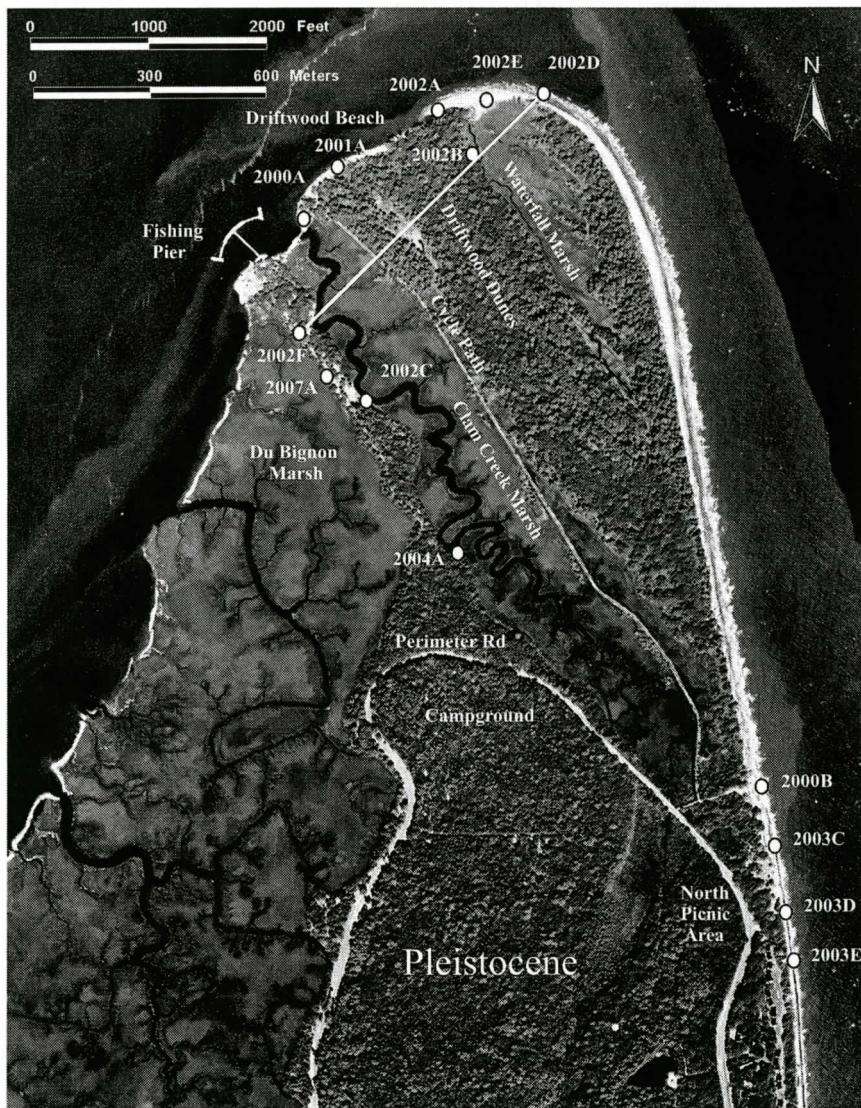


Figure 4. Location of vibracores at the north end of Jekyll Island. Note the truncation of Pleistocene deposits (Silver Bluff barrier and DuBignon Marsh) and the accretion of Holocene beach ridges to the northeast.

sands and clays, while to the south Holocene beach sands rest on muddy inlet fill with abundant aragonitic shell debris.

Man-of-War marsh is developed in the lee of Jekyll spit and does not extend beneath the beach. There are no marsh deposits exposed on the foreshore anywhere along the spit (south of Captain Wylly Road) and vibracore (2000C) from South Dunes picnic area shows a normal sequence of upper shoreface through dune fa-

cies consistent with progradation. This is quite different from the retrogradational sequences recorded beneath the beach at the north end of the island.

3. Western Marshes

To the west of the Pleistocene uplands and Jekyll spit, Jekyll Island is connected to the mainland by a broad swath of salt marsh that is

still undergoing accretion and forms a tombolo now bisected by the Intracoastal Waterway. Limited vibracoring on the east side of Jekyll Creek west of the Pleistocene uplands reveals a relatively thick succession of muddy inlet facies below the modern marsh. Radiometric dating establishes that while surficial deposits are Holocene they are superposed on older Pleistocene deposits. Within the latter sandy units are characteristically micaceous and suggest a source within the Piedmont.

Neogene teeth and bone of both marine (shark, whale) and terrestrial (horse) origin are commonly dredged from the Brunswick River and shark teeth were reported in spoil from the abandoned marina south of the causeway (Henry & Fritz, 1985). Some of these may derive from lag gravels accumulated in back-barrier inlet deposits associated with the Princess Anne and/or Silver Bluff shorelines but many originate from the erosion of older Miocene strata (Voorhies, 1973). Being derived, they are a misleading guide to age.

4. Clam Creek Marsh

The northern point of Jekyll Island comprises a wedge of Holocene marshes and beach ridges accreted to older truncated Pleistocene terranes (figure 4). The oldest beach and dune ridge rests on the truncated margin of DuBignon Marsh, utilized by the road to the fishing pier and with successively younger ridges to the northeast. Drainage is controlled by two small tidal creeks, Clam Creek and the smaller informally named Waterfall Creek. The main group of dune ridges between Clam and Waterfall creeks is informally labeled as Driftwood Dunes after the beach north of the fishing pier.

The accretion of beach ridges and marshes to the seaward side of the north end of the island is anomalous for several reasons. Most importantly it does not fit with the overall pattern of longshore transport. Oertel (1975) points out that both northerly and southerly progradation are possible depending on seasonal winds (northerly winds generated by fall and winter storms and southerly winds in spring and summer, including hurricanes). However, in spite of pro-

gradation to the northeast the main supply of sand to Jekyll Point appears to be from ebb-tidal shoals seaward of St. Simons Sound, in accord with dominant longshore transport. At the same time this accretion has been occurring to the northeast, active erosion is underway to the northwest along the south shore of St. Simons Sound. All these observations suggest that the shoreline is adjusting to some recent change in shoreline equilibrium. The present program of vibracoring was initiated in order to investigate these changes.

DEPOSITIONAL FACIES

Vibracores offer a convenient method of identifying depositional environments in the shallow subsurface. They are particularly useful on Jekyll Island because the geology is obscured by dense vegetation, superficial wind-blown sand and soils. However, interpretations are critically dependent on reliable attributions. Criteria used in assigning depositional environments are summarized in table 1. This table is based on descriptions provided by Henry and Fritz (1985), Farrell and others (1993) Oertel, (1973) and Howard and Reineck (1972) as well as work by students at the University of West Georgia. Although, most cores were completed in Holocene deposits, it is important to distinguish Pleistocene substrate when present. Little difficulty arises characterizing the coarser grained, humate-indurated Pleistocene sands in upland areas but caution is required in the marshes where Holocene backbarrier facies are often superposed on similar Pleistocene lithologies. Radiometrically dated Pleistocene clays often have a greenish hue and sands are commonly highly micaceous.

CLAM CREEK INLET

Vibracores collected between DuBignon Marsh and the north point of the island (figures 4 & 5) confirm that estuarine clays associated with Clam Creek extend continuously to the modern shore beneath Driftwood Dunes, Waterfall Marsh and the modern dune ridge (2004A, 2000A, 2001A, 2002A, 2002B,

HOLOCENE TRANSGRESSION AND RELOCATION OF ESTUARIES

Table 1. Criteria for the recognition of depositional environments in cores.

Environment	Lithologies	Sedimentary Structures & Texture
Dunes	Fine grained sand often stained pale yellow	Usually structureless due to rooting & bioturbation, sands well sorted with slight positive skewness
Backshore-Upper Foreshore	Fine grained sand, light gray to white, broken shell debris in modern sands only	Laminated. Some muddy flasers in runnels. Heavy minerals concentrated in backshore. Bioturbation minor, sands well sorted with slight negative skewness
Lower Foreshore-Shallow shore-face	Fine grained sand slightly darker than above due to mud in burrows	Laminated as above but with <i>Callianassa</i> and other mud-lined burrows, sands less well sorted with slight negative skewness
Marsh	Organic rich mud or muddy sand	Highly burrowed and rooted
Lagoon (Abandoned inlet)	Dark gray mud with sand and shell debris	Laminated. Sand wavy-lenticular & rippled, carbonized plant debris
Active Inlet	Fine sand with mud layers	Thicker bedded than lagoon with shell lags and mud intraclasts, bioturbated sand with mud-lined burrows
Pleistocene uplands	Fine-coarse sand with shell molds	Sands indurated, dark gray or brown due to humate and iron oxides
Pleistocene back-barrier	Clays interbedded with fine-medium sand	Clays greenish gray. Sands micaceous, bioturbated, some decomposed aragonite shells in muds, common plant debris.

2002E, 2000D). The clays are laminated with wavy ripples of fine sand and abundant shell debris, particularly the shells of the clam *Mulinia lateralis*. Significantly, the only rooted marsh facies occur at the surface associated with the modern marshes. This indicates that an open inlet prevailed in the area until quite recently. Unfortunately we are unable to establish the exact dimensions of the inlet fill but the width exceeds 1.5 km. and the depth is greater than our longest core, 7m.

Three main stages of accretion are evident associated with the fill. The oldest deposits form the narrow sand ridge that extends from the fishing pier to the old north picnic area. It mantles the edge of DuBignon Marsh in the north and a scarp cut across Pleistocene upland to the south. The Driftwood Dunes complex was probably initiated east of the modern shoreline and separated from DuBignon Marsh by open water. However, it has clearly been pushed back over washovers and estuarine clays to form a coarsening-upward retrograda-

tional fill. Clam Creek occupies the last remnant of this old inlet. Waterfall Marsh and the modern beach ridge constitute the youngest stage of accretion. They are separated from Driftwood Dunes by another erosional scarp and are perched on top of the older estuarine clays. The fill beneath Waterfall Marsh has a maximum thickness of about 5 m and is much sandier than the older fill. Once again the modern beach ridge has been pushed back to form a coarsening-upward fill of estuarine clays and washovers.

A second group of cores was collected from the beach at the north picnic area in order to confirm an erosional contact at the base of the inlet fill (figure 6). As expected the contact with Pleistocene humate was encountered in two holes (2003E, 2003C) and confirmed by radiometric dating of a wood fragment (45, 820 +/- 3300 BP; 2003C, 13.7', Beta 220145; all dates are conventional radiocarbon ages based on AMS analysis; see table 2)

Shell debris from estuarine fill within Clam

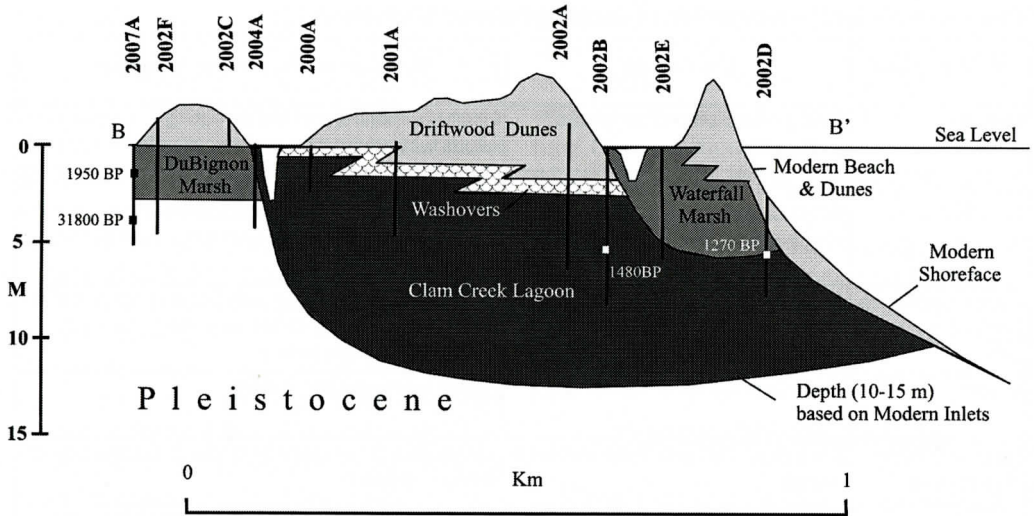


Figure 5. Cross-section across the northern end of Jekyll Island (see figure 4) showing abandoned inlet infilled by lagoonal clays.

Table 2. Core samples for which radiometric dates were obtained.

Sample Number	Location	Material (treatment)	Environment	Measured Radiocarbon Age	13C/12C	Conventional Radiocarbon Age	2σ
Beta 220143 AMS	2002B, 17.0'	<i>M.lateralis</i> (acid etch)	Top of sandy inlet fill Clam Creek inlet	1080 +/- 40 BP	-0.5o/oo	1480 +/-40 BP (no correction for local reservoir)	1120-940 BP
Beta 220144 AMS	2002D, 13.6'	<i>M.lateralis</i> (life position) (acid etch)	Base of inlet fill (Waterfall Inlet)	870 +/- 40 BP	-0.7 o/oo	1270 +/- 40 BP (no correction for local reservoir)	910-720 BP
Beta 220145 AMS	2003C, 13.7	Wood fragment (acid/alkali/acid)	Mud substrate below Clam Creek Inlet	45680 +/- 3300 BP	-16.5 o/oo	45820 +/- 3300 BP	
Beta 230797 AMS	2007A, 5.2'	Charred plant debris (acid/alkali/acid)	Muddy inlet fill (Dubignon Marsh)	1790 +/- 40 BP	-15.1 o/oo	1950 +/- 40 BP	1990-1820 BP
Beta 230798 AMS	2007A, 13.6'	Plant debris (acid/alkali/acid)	Sandy Inlet fill lacking shells, beneath Dubignon Marsh	31850 +/- 320 BP	-27.9o/oo	31800 +/- 320 BP	

Creek inlet gives a radiometric age of 1480 +/- 40 BP (2002B 17'; Beta 220143), while fragments of plant debris from beds beneath DuBignon Marsh that are incised by Clam Creek inlet yield a radiometric age of 1950 +/- 40 BP (2007A 5.2'; Beta 230797). A precise date of 1270 +/- 40 BP (2002D 13.6'; Beta 220144) is

given for the base of Waterfall inlet by specimens of *Mulinia* found in life position at the contact with the Clam Creek sequence. The sample from Clam Creek inlet was collected at the contact between an older group of muddy sands and a younger group of silty muds that may coincide with the transition from active to

HOLOCENE TRANSGRESSION AND RELOCATION OF ESTUARIES

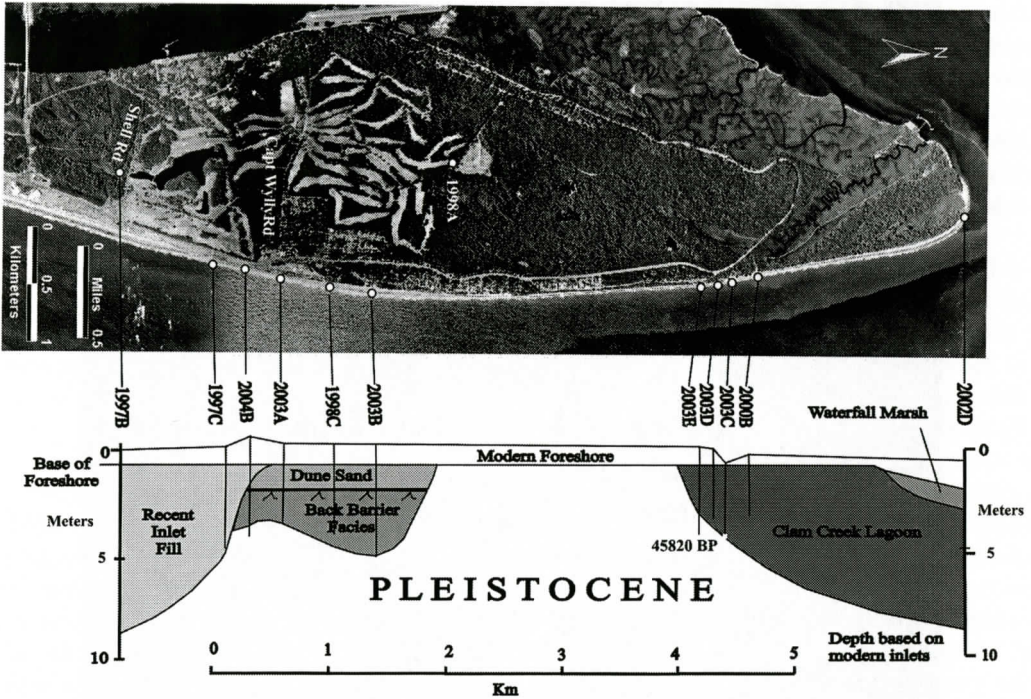


Figure 6. Longitudinal section based on vibracores along Jekyll beach. The section shows Clam Creek inlet to the north and old 'Jekyll' inlet to the south separated by a core of Pleistocene substrate.

abandoned inlet. The 1950 BP date is derived from overbank deposits probably deposited while the channel was active.

From the dimensions of the inlet fill the Holocene wedge northeast of Clam Creek clearly marks the location of a major inlet rather than a small tidal creek. Most likely it indicates a former location of St. Simon's Sound. However, even allowing for changing meanders, the north-northwesterly trend of this inlet in no way matches the likely outfall of Brunswick River. Rather, it appears as a continuation of Mackay and Frederica rivers on the north side of St. Simons Sound. It suggests that instead of turning northeast Brunswick River formerly drained southeast into St. Andrews Sound via Jekyll Creek (figure 7). In this case Jekyll Island lay at the southeast end of the Brunswick peninsula and DuBignon Marsh was continuous with the Marshes of Glynn. The neck of marsh between Brunswick and Mackay rivers was less than three miles (5 km) wide, and given the low relief and lack of hard substrate, relatively easily

breached, especially if large volumes of water were impounded in the estuaries following storms. A single large storm would be enough to cause avulsion.

The narrow sand ridge along the road to the fishing pier was probably originally a marsh hammock formed by storm washover when Clam Creek inlet was open to the southeast (cf. Cleary and others, 2004), while Driftwood Dunes migrated from the northeastern side of the inlet following the breach. Most likely sand to form the Driftwood Dunes was derived from the destruction of St. Simons spit. Based on this scenario it follows that the inlet was open at 1950 BP but closed by 1480 BP.

Radiometric dating of plant debris from below DuBignon Marsh (figure 5) indicates a relatively thin Holocene sequence (about 2.7m) underlain by Pleistocene sands (31,800 +/- 320 BP; 2007A, 13.6', Beta 230798) and, below these, muds containing aragonite shells (*Cyrtopleura*). These, questionably, alluvial sands and marine muds are much older than the fill

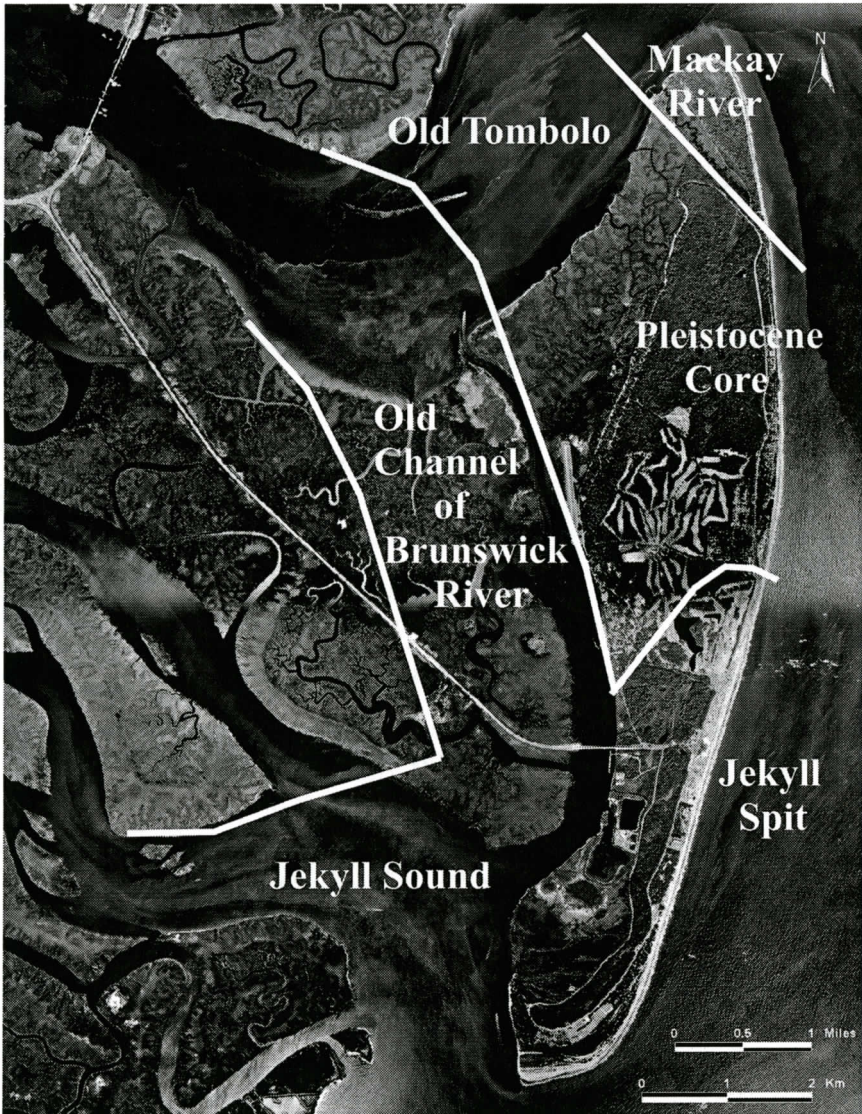


Figure 7. Air photo and schematic map showing former locations of 'Mackay River', 'Brunswick River' and 'Jekyll Sound' prior to the diversion of Brunswick River into St. Simons Sound.

within Clam Creek inlet and older than back-barrier facies cored at comparable depths behind Cumberland Island (< 3 ka; Farrell and others, 1993).

BRUNSWICK RIVER

As a direct consequence of this proposed switch, discharge through St Simons Sound would have increased at the expense of St. An-

draws Sound. The result was increased erosion through St. Simons Sound and rapid elongation of Jekyll spit into St Andrews Sound. St. Simons Sound is one of the narrowest and deepest inlets among the Sea Islands, squeezed between Pleistocene headlands both to the north and south. Both the north and south shores are undergoing active erosion and St Simons Island is the only island lacking a spit at the southern end. Loss of this spit is a predictable result of

the diversion of Brunswick River.

We lack absolute dates to establish a record of the elongation of Jekyll spit but there are no prehistoric aboriginal sites south of the causeway (Crook, 1985; unpublished data). The most southerly site (Huddle site, figure 2) is located on an early recurved spit just north of the causeway and dates to the Savannah Phase (AD 1150-1350; Williams & Thompson, 1991). Shell mounds were typically located on the lee-side of islands adjacent to salt-marsh that was the source of the oyster shell.

THE ALTAMAHA

Pleistocene sands beneath DuBignon Marsh (1998B, 2004A, 2007A) as well as beneath the modern beach north of the spit (2004B, 1998C) are notably micaceous; in distinct contrast to modern sands. The most likely source of mica is the Altamaha River, the only local river with tributaries rising in the Piedmont. More work is needed to determine whether this mica was derived from the shoreface, or if the Altamaha once occupied the low country between the Silver Bluff and Princess Anne barriers and perhaps the gap between Jekyll and Cumberland islands. The single dated sample (31,800 +/-320 BP.) from this inlet fill coincides with the latter part of marine isotope stage 3 (Shackleton & Opdyke, 1973; Gibbard & van Kolfshoten, 2005) when the shoreline was probably much further east. If so, this fill is most likely alluvial rather than estuarine and supports the latter hypothesis.

COMPARISON WITH OTHER ISLANDS

St. Simons Sound is not unique in showing evidence of relatively recent diversion. In fact, an inspection of many of the inlets on the Georgia coast suggests that southeasterly channels have recently been abandoned in favor of a more direct route to the sea (figure 1). Blackbeard Marsh between Blackbeard and Sapelo islands, Hampton Marsh between Sea Island and St. Simons Island and Brockington Marsh between Little Cumberland and Cumberland is-

lands all appear to be parts of abandoned inlets and lie south of modern inlets. Localities where capture is suspected include Sapelo River, which may have emptied into Doboy Sound, the Ogeechee through St. Catherines Sound; and, more speculatively, Newport River, which may have flowed between Sapelo and Blackbeard islands (figures 8 & 9).

Recent work (Bishop and others, 2007; Linsley and others, in press) suggests that St. Catherines Island was originally paired with a Holocene island analogous to Blackbeard Island and thus that Seaside Marsh on the northeast end of St. Catherines Island conceals yet another abandoned inlet. This interpretation is supported by vibrocoring carried out by Linsley (1993) and Bishop and others (2007). Linsley (1993) encountered sandy estuarine deposits with a mixed fauna of marine and brackish shells beneath Holocene marsh while Bishop and others (2007) reported more than 9m of marsh mud in the same vicinity (Linsley and others, in press). Whether or not other marshes coincide with buried inlets remains to be tested, but, all seem to have been displaced to the southeast in response to longshore transport. In the Sapelo-Blackbeard doublet both margins of the inlet (albeit modified by washover) may be preserved while the seaward part of the doublet has been lost to erosion on St. Catherines (Bishop and others, 2007; Thomas and others, in press) and on Jekyll only a fraction of the inlet-fill is preserved. If these are the remnants of old inlets there is the implication that their seaward margins were defined by spits; St. Simons spit in the case of Brunswick River.

The possibility that Blackbeard Island originated as a dissected spit needs to be investigated. Certainly, a major part of the island shows beach ridges prograding to the south (Oertel, 1975) in the manner of a spit. St Catherines spit is divided in two parts by Zapala scarp that marks the former northern limit of Sapelo Sound (Bishop and others, 2007; Linsley and others, in press). North of the scarp, on Cracker Tom Hammock, the older part of the spit consists of cusped beach ridges reminiscent of Blackbeard Island. Here the spit rests on a Pleistocene substrate (Booth and others, 1999),

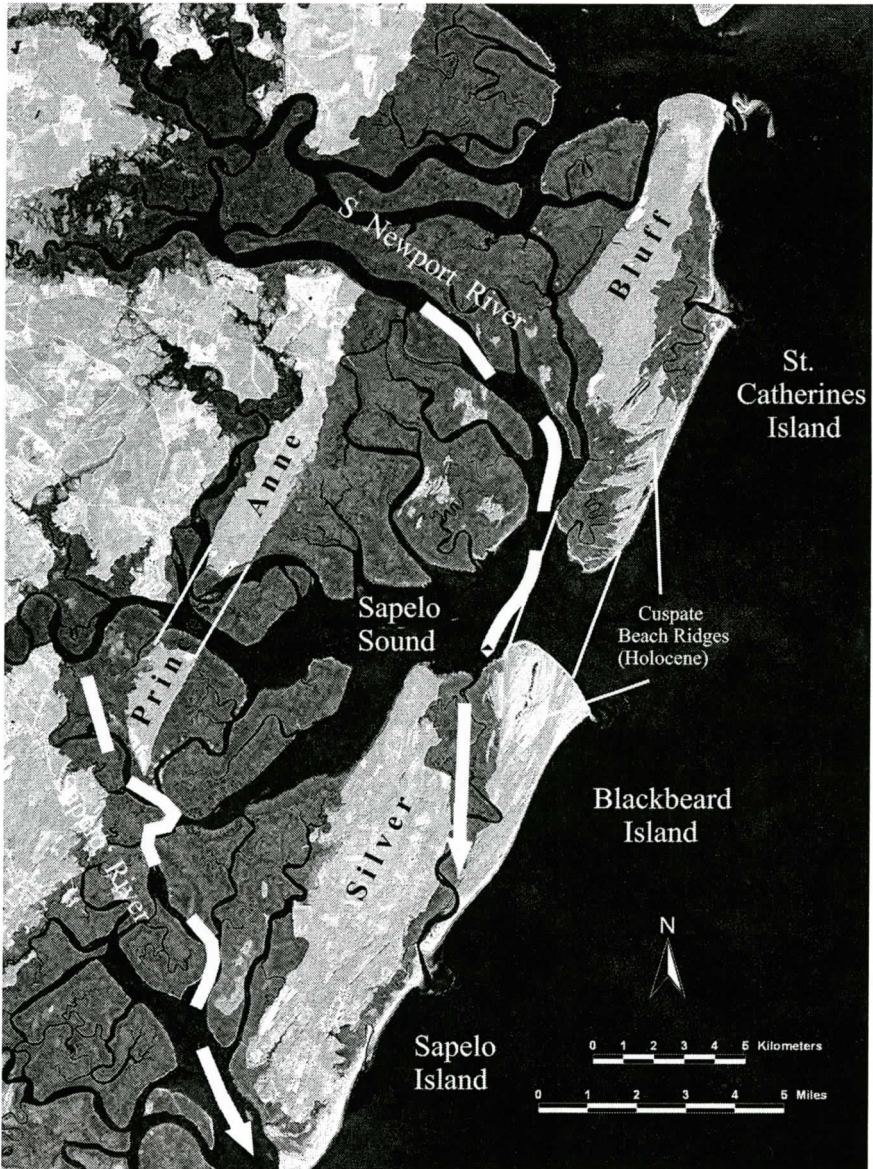


Figure 8. Satellite imagery supporting the contention that Blackbeard Island is a portion of St. Catherines spit dissected by the relocation of Newport River and perhaps also Sapelo River. The swath of cusate beach ridges on St. Catherines Island is Cracker Tom Hammock bounded to the south by Zapala scarp.

while to the south of the scarp it has prograded over Holocene inlet fill. Elevations are generally higher on both Blackbeard Island and Cracker Tom Hammock than on the younger part of St. Catherines spit. More than likely this is due to differential subsidence related to higher compaction rates in recent inlet fill. The similarity

in geomorphology between the older part of St. Catherines spit and Blackbeard Island strongly suggests that they are one and the same (figure 8). From archaeological data (Thomas and others, in press) Cracker Tom Hammock predates 2900 BP (St. Simons period), while beach ridges south and east of Zapala scarp are younger

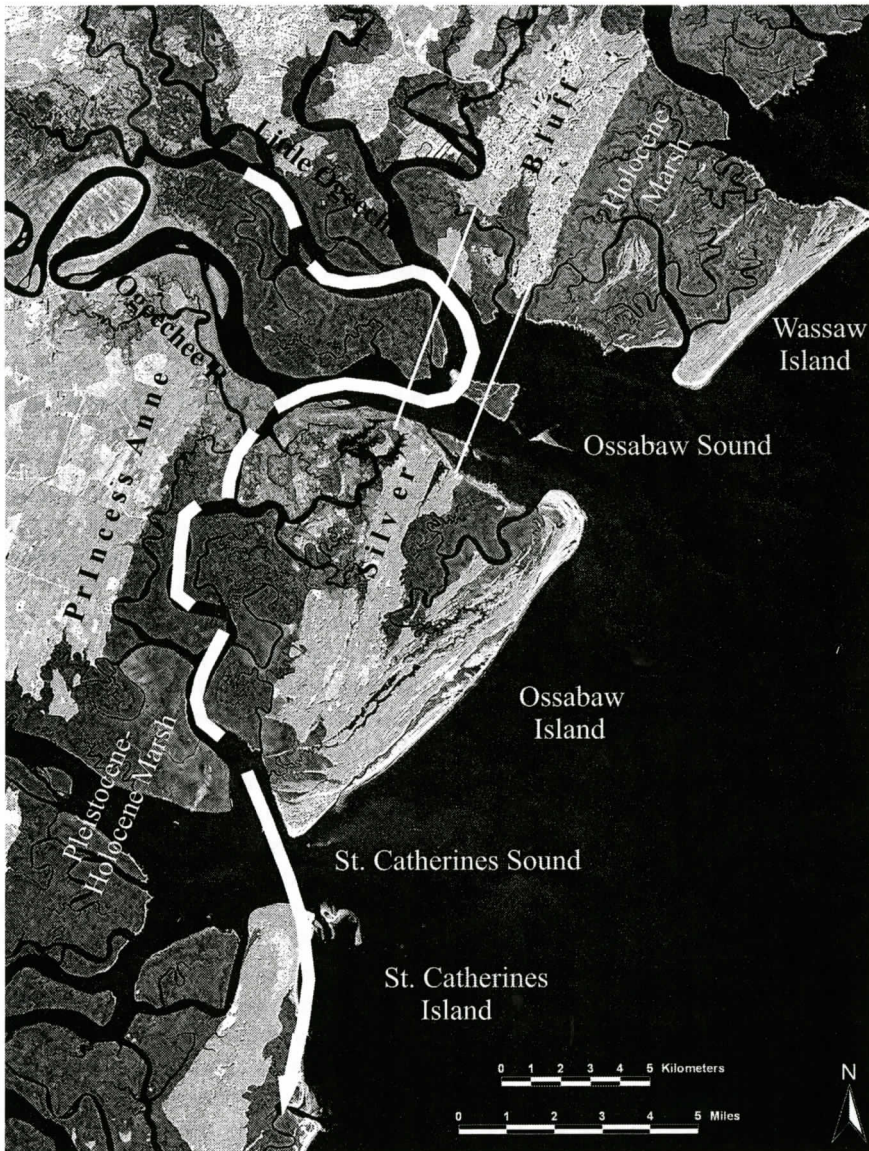


Figure 9. Satellite imagery suggesting that the Ogeechee River originally entered the Atlantic through St. Catherines Sound. Note the way in which Ossabaw Sound has been widened so that it erodes the Silver Bluff Formation on both banks. By contrast St. Catherines Sound has been infilled from both sides by prograding spits.

(Deptford period and later). Although lacking confirmation in the field, there is also strong circumstantial evidence for relocation of the Ogeechee River in a manner similar to the Brunswick River. The Ogeechee appears to have been diverted from St. Catherines Sound and now bisects both the Silver Bluff and Ho-

locene beach ridges (figure 9). It may be inferred that the Silver Bluff barrier was breached by erosion on the east side of a large meander now preserved at the confluence of the Ogeechee and Little Ogeechee rivers. As with the Brunswick River, avulsion occurred within the flooded marshes behind the Silver Bluff

barrier, again probably as a result of extreme high water during a single storm. A seismic profile along the shelf seaward of St. Catherines Sound (G2 of Oertel and others, 1991) shows a large paleochannel, possibly the Ogeechee, beneath the modern inlet and this has been traced across the shelf by Littman (2000). Another paleochannel seaward of Wassaw Island (G1 of Oertel and others, 1991) appears to be too far north to be associated with the Ogeechee.

These observations imply that the changes observed at St Simons Sound may be part of a regional trend rather than an isolated event contingent on storm erosion.

WAVE AND TIDAL MECHANISMS

Oertel (1975) described a combination of two systems that shape islands and inlets in the Georgia Bight. The first is a wave-driven system (river of sand) that leads to dominant longshore transport to the south; erosion on the north end of islands and spit development on the south. The second is a tide-driven system that breaks the longshore transport into cells (inlet sediment cells), prevents migration and encourages relatively straight inlets. Short islands with straight inlets currently form in tide-dominated, mesotidal situations like those at the apex of the Georgia Bight (Hayes, 1994), while long, thin spit-shaped islands with displaced inlets occur on wave-dominated microtidal coasts like those epitomized in the Carolinas. Although, the Sea Islands are currently tide-dominated, the geometry of earlier Pleistocene barriers indicates the possibility of a wave-dominated regime under broadly similar bathymetric conditions during the past (Winkler & Howard, 1977; Rhea, 1986).

The spacing of inlets on the Georgia coast is determined by the balance between wave and tidal processes. At the same time the actual position of the inlets is constrained by the dispersal of rivers crossing the coastal plain and the distribution of old Pleistocene barriers and marshes. Low-lying tracts of marsh are clearly more conducive for the relocation of inlets than indurated beach ridges. Thus it is not surprising that Brunswick River relocated at St. Simons

inlet. The pattern of tidal creeks in the marsh landwards of the Silver Bluff barrier suggests that a number of inlets may have experienced similar jumps as explained above.

Oertel (1975) drew attention to an apparent narrowing of inlets between the Sea Islands as a result of Holocene deposition on the northern as well as southern ends of some islands. This is especially clear at St. Catherines Sound, St. Andrews Sound and St. Mary's River, although not at St. Simons and Sapelo sounds. He suggested a number of possible causes including reduction in the volume of the backbarrier tidal prism due to infilling of lagoons and accretion of marshes, local reversals in the direction of longshore transport, and adjustments due to shoreline retreat. Redirection of distributaries from one inlet to another should be added as an important alternative.

It is estimated that more than 75% of mobile sand on the central part of the South Carolina shore is held in ebb-tidal deltas (Hayes, 1994). Changes in patterns of erosion and sedimentation are likely associated with changes to these huge sand reservoirs (Oertel, 1975; Davies, 1994a). In particular, these ebb-tidal deltas are responsible for local reversals in the direction of longshore transport that leads to accretion immediately down-drift (i.e. on the north end of drumstick shaped islands). Both straightening and abandonment of an inlet have the potential of releasing large volumes of sand to the barrier island in the lee of the tidal delta. Straightening, immediately transfers sand from one sediment cell to the next down-drift, either through dissection and detachment of a spit or as a result of the rerouting of ebb-tidal channels (Oertel, 1977). Abandonment, even if only partial, reduces tidal volume and leads to sedimentation at the inlet throat. In particular, the reduction of flow at St. Andrews Sound was likely the result of loss of drainage from Brunswick River and the narrowing of St. Catherines Sound may be related to loss of the Ogeechee. Although these switches may be temporally independent they derive from the same cause; straightening of inlets due to rising sea level.

The volume of tidal-prisms and effectiveness of longshore transport are both critically depen-

dent on relative sea level because of its effect on accommodation space within backbarrier environments and rate of sediment supply to the shoreface. Marine transgression tends to favor the tidal system. The volume of the back-barrier tidal prism (water trapped in inlets and marshes), as well as tidal-current velocity, increases. At the same time sediment is trapped upstream in the estuaries. As base level rises, inlets are destabilized and adjust by breaching spits and straightening their estuaries. Conversely, during stillstand or minor regression, the volume of back-barrier tidal prisms is reduced and sand is flushed into the longshore transport system. These conditions tend to stabilize the estuaries, reduce ebb-tidal currents and reinforce the longshore transport system leading to spit building and inlet migration. One possible explanation of the variation between wave and tide dominated shorelines recognized by Rhea (1986) for the Pleistocene may depend on whether shorelines were abandoned after a period of rapid transgression or slow retreat. A rapid retreat following transgression would leave a tide-dominated coast while a slow retreat would favor a wave-dominated coast. Currently, the interface between wave- and tide-dominated morphology occurs at the Santee-Pee Dee delta in the north and St. John's River in the south, but the tide dominated sector may be expected to expand (transgression) and contract (regression) over time.

Based on this scenario the straightening of inlets on the Georgia coast is most likely a response to modern sea level rise, while the abandoned inlets may suggest a more effective wave-driven longshore transport system in the recent past, perhaps related to a slower rate of sea level rise, stillstand or even slight regression. Alternatively, the abandoned inlets may be antecedent features established earlier during the Pleistocene.

Opinion is divided concerning the trajectory of sea level rise during the Holocene. The most recent data (Fleming and others, 1998) suggests a relatively smooth curve with a uniform rise of about 10 m /century from around 15 ka to 7 ka and a constant value of between 3-5m during the last 7 ka. However, this curve deliberately

emphasizes eustatic effects while avoiding local isostatic adjustments. In the case of a uniform rise in relative sea level the abandoned inlets are most likely antecedent features. On the other hand if the supposition of a slight regression or stillstand around -3m between 4300-3600 BP is correct (DePratter & Howard, 1981; Gayes and others 1992; Colquhoun and others, 1995) this might account for a wave-dominant system. Archaeologists identify this stillstand as a time of major change in the coastal ecosystem that apparently disrupted the St. Simons cultural phase (4350-3000 BP) and led to replacement by the younger Deptford, Swift Creek, Wilmington and Savannah phases (2400-450 BP) (Crook, 2006, 2007). Our radiometric dates from the northern end of Jekyll Island indicate that Brunswick River was captured to St. Simons Sound some time around 1480 BP., consistent with either alternative.

CONCLUSIONS

The straightening of estuaries at the head of the Georgia Bight corresponds to the transition from a wave dominated system in the Carolinas and Florida peninsula to a tide dominated system in the Sea Islands. The process is especially favored by the modern transgression which, by raising base level, has increased the volume of backbarrier tidal prisms and trapped sediment within the estuaries and marshes, thus reducing the supply of sand to the shoreface. The end effect is to favor tidal over wave processes and break the longshore transport system into a series of compartmentalized cells. Within this system large volumes of sand are stored in ebb-tidal shoals.

The location of estuaries is controlled by antecedent drainage and particularly by the distribution of Pleistocene barrier islands and marshes that are being selectively flooded by rising sea levels. Drainage changes due to avulsion are relatively easy within the tangle of tidal channels characteristic of the backbarrier but are constrained by the uplands formed by Pleistocene barrier islands. Such changes may affect the longshore transport system by releasing sand; through dissection of spits or redirection

of ebb-tidal channels. Brunswick River formerly debouched through St. Andrews Sound but relocated to St. Simons Sound some time between 1950 and 1480 BP, during the Deptford archaeological phase. In so doing it abandoned a southeasterly inlet for a more direct route to the coast. In a similar way the Ogeechee appears to have abandoned a previous estuary at St. Catherines Sound in favor of its present outfall in Ossabaw Sound, and Sapelo Sound probably formed by the breaching of St. Catherines spit. Such changes offer a satisfactory explanation for the adjustments in inlet width recognized by Oertel (1975). The narrowing of St. Andrews, St. Catherines and perhaps Doboy sounds are the result of loss of tidal distributaries while St. Simons, Sapelo, and Ossabaw sounds are newly expanded.

ACKNOWLEDGEMENTS

This paper is the result of undergraduate research carried out in the course of annual field trips to Jekyll Island. It is a tribute from the University of West Georgia to Dr. Jim Henry for his many years of research and service on the Georgia coast. The work was supported in part by a faculty research grant from the University of West Georgia. Special thanks are due to Dave Bush and Rob Young who first encouraged the vibracoring program and to John Congleton who helped with the satellite and airphoto imagery; also to the numerous undergraduates who helped manhandling core and equipment. Thanks also to Irv Garrison and Dave Bush for their helpful reviews.

REFERENCES

- Baldwin, W.E., Morton, R.A., Putney, T.R., Katuna, M.P., Harris, M. S., Gayes, P.T., Driscoll, N.W., Denny, J.F., Schwab, W.C., 2006, Migration of the Pee Dee River system inferred from ancestral paleochannels underlying the South Carolina Grand Strand and Long Bay inner shelf: *Geological Society of America, Bulletin* v. 118, p 533-549.
- Bishop, G.A., Hayes, R.H., Meyer, B.K., Rollins, H.E., Rich, F.J., Thomas, D.H., Vance, R.K., 2007, Transgressive barrier island features of St. Catherines Island, Georgia; p. 39-85, *Guide to fieldtrips, Geological Society of America, Southeastern Section 2007*; *Geology & Geography, Georgia Southern Univ. Contribution* 1, 198 p.
- Booth, R.K., Rich, F.J., Bishop, G.A., 1999, Palynology and depositional history of late Pleistocene and Holocene coastal sediments from St. Catherines Island, Georgia, U.S.A.; *Palynology* v. 23, p. 67-86.
- Chowns, T. M., Schultz, B. S., Griffin, J. R., 2002, Jumping inlets, spits and islands on the Georgia coast, USA; *Geological Society of America, Abstracts with Programs* v.34, no 2, p.110.
- Chowns, T. M., Schultz, B. S., Griffin, J. R., 2006, Recent changes on Jekyll Island, Georgia, caused by relocation of Brunswick River; *Georgia Geological Society Guidebook*, v 26, p1-14.
- Cleary, W., Fitzgerald, D., Buynevich, I., Marden, T., Knierim, A., Doughly, D, 2004, Inlet-associated marsh islands: North Inlet, South Carolina; *Geological Society of America, Abstracts with Programs*, v.36, no. 2, p.52
- Colquhoun, D.J., Brooks, M.J., Stone, P.A., 1995, Sea-level fluctuation: emphasis on temporal correlations with records from areas with strong hydrologic influences in the southeastern United States: *Journal of Coastal Research, Special Issue* 17, p 191-196.
- Crook, M.R., 1985, An archaeological survey of Jekyll Island, Georgia: unpublished report prepared for the Jekyll Island Authority, 50 p.
- Crook, M.R., 2006, An introduction to the archeology of Jekyll Island; *Georgia Geological Society Guidebook* v. 26, p. 25-29
- Crook, M.R., 2007, Prehistoric pile dwellers within an emergent ecosystem: an archeological case of hunters and gatherers at the mouth of the Savannah River; *Human Ecology* v 35, p.223-337.
- Davis, R. A., 1994a, Barrier Island Systems- a Geologic Overview in Davis R.A. (ed.) *Geology of Holocene Barrier Island Systems*: Springer-Verlag, chap. 1, p. 1-46.
- Davis, R. A., 1994b, Barriers of the Florida Gulf Peninsula; in Davis R.A. (ed.) *Geology of Holocene Barrier Island Systems*: Springer-Verlag, chap. 5, p. 167-205.
- Davis, R.A., Hayes, M.O., 1984, What is a wave-dominated coast?; *Marine Geology* v.60, p.313-329.
- DePratter, C.B., Howard, J.D., 1981, Evidence for a sea level lowstand between 4500 and 2400 years B.P. on the southeast coast of the United States; *Journal of Sedimentary Petrology* v. 51, p. 1287-1295.
- Farrell, K.M., Hoffman, C.W., Henry, V.J., 1993, Geomorphology and facies relationships of Quaternary barrier island complexes near St. Mary's, Georgia: *Georgia Geological Society Guidebook* v. 13, 98 p.
- Fleming, K., Johnston, P., Zwartz, D., Yusuke, Y., Lambeck, K., Chappell, J., 1998, Refining the eustatic sea-level curve since the Last Glacial Maximum using far- and intermediate-filed sites; *Earth & Planetary Science Letters*, v.163, p. 327-342.
- Gayes, P.T., Scott, D.B., Collins, E.S., Nelson, D.D., 1992, A Late Holocene sea-level irregularity in South Caro-

HOLOCENE TRANSGRESSION AND RELOCATION OF ESTUARIES

- lina; Society of Economic Paleontologists and Mineralogists, Special Publication 48 p. 154-160.
- Gibbard, P., van Kolfschoten, T., 2005, The Pleistocene and Holocene Epochs, p. 441-452, in Gradstein, F. M., Ogg, J. G., Smith, A. G. (eds.); A Geologic Time Scale 2004, Cambridge University Press, Cambridge, 589 p.
- Hails, J.R., Hoyt, J.H., 1969, An appraisal of the evolution of the lower Atlantic coastal plain of Georgia, USA: Institute of British Geographers, Trans. & Papers, v. 46, p. 53-68.
- Hayes, M.O., 1994, The Georgia Bight Barrier System; in Davis R.A. (ed.) Geology of Holocene Barrier Island Systems: Springer-Verlag, chap. 7, p. 233-304.
- Henry, V.J., 2005, Geology of the Georgia coast; www.georgiaencyclopedia.org
- Henry, V.J., Fritz, W.J., 1985, Coastal processes and barrier island development, Jekyll Island, Georgia; Georgia Geological Society Guidebook for 20th Annual Field Trip p. 20-57.
- Howard, J.D., Reineck, H.-E., 1972, Georgia Coastal Region, Sapelo Island, U.S.A.: Sedimentology and Biology. IV Physical and biogenic sedimentary structures of the nearshore shelf: Senckenbergiana Maritima; b.4, p. 81-123.
- Howard, J.D., Frey, R.W., Reineck, H.-E., 1972, Georgia Coastal Region, Sapelo Island, U.S.A.: Sedimentology and Biology: Introduction; Senckenbergiana Maritima; b.4, p. 3-14.
- Hoyt, J.H., 1967, Barrier island formation; Geological Society of America Bulletin; v. 78, p. 1125-1136.
- Hoyt, J.H., Hails, J.R., 1974, Pleistocene stratigraphy of southeastern Georgia p. 191-205 in Oaks, R.Q., DuBar, J.R.(eds.), Post-Miocene stratigraphy, central and southern Atlantic coastal plain: Utah University Press, Logan Utah.
- Hoyt, J.H., Henry, V.J., 1967, Influence of island migration on barrier-island sedimentation: Geological Society of America Bulletin v. 78, p.77-86.
- Linsley, D.M., 1993, Depositional environments of St. Catherines Island: Their relationship to Late Quaternary sea-level change and application to late Paleozoic cyclic stratigraphy; unpublished PhD thesis, University of Pittsburgh, 186 p.
- Linsley, D.M., Bishop, G.A., Rollins, H.B., (in press), Stratigraphy and geologic evolution of St. Catherines Island: in Thomas, D.H., (ed.) Native American landscapes of St. Catherines Island, Georgia; American Museum of Natural History, Anthropological Papers.
- Littmann, S.L., 2000, Pleistocene/Holocene sea level change in the Georgia Bight: a paleoenvironmental reconstruction of Gray's Reef National Marine Sanctuary and J. Reef; unpublished MS thesis, University of Georgia.
- Oertel, G.F., 1973, Examination of textures and structures of mud in layered sediments at the entrance of a Georgia tidal inlet: Journal of Sedimentary Petrology v. 43 p. 33-41.
- Oertel, G.F., 1975, Post Pleistocene island and inlet adjustment along the Georgia coast: Journal of Sedimentary Petrology v. 45, p.150-159.
- Oertel, G.F., 1977, Geomorphic cycles in ebb deltas and related patterns of shore erosion and accretion; Journal of Sedimentary Petrology, v. 47, p.1121-1131.
- Oertel, G. F., Henry, V. J., Foyle, A.M., 1991, Implications of tide-dominated lagoon processes on the preservation of buried channels on a sediment-starved continental shelf; in Swift, D. J.P., Oertel, G. F., Tillman, R. W., Thorne, J. A., (eds.) Shelf Sand and Sandstone bodies; geometry, facies and sequence stratigraphy; International Association of Sedimentologists special pub 14, p 379-394.
- Rhea, M.W., 1986, Comparison of Quaternary shoreline systems in Georgia: Morphology, drainage and inferred processes of formation; unpub. MS. thesis, University of Georgia, 73 p.
- Shackleton, N.J., Opdyke, N.D., 1973, Oxygen isotope and paleomagnetic stratigraphy of equatorial Pacific core V28-238: oxygen isotope temperatures and ice volumes on a 10⁵ year and 10⁶ year scale; Quaternary Research, v.3, p. 39-55.
- Thomas, D.H., Rollins, H. B., DePratter, C.B., (in press), The changing shape of St. Catherines Island: in Thomas, D.H.,(ed.) Native American landscapes of St. Catherines Island, Georgia; American Museum of Natural History, Anthropological Papers.
- Voorhies, M. R., 1973, Vertebrate fossils of coastal Georgia; a field geologist's guide, in Frey, R.W., (ed.) The Neogene of the Georgia coast; Georgia Geological Society 8th Annual Field Trip, University of Georgia, Athens GA.
- Williams, M., Thompson, V., 1991, A guide to Georgian Indian pottery types; Early Georgia v. 27 (1), p.1-166.



HIGH RESOLUTION SHALLOW GEOLOGIC CHARACTERIZATION OF A LATE PLEISTOCENE EOLIAN ENVIRONMENT USING GROUND PENETRATING RADAR AND OPTICALLY STIMULATED LUMINESCENCE TECHNIQUES: NORTH CAROLINA, USA

¹DAVID MALLINSON, ²SHANNON MAHAN, ³CHRISTOPHER MOORE

¹*Dept. of Geological Sciences, East Carolina University, Greenville, NC 27858, mallinsond@ecu.edu*

²*USGS Optically Stimulated Luminescence Dating Laboratory, Denver Federal Center, Denver CO, 80225*

³*Coastal Resources Management Program, East Carolina University, Greenville, NC 27858*

ABSTRACT

Geophysical surveys, sedimentology, and optically-stimulated luminescence age analyses were used to assess the geologic development of a coastal system near Swansboro, NC. This area is a significant Woodland Period Native American habitation and is designated the "Broad Reach" archaeological site. 2-d and 3-d subsurface geophysical surveys were performed using a ground penetrating radar system to define the stratigraphic framework and depositional facies. Sediment samples were collected and analyzed for grain-size to determine depositional environments. Samples were acquired and analyzed using optically stimulated luminescence techniques to derive the depositional age of the various features. The data support a low eolian to shallow subtidal coastal depositional setting for this area. LIDAR data reveal ridge and swale topography, most likely related to beach ridges, and eolian features including low-relief, low-angle transverse and parabolic dunes, blow-outs, and a low-relief eolian sand sheet. Geophysical data reveal dominantly seaward dipping units, and low-angle mounded features. Sedimentological data reveal mostly moderately-well to well-sorted fine-grained symmetrical to coarse skewed sands, suggesting initial aqueous transport and deposition, followed by eolian reworking and bioturbation. OSL data indicate initial coastal deposition prior to ca. 45,000 yBP, followed by eolian reworking and low dune stabilization at ca. 13,000 to 11,500 yBP, and

again at ca. 10,000 yBP (during, and slightly after the Younger Dryas chronozone).

INTRODUCTION

Numerous geological studies have been performed of the barrier islands fronting the Atlantic Coastal Plain of North Carolina (Godfrey and Godfrey, 1976; Herbert, 1978; Steele, 1980; Heron and others, 1984; Inman and Dolan, 1989; Riggs and Ames, 2003; Culver and others, 2006; etc.). Most of these studies have focused on the processes governing barrier island formation and evolution, as well as the age of the barrier islands in general, and the age of different components of the barriers. The barrier islands along the Atlantic Coastal Plain are Holocene in age (<10,000 yBP), and represent the updip limit of the developing stratigraphic sequence corresponding to the present transgressive to highstand sea-level event. The Holocene barrier/estuarine system is perched on late Pleistocene sequences that formed between ca. 125 thousand years ago (ka) and ca. 51 ka (Riggs and others, 1992; Mallinson and others, 2005; Mallinson and others, 2007a; Mallinson and others, 2007b). The updip limit of the Pleistocene sequence is landward of the modern system, and typically forms the mainland estuarine shoreline. Few investigations have been performed to determine the age and origin of the mainland shoreline features, although Pleistocene and Holocene sea-level and paleoclimate records are preserved here.

In addition to the potential record of sea-level and paleoclimate change in this setting, the backbarrier mainland shoreline commonly is

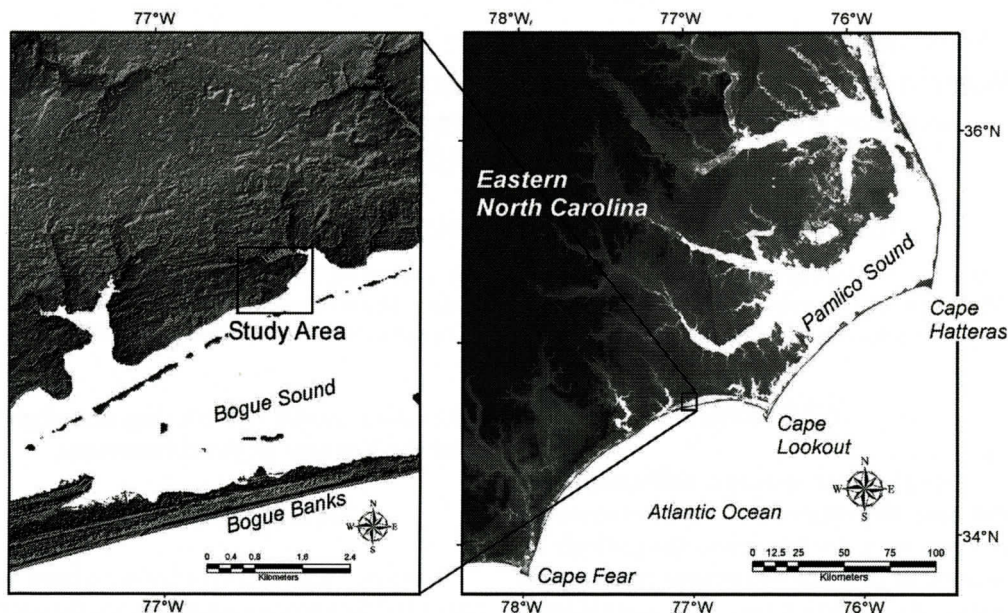


Figure 1. Location of the Broad Reach archaeological site in coastal North Carolina. Elevation data were acquired by LiDAR and are available at www.ncfloodmaps.com/default_swf.asp

the setting for archaeological sites containing artifacts of Native American communities. Native Americans typically utilized high ground adjacent to productive coastal waters. The site investigated for this study is a significant archaeological site, the Broad Reach Archaeological site, which contains an ossuary of some 30 individuals, along with middens and artifacts of the Woodland Period (ca. 500-1000 yBP) (Mathis, 1993). A geological investigation was undertaken to ascertain the general geomorphic environment in which this community existed, and to aid in finding additional artifacts using high resolution ground penetrating radar techniques. A bonus was the opportunity to determine the origin and age of the geomorphic features, the shallow geologic framework and development, the sedimentologic and geophysical attributes, and paleoclimate significance. These geological attributes are the focus of this manuscript. Due to the initial archaeological focus of the investigation (with artifacts situated only to ca. 0.5 m depth), the geological component was purposefully confined to the shallow (<4 m depth) sediment column.

STUDY AREA

The Broad Reach archaeological site is located along the southeast coast of North Carolina, in Carteret County (Figure 1). The coastal region faces southward in this area, and is microtidal. The study location occurs along the low-energy estuarine shoreline of Bogue Sound, and is sheltered from open ocean wave energy of the Atlantic by the presence Bogue Banks, a 39 km long barrier island (Figure 1) (Steele, 1980; Heron and others, 1984). Wind directions are dominantly from the south during summer months and from the northwest during winter months.

The elevation of the study area ranges from 0 to 5.8 m (NAVD88), with higher elevations to the west (ca. 4 m ave.) and lower elevations to the east (ca. 1.5 m ave.) (Figure 2). The relief of the area defines subtle ENE trending ridge and swale topography (Figure 1), characteristic of beach ridge morphology.

Previous studies of this specific area are limited to the archaeological components (Mathis, 1993). Geological investigations have been restricted to Bogue Banks or Bogue Sound (Steele, 1980; Heron and others, 1984; Sproat,

GEOLOGY OF A LATE PLEISTOCENE EOLIAN ENVIRONMENT

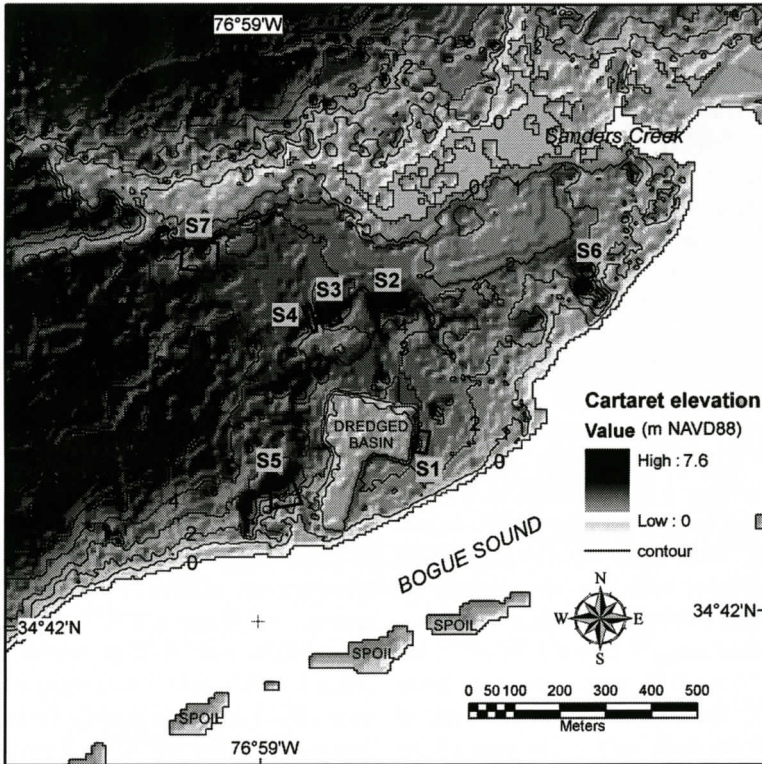


Figure 2. Shaded relief map of the study area with 1 m contours based on LiDAR data, and sites assessed in this study.

1999). The field site consists of a Pleistocene beach ridge complex that is situated above Tertiary strata (at a depth of ca. 5 m below msl) (Steele, 1980).

METHODS

Ground penetrating radar surveys were conducted using a Geophysical Survey Systems (GSSI) SIR-2000 unit, and a 500 MHz antenna. A recording window of 250 ns was used, which provided potential data acquisition to a depth of ca. 8.3 m (using a dielectric of 25, typical of saturated sands). Surveys were conducted using a survey wheel, and 10 scans per meter, and 512 samples per scan. 3-d subsurface surveys were performed where minimal ground-cover was present and utilized either 0.5-m or 1-m spaced survey lines. Survey lines were georeferenced using a Trimble differential GPS. GPR Data were processed using Radan v6.5 software

(©GSSI). Data were bandpass filtered and gain-enhanced.

Stratigraphy was documented at man-made bluffs or backhoe cuts. Sediment samples for grain size analyses were collected at 20 cm intervals at exposures. Sediment samples were split in the laboratory, and analyzed for grain-size using sieves and Roe-tap at 0.5 phi intervals according to standard methodology (Folk, 1974). Grain size statistics (mean, inclusive sorting and skewness) were determined using the GRADISTAT program (Blott and Pye, 2001) and the statistical methods of Folk and Ward (1957).

Samples for optically stimulated luminescence dating were acquired from exposures at 4 sites. Samples were sent to the US Geological Survey Luminescence Dating Laboratory in Denver, CO for analysis. Standard procedure includes treatment with 10% HCl and 30% H₂O₂ to remove carbonates and organic matter,

then sieving to extract the 150-170 μ m-size fraction. Quartz and feldspar grains were separated by density using Na-polytungstate ($\rho=2.58$ gcm⁻³). The quartz fraction was etched using 40% HF for 80 min followed by 12N HCl for 30 min to remove the outermost layer affected by alpha radiation. The quartz grains were mounted on stainless steel discs using Silkospray™. Dose recovery and preheat plateau tests were performed to ensure that the sediments were responsive to optical techniques and that the proper temperatures were used in producing the D_e values. Acceptable preheat temperatures ranged from 200-280°C. Samples were analyzed by SAR (Murray and Wintle, 2000) using a RISØ array of blue LEDs centered at 470 nm. Detection optics comprised Hoya 2xU340 and Schott BG-39 filters coupled to an EMI 9635 QA Photomultiplier tube. Measurements were taken with a RISØ TL-DA-15 reader. β radiation was applied using a 25 mCi ⁹⁰Sr/⁹⁰Y in-built source. The OSL measurements were made at 125°C for 40 seconds after preheat of 220°C for 10 seconds with a cut heat of the same time. An IRSL stimulation of 100 seconds before the blue-light stimulation of 40 seconds was used to completely drain any residual feldspar contamination. Approximately 30 to 50 aliquots per sample were run for the SAR blue-light equivalent dose determination.

The elevation of the ground surface at each site was determined using LiDAR data (www.ncfloodmaps.com). Sample elevations were then measured from the ground surface with a measuring tape. These data use the NAVD 88 vertical datum, and provide a reported accuracy of ± 25 cm.

RESULTS

Seven sites were selected for evaluation by the archaeological group, based upon knowledge of artifacts in the area (Figure 2). Site elevations and analyses performed are listed in Table 1. A description of the lithostratigraphy, geophysical characteristics, and grain size characteristics is presented for each site. Optically stimulated luminescence ages are presented at the end of the Results section in order to place the physical results in a chronostratigraphic framework.

Lithostratigraphy

The lithostratigraphic framework of all sites is generally characterized by variably orange (Fe-stained), mottled to laminated, fine-grained quartz sand (Figures 3 to 7). Gravel-sized iron-concretions were evident within the profile at Sites 1 and 3. Site 2 was unique in the occurrence of a burrowed, heavily Fe-stained B-horizon at 3.5 m below ground surface. In other sites, no obvious lithostratigraphic horizons were present.

Site 1

Site 1 is located adjacent to the marina basin and the major archaeological dig (Figure 2). Elevation of the site is ca. 2.7 m. A 40 x 20 meter 3-d ground penetrating radar survey was performed in this area, using a 500 MHz antenna. Radar attenuation occurred at approximately 2.5 to 3 m subsurface.

Exposure of the sediments was made possible by digging a 1.8-m deep trench with a back-

Table 1. Characteristics of investigated sites, surveys and sample information.

Site	Elevation	GPR survey	Exposure	Sediment	OSL analyses
1	2.7	40 x 20 m 3-d	1.8 m trench	8	1
2	4.5 to 4.9	8 2-d lines	Cut bank	7	1
3	4.3 to 5.2	20 x 35 m 3-d	2.0 m trench	6	1
4	3.7 m	2 2-d lines	none	none	none
5	3.7 to 5.8	5 2-d lines	none	none	none
6	5.8	11 x 16 m 3-d	1.8 m trench	9	2
7	3 to 5.2	5 2-d lines	0.8 m pit	6	none

GEOLOGY OF A LATE PLEISTOCENE EOLIAN ENVIRONMENT

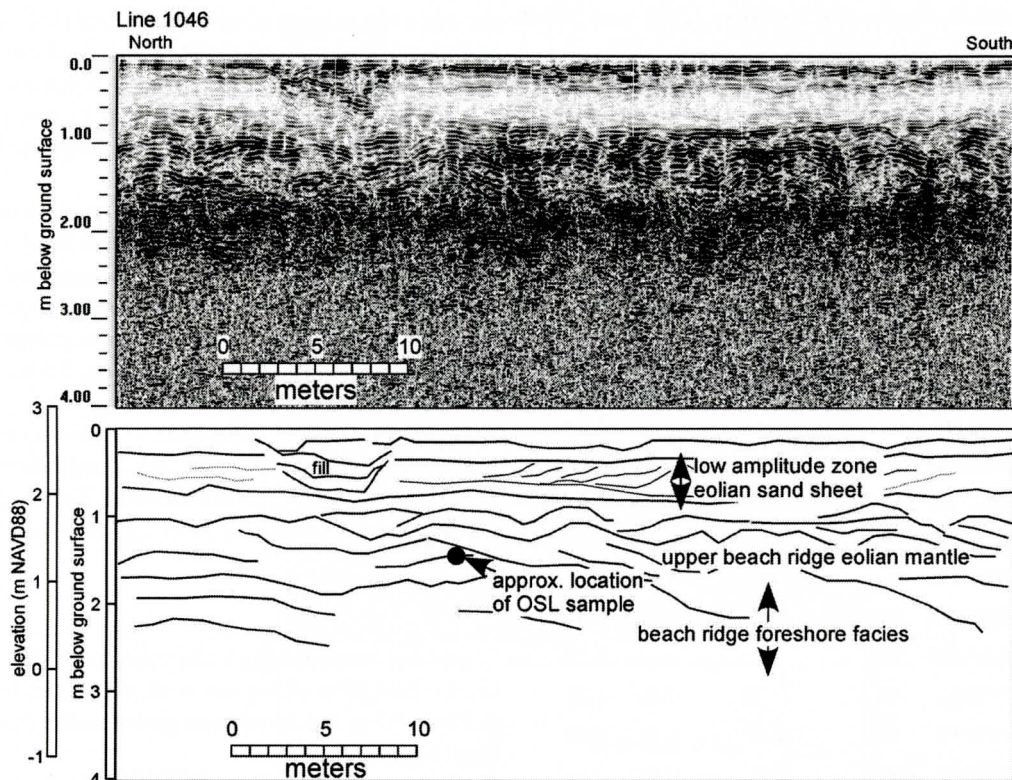


Figure 3. Processed ground penetrating radar data (top) with a line interpretation (bottom) revealing a lower beach ridge unit consisting of seaward (south) dipping reflections, with hummocky bedding, and an upper eolian sand sheet unit.

hoe. Sediments are variably orange (Fe-stained), mottled, fine-grained quartz sand, with scattered gravel-sized iron-concretions. No obvious lithostratigraphic horizons were present.

The radar-stratigraphic character consists of an upper, nearly radar transparent (very low amplitude response) zone between ca. 0.2 and 0.8 m, revealing subtle structure (Figure 3), including northward-dipping small-scale clinoforms. Beneath this zone, the reflection amplitude increases, and reflections exhibit subtle mounded structures, with very low angle, dominantly seaward dipping forms, to approximately 3 m. There is a minor increase in amplitude at ca. 1.7 m.

One significant high-amplitude feature was noted in the NW corner of the surveyed area in the upper 60 cm. The feature was excavated and found to be fill material (Figure 3) consisting of coquina (loosely consolidated shell hash). Other

small high amplitude reflections were found to correspond to possible post holes.

Grain size analyses show little variation from 0 to 2 m below ground surface. Sediment is well sorted, coarse skewed, fine sand (ranging from a mean of 2.49 to 2.59 phi; Table 2).

Site 2

Site 2 is located along a low relief east-west trending ridge, covered with pines (Figure 2). The ridge is approximately 4.9 m in elevation at the highest point, and stands approximately 2 to 2.5 m above the surrounding area. Due to the tree cover, a 3-d survey was not possible in this area. A total of eight GPR survey lines were run at this site; four in the N-S direction, and four in the E-W direction.

Exposure of the sediments along a man-made cut bank at the southern edge of the ridge permitted a stratigraphic assessment. Sediments

Table 2. Grain size statistics (Folk and Ward, 1957), are variably orange (Fe-stained), mottled to laminated, fine-grained quartz sand. A prominent burrowed, heavily Fe-stained B-horizon is evident at approximately 3.5 m below ground surface, and occurs in contact with laminated sand below.

Sample	depth (cm)	Mean phi	Sort	Skew
BRS1-20	20	2.58	0.42	-0.20
BRS1-40	40	2.58	0.42	-0.21
BRS1-60	60	2.56	0.42	-0.23
BRS1-80	80	2.52	0.47	-0.20
BRS1-100	100	2.59	0.44	-0.21
BRS1-120	120	2.55	0.50	-0.23
BRS1-140	140	2.49	0.50	-0.24
BRS1-160	160	2.52	0.45	-0.17
BRS2-60	60	2.49	0.48	-0.23
BRS2-100	100	2.46	0.47	-0.11
BRS2-120	120	2.51	0.47	-0.21
BRS2-270	270	2.57	0.36	-0.16
BRS2-350	350	2.31	0.70	-0.42
BRS2-365	365	2.48	0.43	-0.17
BRS2-385	385	2.46	0.44	-0.13
BRS3-20	20	2.30	0.60	-0.21
BRS3-40	40	2.32	0.61	-0.26
BRS3-60	60	2.25	0.58	-0.20
BRS3-80	80	2.22	0.59	-0.18
BRS3-100	100	2.21	0.58	-0.16
BRS3-120	120	2.21	0.60	-0.19
BRS6-20	20	2.52	0.48	-0.20
BRS6-40	40	2.56	0.46	-0.30
BRS6-60	60	2.42	0.55	-0.25
BRS6-80	80	2.06	0.86	-0.33
BRS6-100	100	1.95	0.77	-0.09
BRS6-120	120	2.02	0.71	-0.12
BRS6-140	140	2.04	0.67	-0.09
BRS6-160	160	1.90	0.77	-0.05
BRS6-180	180	2.12	0.67	-0.20
BRS7-1-40	40	2.06	0.60	-0.07
BRS7-1-60	60	2.15	0.61	-0.12
BRS7-1-80	80	2.18	0.61	-0.14
BRS7-2-40	40	2.15	0.59	-0.10
BRS7-2-60	60	2.17	0.57	-0.09
BRS7-2-80	80	2.14	0.55	-0.04

The radar-stratigraphic character consists of an upper, low amplitude reflection zone between ca. 0.2 and 1.6 m (Figure 4). Beneath this zone, the reflection amplitude increases, and reflections exhibit subtle mounded structures. High-amplitude reflections occur at ca. 3.5 and 4.4 m below ground surface.

Grain size analyses show little variation from 0 to 2 m below ground surface. Sediment is well sorted, coarse to very coarse skewed, fine sand (ranging from a mean of 2.31 to 2.57 phi; Table 2).

Site 3

Site 3 is located along a low relief ridge (Figure 2). Elevation of the site is ca. 4.3 to 5.2 m. A 20m x 35 m 3-d survey was performed in this area (Figure 5).

Exposure of the sediments was made possible by digging a 2.0-m deep trench with a backhoe. Sediments are variably orange (Fe-stained), mottled, fine-grained quartz sand, with scattered gravel-sized iron-concretions. No significant stratigraphic horizons were noted.

The radar-stratigraphic character consists of an upper, high amplitude reflection zone between ca. 0 and 0.3 m (Figure 5) which corresponds to the A and O soil horizons. Beneath this zone, the reflection amplitude decreases, and reflections exhibit subtle mounded structures. A medium amplitude horizontal reflection is evident at ca. 1 m, and a high amplitude, slightly hummocky continuous reflection is apparent at ca. 2 m. A discontinuous northward dipping medium amplitude reflection is seen at ca. 4 m.

Grain size data are extremely uniform from 0 to 1.2 m below ground surface. Sediment is moderately well sorted (0.58 to 0.61), coarse skewed (-0.16 to -0.26), fine sand (ranging from a mean of 2.21 to 2.32 phi; Table 2).

GEOLOGY OF A LATE PLEISTOCENE EOLIAN ENVIRONMENT

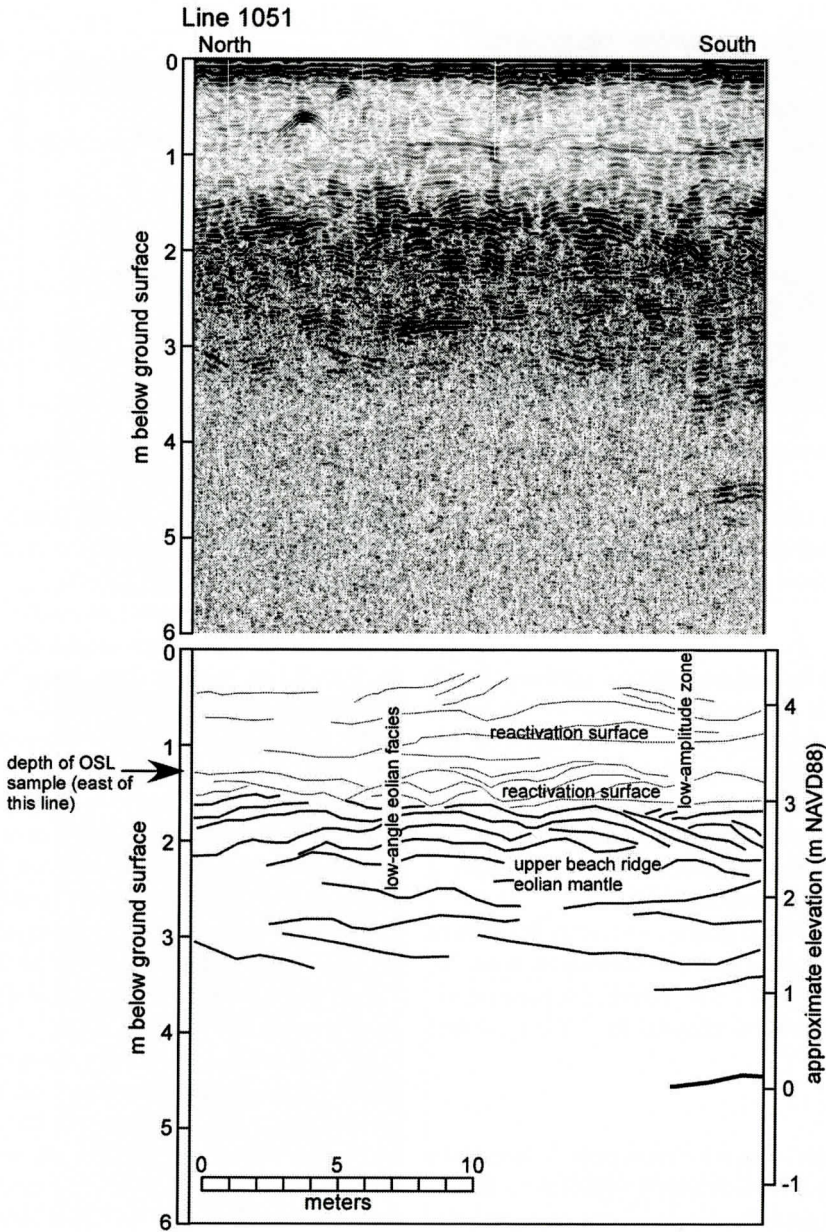


Figure 4. Processed ground penetrating radar data (top) and line interpretation (bottom) illustrating low-angle, mounded dune facies.

Site 4

Site 4 is located immediately to the west of Site 3 (Figure 2). Elevation of the site is ca. 3.7 m. Due to the presence of large debris mounds from land-clearing, only two lines were surveyed in this area. No exposures were dug, and no sediment samples were acquired.

The radar-stratigraphic character is virtually identical to Site 4, and consists of an upper, high amplitude reflection zone between ca. 0 and 0.3 m which corresponds to the A and O soil horizons. Beneath this zone, the reflection amplitude decreases, and data reveal low angle, seaward-dipping reflections. High amplitude

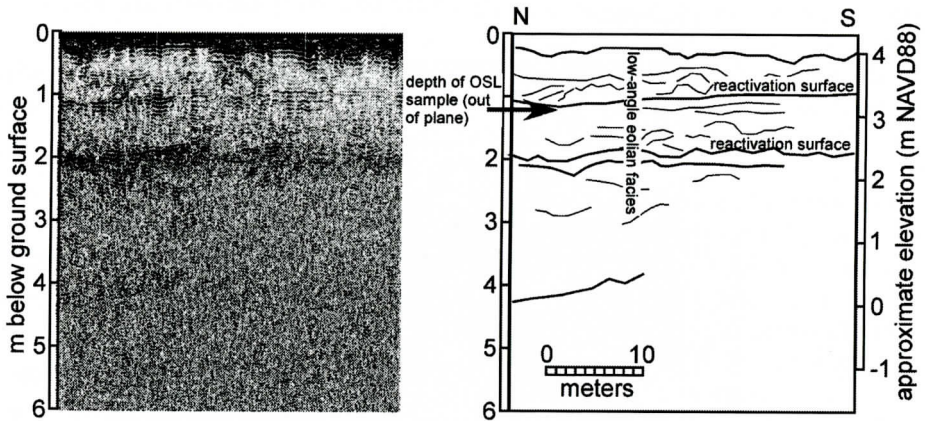


Figure 5. Site 3 - Processed ground penetrating radar data (left) and line interpretation (right).

reflections occur between ca. 2 and 2.5 m, and a discontinuous medium to high amplitude reflection occurs at ca. 3.5 m.

Site 5

Site 5 is located on a narrow northeast trending ridge in the southwest corner of the Broad Reach study area (Figure 2). Elevation of this site is approximately 3.7 to 5.8 m. Due to the presence of debris from land-clearing, tree cover, and dense undergrowth, a 3-d survey was not possible in this area. GPR data were collected along five survey lines.

The radar-stratigraphic character consists of an upper, low amplitude reflection zone between ca. 0.2 and 1.8 m. Within this zone reflections exhibit subhorizontal to subtle mounded structures.

Site 6

Site 6 occupies a location near the crest of a topographic high situated adjacent to Bogue Sound (Figure 2). A homestead occupied this general site. The maximum elevation of the topographic feature is ca. 5.8 m above msl. A 3-d subsurface survey was performed on the northern side of the crest at an elevation of ca. 3.7 to 4.0 m (Figures 6 and 7). Grid parameters were 11m x 16m, with 0.5m line spacing and 23 lines.

Exposure of the sediments was made possible by digging a 1.8-m deep trench with a backhoe. Sediments are variably orange (Fe-

stained), mottled, fine-grained quartz sand. No significant stratigraphic horizons were evident in the trench.

The radar-stratigraphic character generally consists of an upper, high amplitude zone from ca. 0 to 0.3 m, with an underlying low amplitude reflection zone between ca. 0.3 and 1 to 1.5 m (Figures 6 and 7). Several east-west trending high amplitude zones occur in the shallow subsurface to a depth ca. 0.5 m, suggesting shallow disturbance of the site. A series of very high amplitude reflections occur between 1 and 2 m, associated with east-southeast gently dipping clinoforms (Figures 6 and 7). Overall, the general dip pattern indicates seaward accretion, but a zone of small-scale northward dipping clinoforms is present at a depth of ca. 1.5 to 1.8 m.

Grain size analyses show a change from unimodal to bimodal distributions at ca. 1 m below surface. Sediment is generally moderately sorted (below 80 cm) to moderately well sorted (above 80 cm), medium to fine sand (ranging from a mean of 1.90 to 2.56 phi; Table 2). The sediments are symmetrical to coarse skewed.

Site 7

Site 7 is located in the northwest corner of the study area, in a variably cleared and vegetated area (Figure 2). The area is characterized by moderate relief, with high ground to the northwest. Elevation varies from 3 m to 5.2 m. Due to the vegetation and debris, a 3-d survey was not possible in this area. Five 2-d gpr lines were

GEOLOGY OF A LATE PLEISTOCENE EOLIAN ENVIRONMENT

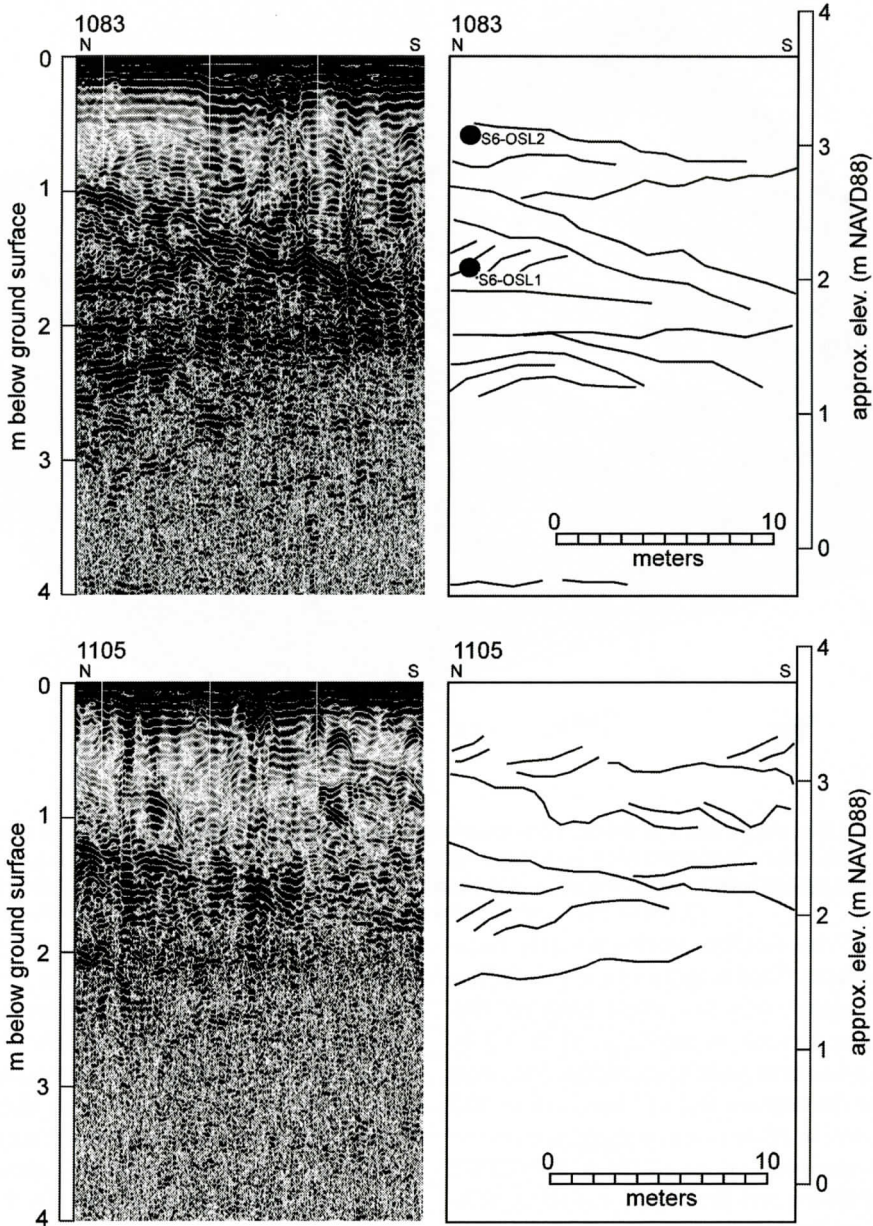


Figure 6. Processed GPR lines 1083 (top) and 1105 (bottom) from Site 6. Processed data are shown on the left, and a line interpretation is shown on the right.

collected in this area. A ca. 30 cm exposure was available for collection of sediment samples, where archaeological test sites were located.

Due to the limited exposure, the detailed stratigraphy was not determined. A small pit was dug to ca. 80 cm below the surrounding soil surface. The upper 20 cm contained the O and

A horizons, and graded downward to an E horizon. Exposed sediments are variably light brown (organic stained) to slightly yellowish-orange (Fe-stained), mottled, fine-grained quartz sand. No significant stratigraphic horizons were evident.

The radar-stratigraphic character consists of

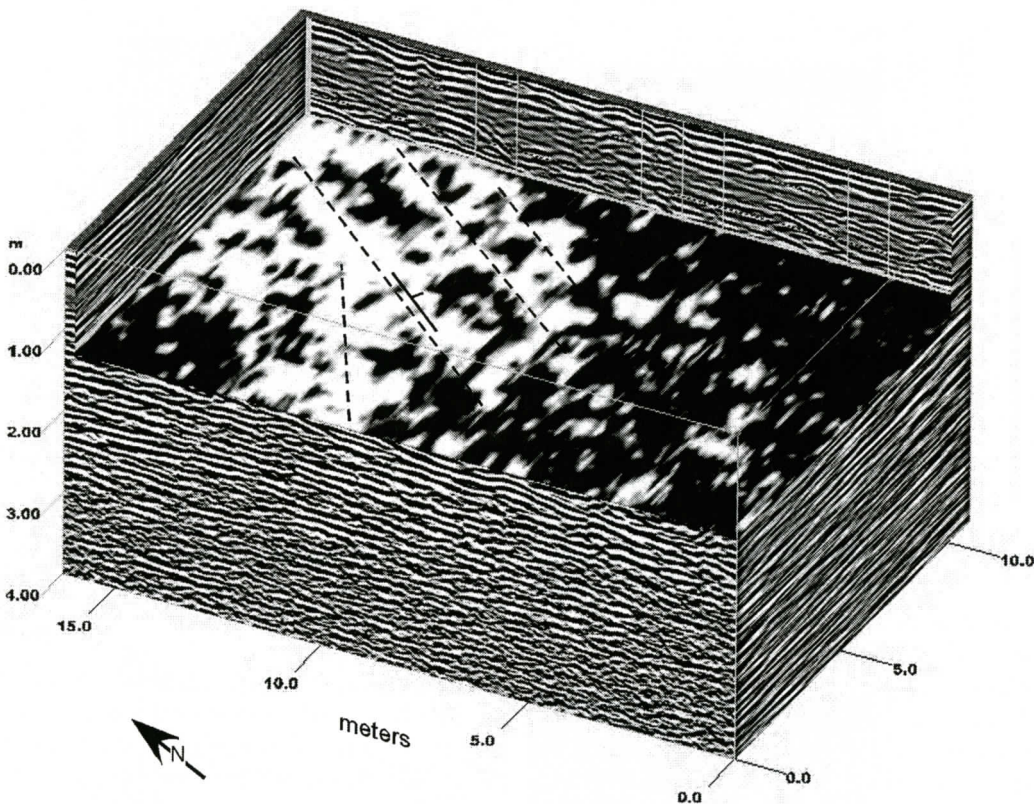


Figure 7. 1.2 m depth slice at Site 6. The orientation is indicated by the north arrow at the bottom of the figure. White indicates high amplitude reflections. Dashed lines emphasize the strike of the clinoforms (NNE), which dip to the east-southeast and indicate sediment transport from the west.

somewhat chaotic (few continuous reflections) to subhorizontal and broadly mounded bedding, with a general, very low angle eastward dip. There is an increase in amplitude at ca. 1.7 m. Several prominent point source reflections were noted on the western end of Line 1111 at <0.5 m, and may be roots or cultural artifacts.

Grain size analyses were only performed to a depth of 80 cm and show little variation. Sediment is moderately well sorted (0.54 to 0.63), fine sand (ranging from a mean of 2.06 to 2.18 phi; Table 2). The sediments are symmetrical to coarse skewed (-0.04 to -0.14).

Optically Stimulated Luminescence Ages

Five OSL ages were determined at three different sites. Data and ages are presented in Fig-

ures 8, and 9 and Table 3. Two-sigma standard deviations are shown on Figure 8. In general, all samples, except S1-OSL1, have low standard deviations, producing high confidence in the assigned ages. S1-OSL1 has a poorer standard deviation which is reflected in the broad distribution of D_e (equivalent dose) seen in Figure 8. The D_e distribution of this sample suggests the incorporation of partially bleached grains. All samples are young enough that saturation is not an issue.

The ages decrease upward and seaward. Four of the five samples provide ages that are Holocene in age, and differ statistically by a maximum of 3600 years, or a minimum of 1400 years. The two samples from the same site, although separated by 1 m, yield statistically identical ages. The oldest age, 42.4 ± 3.72 ka corresponds to the stratigraphically and eleva-

GEOLOGY OF A LATE PLEISTOCENE EOLIAN ENVIRONMENT

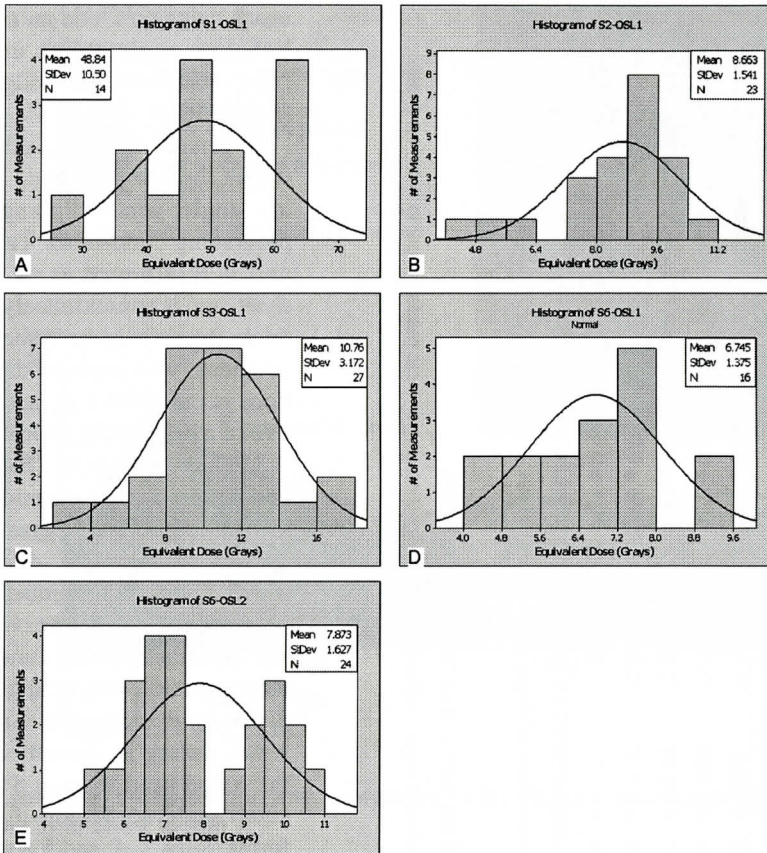


Figure 8. Frequency distribution histograms of Equivalent Dose – D_e (Grays). The age of the sample is calculated by dividing the D_e by the dose rate (Gy/ka) (see Table 2).

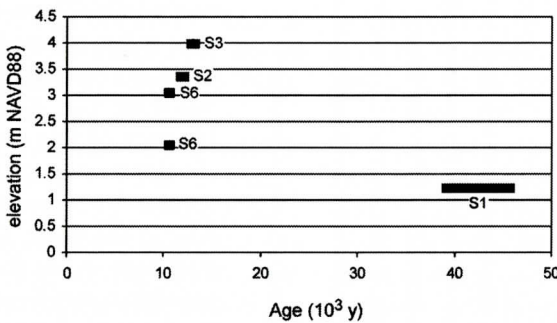


Figure 9. Elevation (vertical axis) in m above MSL (NAVD88), versus OSL age (horizontal axis) in 10^3 years BP (or ka). The width of the age bars represents the 2-sigma error. A significant hiatus apparently occurs at approximately 1.5 to 2.0 m elevation.

tionally lowest sample.

DISCUSSION

A compilation of all results are presented in

Table 4, and summarize the lithostratigraphy, geophysical framework, the grain size data, and interpretation for each site. Geomorphic, geophysical and sedimentological data suggest that the sediments in this area represent a lower

Table 3. OSL sample information.

Table 1: GAMMA SPECTROMETRY, COSMIC AND TOTAL DOSE RATES, EQUIVALENT DOSES AND AGES FOR BROAD REACH, NORTH CAROLINA

Sample #	elevation (m NAVD88)	K (%)	Th (ppm)	U (ppm)	Water Content (%) ^a	Cosmic Dose Rate (Gy/ka) ^b	Total Dose Rate (Gy/ka) ^c	De (Gy) ^d	n ^e	Age (ka) ^f
S1-OSL1	1.24	0.87 ± 0.08	1.30 ± 0.12	0.36 ± 0.05	9 ± 0.5	0.17 ± 0.02	1.07 ± 0.05	45.3 ± 3.24	16 (25)	42.4 ± 3.72
S2-OSL1	3.37	10.37 ± 0.03	1.71 ± 0.12	0.59 ± 0.04	3 ± 0.25	0.18 ± 0.02	0.73 ± 0.03	8.66 ± 0.22	23 (25)	11.9 ± 0.61
S3-OSL1	4	0.31 ± 0.04	2.53 ± 0.13	1.07 ± 0.05	6 ± 0.25	0.18 ± 0.02	0.83 ± 0.03	10.8 ± 0.31	27 (29)	13.0 ± 0.60
S6-OSL1	3.06	0.20 ± 0.02	1.88 ± 0.12	0.87 ± 0.05	5 ± 0.25	0.17 ± 0.02	0.64 ± 0.03	6.75 ± 0.16	16 (20)	10.5 ± 0.50
S6-OSL2	2.06	0.31 ± 0.04	1.75 ± 0.12	0.81 ± 0.05	8 ± 0.5	0.19 ± 0.02	0.74 ± 0.03	7.77 ± 0.19	26 (28)	10.5 ± 0.53

^aFrom field moisture, ages measured at 15% moisture content, mid-way between field and saturation moisture values.

^bCosmic doses and attenuation with depth were calculated using the methods of Prescott and Hutton (1994).

^cTotal dose rate is measured from 15% water content.

^dReported to one sigma, fit to an exponential + linear regression and calculated as a simple averaged mean.

^eNumber of replicated equivalent dose (De) estimates used to calculate the mean. Second number is total measurements made including failed runs with unusable data.

^fLab used fine sand grains (250-180 micron size).

beach ridge unit, and an upper low-relief, low-angle eolian unit, sourced from reworked beach ridge sediments (Figure 10).

In general, at Site 1, subtle structure within the low amplitude zone reveals low-angle, gently dipping, northward prograding clinofolds. This low-angle unit is interpreted as an eolian sand sheet, and is approximately 0.8 to 1.0 m thick. Beneath the sand sheet, mounded structures with seaward-dipping reflections occur at >0.8 m, and are suggestive of a beach ridge morphology.

Higher relief areas (Sites 2, 3, 4, 5 and 6) yielded geophysical and sedimentological data suggestive of sediments that were deposited in association with low-relief dunes (simple parabolic and transverse dunes). The asymmetry of the dune at Site 2 indicates a northward facing slip face, indicating dominantly southeasterly winds during its formation. Likewise, the eolian sand sheet at Site 1 exhibits small scale northward-dipping clinofolds. Sites 3, 4, and 5 appear to occupy a transverse dune ridge (Figure 2). An apparent blow-out to the south of Site 3 also suggests dominantly southeast winds. The seaward side of the dune at Site 6 is eroded at the shoreline, so it is not clear what the morphology of that dune was. However, the internal structure of Site 6 reveals large-scale clinofold structures dipping to the east-southeast, with smaller clinofolds dipping to the north. These data suggest dominant winds from the west, with variable winds from the south during the deposition of this feature. The overall geomorphology is consistent with a low-angle eolian sand sheet with small nascent parabolic and transverse dunes.

The grain-size data are somewhat ambiguous. The sediments are dominantly well to moderately-well sorted, leptokurtic to very leptokurtic fine sands, typical of eolian deposits. How-

GEOLOGY OF A LATE PLEISTOCENE EOLIAN ENVIRONMENT

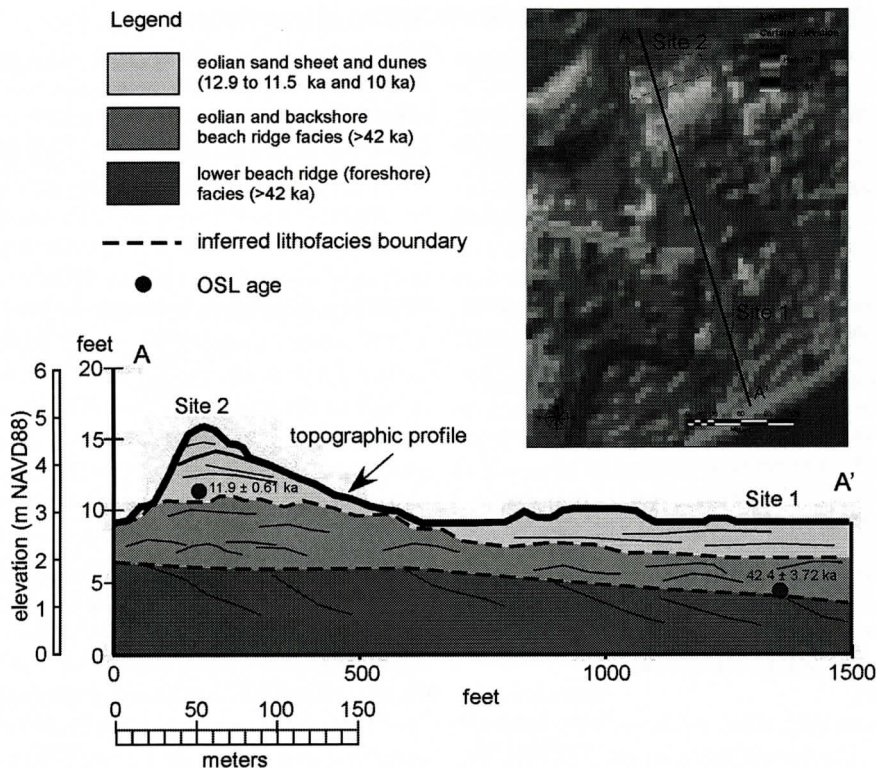


Figure 10. Geological cross-section and interpretation including depositional facies and ages along a profile from Site 2 to Site 1.

ever, overall, the sediments are coarse skewed. Mason and Folk (1958) and Friedman (1961) suggest that coarse skewed deposits are atypical of eolian systems. Friedman (1961) demonstrates the existence of some negatively skewed eolian deposits, but they are rare in his study. On the other hand, Shepard and Young (1961) demonstrate that coarse skewness dominates their eolian samples in regions with dominantly onshore winds. A portion of the coarse skew is a result of the incorporation of pedogenic iron concretions in the samples. The coarse skewness of the sedimentological data could be interpreted as reflecting a subtidal to intertidal depositional origin, however, all other factors point toward eolian (lack of fossil material, lack of heavy mineral laminations, lack of coarse-grained material, high degree of sorting). Fryberger and others (1979) shows that many samples from a low-angle eolian sand sheet are bimodal, similar to those samples from Site 6.

Other factors may account for coarse skew in eolian deposits (in addition to the incorporation of Fe-concretions). Fryberger and others (1979) and Garcia-Hidalgo (2002) discuss the occurrence and textural characteristics of eolian sand sheets. Their data indicate that in the upwind, source location for sand sheet development, the sorting may be poorer than in downwind regions. Given the location of the Broad Reach study area and likelihood that the underlying beach ridge deposits are the source of the eolian deposits, it is probable that local reworking and deflation of the beach ridge deposits provided the eolian sediments. Reversing and variable wind conditions yield laminated sediments of varying grain size (Fryberger and others, 1979), which, upon bioturbation and deflation processes, may yield negatively skewed and even bimodal sediments similar to what is seen in the Broad Reach study area.

OSL ages (Table 2) indicate the existence of

Table 4. Summary of Characteristics with Interpretations of Investigated Sites.

Site	Lithofacies	GPR facies	Mean Grain size (phi)	Sort	Skew	Interpretation
1	orange (Fe-stained), mottled, fine-grained quartz sand, with scattered sand to gravel-sized iron-concretions	Upper low amp. zone; low-angle mounded bedding; low angle seaward dipping reflections	2.49 to 2.59	well sorted	coarse skew	Upper: low-angle eolian sand sheet Lower: eolian and backshore mantle on beach ridge
2	orange (Fe-stained), mottled to laminated, fine-grained quartz sand, with scattered sand to gravel-sized iron-concretions. Burrowed, heavily Fe-stained B-horizon at 3.5 m below ground surface, in contact with laminated sand below	Upper low amp. zone; low-angle mounded bedding; reactivation surfaces	2.31 to 2.57	well sorted	coarse to very coarse skew	Low-angle eolian parabolic dune
3	orange (Fe-stained), mottled, fine-grained quartz sand, with scattered sand to gravel-sized iron-concretions	Upper low amp. zone; low-angle mounded bedding; reactivation surfaces	2.21 to 2.32	moderately well sorted (0.60 to 0.62)	coarse skew	Low-angle eolian parabolic to transverse dune
4	N/A	Upper low amp. zone; low-angle mounded bedding	N/A	N/A	N/A	Low-angle eolian sand sheet
5	N/A	Upper low amp. zone; low-angle mounded bedding	N/A	N/A	N/A	Low-angle eolian; parabolic to transverse dune
6	variably orange (Fe-stained), mottled, fine-grained quartz sand	Upper low amp. zone; mounded bedding	1.90 to 2.56	moderately sorted (below 80 cm) to moderately well sorted (above 80 cm), bimodal at 60-100, and 160 cm	symmetrical to very coarse skew	Low-angle eolian; parabolic to transverse dune
7	variably orange (Fe-stained), mottled, fine-grained quartz sand	Upper low amp. zone; low-angle, mounded bedding	2.06-2.18	moderately well sorted (0.54 to 0.63)	Symmetrical to coarse skew -0.27 to -0.53	Low-angle eolian sand sheet

at least three depositional periods. An older substrate at a lower elevation is indicated at Site 1, possibly associated with the beach ridges to the west. A beach ridge interpretation is consistent with the GPR data which reveal low angle seaward dipping beds below ca. 1 m depth. The histogram of the OSL data for Site 1 (Figure 8) presents a poorly defined distribution, and suggests three different age populations. This kind of distribution may result from mixing of older and younger grains (Bateman and others, 2003), which is also supported by the mottled, bioturbated appearance of the sediments at Site 1. These data indicate that the beach ridge deposits are significantly older than the overlying surficial sand sheet and dunes, and probably correspond to a relative sea-level highstand at some time greater than ca. 45 ka. Other coastal features of this general age have been identified in eastern North Carolina, Virginia, and Florida (Burdette, 2005; Scott, 2006; Rink and Forrest, 2006; Mallinson and others, 2007a; 2007b).

The surficial sand sheet and associated low-relief dunes formed during two episodes during and immediately following the Younger Dryas (YD) chronozone (ca. 12.9 to 11.6 ka) (Alley and others, 1993). The dune ridges associated with Sites 2, 3, 4 and 7 apparently formed and stabilized during the YD time interval. Clinoform dip directions suggest dominantly southerly winds. The histogram of the OSL sample S6-OSL2 shows a bimodal distribution (Figure 8), suggesting two separate age populations. The mean of both provides the age shown in Table 2 (10.5 ± 0.53 ka). However, evaluating each population separately yields ages of ca. 12.8 ka, and 9.5 ka. The older age is consistent with formation during the YD, and correlates with the age of the dunes at Sites 2 and 3. The younger age is consistent with the overlying sample (S6-OSL1), and suggests reactivation of the upper dune sediments at this time, with sediment transport occurring via winds from the west-northwest. Reactivation at ca. 10 ka coincides with a cold shift which has been documented in Greenland Ice Sheet cores and records of glacial advancement (GISP2; Mayewski and others, 1997; Nesje and others, 2001).

The characteristics of this eolian environment are similar to those described for the Due-ro Basin of Spain (Garcia-Hidalgo and others, 2002), which is considered a wet eolian environment as defined by Kocurek and Havholm (1993). Wet eolian environments are controlled by the availability of sand, wind, and a shallow, seasonally fluctuating water table, with sand accumulation and preservation occurring during elevated water table conditions. The age of this eolian system, then, may reflect accumulation and stabilization as a result of a rising water table in response to an increase in regional precipitation. This hypothesis is consistent with evidence of an increase in river discharge in the southeastern U.S. based on channel morphologies, suggesting higher precipitation rates than present during the late Pleistocene to early Holocene (Leigh, 2006).

CONCLUSIONS

Ground penetrating radar data reveal two characteristic depositional facies:

- A lower low-angle seaward dipping unit, consistent with beach ridge development
- An upper low-angle horizontally bedded to mounded unit that defines the eolian sand sheet and associated low-angle dunes.

Granulometric investigations of the sediments are ambiguous as to the depositional environments. Sediments are typically moderately-well to well sorted, leptokurtic to very leptokurtic, coarse skewed, fine grained, highly bioturbated quartz sand. The coarse skewness is proposed to have formed due to variable wind directions and speeds, local deflation, and significant bioturbation.

The study area consists of at least three chronostratigraphic units:

1. An initial beach ridge unit dated to at least 45 ka.
2. An eolian low-angle sand sheet and dune complex that corresponds to the Younger Dryas chronozone (12.9 to 11.6 ka).
3. An eolian low-angle dune system that represents reactivation of the earlier dune system, and dates to ca. 10 ka.

ACKNOWLEDGEMENTS

The authors would like to thank Heather Milis for her contributions and discussions in the field, and Andrew Ivester for his constructive review. This work was funded by the North Carolina Office of Archives and History - State Historic Preservation Office, and TRC Garrow Associates, Inc.

REFERENCES CITED

Alley, R. B., D. A. Meese, A. J. Shuman, A. J. Gow, K. C. Taylor, P. M. Grootes, J. W. C. White, M. Ram, E. D. Waddington, P. A. Mayewski, and G. A. Zielinski, 1993. Abrupt accumulation increase at the Younger Dryas termination in the GISP2 ice core. *Nature*, v. 362, p. 527-529.

Bateman, M.D., Frederick, C.D., Jaiswal, M.K., and Singhvi, A.K., 2003. Investigations into the potential effects of pedoturbation on luminescence dating. *Quaternary Science Reviews*, v. 22, p. 1169-1176.

Blott, S.J., and Pye, K., 2001. Grain Size Statistics Program. *Earth Surface Processes and Landforms*, v. 26, p. 1237-1248.

Burdette, K.E., 2005. Chronostratigraphy and Geologic Framework of the Currituck Sand Ridges, Currituck County, NC. Unpub. M.S. Thesis, East Carolina University, Greenville, NC, 184 p.

Culver, S.J., Ames, D.V., Corbett, D.R., Mallinson, D.J., Riggs, S.R., Smith, C.G., and Vance, D.J., 2006. Foraminiferal and Sedimentary Record of Late Holocene Barrier Island Evolution, Pea Island, North Carolina: The role of Storm Overwash, Inlet Processes, and Anthropogenic Modification. *Journal of Coastal Research*, v. 22, p. 836-846.

Folk, 1974. *Petrology of Sedimentary Rocks*. Hemphill Publ., Austin TX.

Folk RL, and Ward WC. 1957. Brazos River bar: a study in the significance of grain size parameters. *Journal of Sedimentary Petrology*, v. 27, p. 3-26.

Friedman, G., 1961. Distinction between dune, beach and river sands from their textural characteristics. *Journal of Sedimentary Petrology*, v. 31, p. 514-529.

Fryberger, S., Ahlbrandt, T., and Andrews, S., 1979. Origin, sedimentary features, and significance of low-angle eolian "sand sheet" deposits, Great Sand Dunes National Monument and vicinity, Colorado. *Journal of Sedimentary Petrology*, v. 49, p. 733-746

Garcia-Hidalgo, J., Temino, J., and Segura, M., 2002. Holocene eolian sediments on the southern border of the Duero Basin (Spain): Origin and development of an eolian system in a temperate zone. *Journal of Sedimentary Research*, v. 72, p. 30-39.

Godfrey, P.J., and Godfrey, M.M., 1976. Barrier Island Ecology of Cape Lookout National Seashore and Vicinity, North Carolina. National Park Service Scientific Monograph Series No. 9, 160 p.

Herbert, J., 1978. Post-Miocene Stratigraphy and Evolution of Northern Core Banks, NC. Unpub. M.S. Thesis, Dept. of Geology, Duke University, Durham, NC. 133 p.

Heron, Jr., S.D.; Moslow, T.F.; Berelson, W.M.; Herbert, J.R.; Steele Iii, G.A., And Susman, K.R., 1984. Holocene sedimentation of a wave-dominated barrier-island shoreline: Cape Lookout, North Carolina. *Marine Geology*, v. 60, p. 413-434.

Inman, D.L. and Dolan, R., 1989. The Outer Banks of North Carolina: Budget of sediment and inlet dynamics along a migrating barrier system. *Journal of Coastal Research*, v. 5, p. 193-237.

Kneller, M., and Peteet, D., 1999. Late-glacial to early Holocene climate changes from a central Appalachian pollen and macrofossil record. *Quaternary Research*, v. 51, 133-147.

Kocurek, G., and Havholm, K.G., 1993, Eolian sequence stratigraphy—a conceptual framework, *in* Posamentier, H., and Weimer, P. eds., *Recent Advances in Siliciclastic Sequence Stratigraphy*: American Association of Petroleum Geologists, Memoir 58, p. 393-409.

Leigh, D.S., 2006. Terminal Pleistocene braided to meandering transition in rivers of the Southeastern USA. *Catena*, v. 66, p. 155-160.

Mallinson, D., Riggs, S., Culver, S., Thieler, R., Foster, D. Corbett, D., Farrell, K., and Wehmiller, J., 2005. Late Neogene and Quaternary evolution of the northern Albemarle Embayment (Mid-Atlantic Continental Margin, USA). *Marine Geology*, v. 217, p. 97-117.

Mallinson, D., Burdette, K., Rink, J., Mahan, S., Brook, G., Smith, C., Parham, P., Culver, S., and Riggs, S., 2007b. Assessing the chronostratigraphy of late Pleistocene and Holocene coastal lithosomes using optically stimulated luminescence techniques: intriguing results from NC and FL. *GSA Abstracts with Programs*, v. 39, p. 2

Mallinson, D., Burdette, K., Mahan, S., and Brook, G., 2007a. Optically Stimulated Luminescence Age Controls on Late Pleistocene and Holocene Coastal Lithosomes: North Carolina, USA. *Quaternary Research*, doi:10.1016/j.yqres.2007.10.002.

Mason, C., and Folk, R., 1958. Differentiation of beach, dune, and Aeolian flat environments by size analysis, Mustang Island, Texas. *Journal of Sedimentary Petrology*, v. 28, p. 211-226.

Mathis, M.A., 1993. Broad Reach: The Truth About What We've Missed. In, D. Anderson and V. Horak (eds.), *Site Destruction in Georgia and the Carolinas*. Interagency Archeological Services Division, National Park Service, 100 p.

Mayewski, P.A., Meeker, L.D., Twickler, M.S., Whitlow, S., Yang, Q., Lyons, W.B., and Prentice, M., 1997. Major features and forcing of high-latitude northern hemisphere atmospheric circulation using a 110,000-year long glaciochemical series. *Journal of Geophysical Research*, v. 102, p. 26345-26366.

Murray, A. S., and Wintle, A. G., 2000. Luminescence of

GEOLOGY OF A LATE PLEISTOCENE EOLIAN ENVIRONMENT

- dating of quartz using an improved single-aliquot regenerative-dose protocol. *Radiation Measurements*, v. 32, p. 57-73.
- Nesje, A., Matthews, J.A., Dahl, S.O., Berrisford, M.S., and Andersson, C., 2001. Holocene glacier fluctuations of Flatbreen and winter-precipitation changes in the Jostedalbreen region, western Norway, based on glaciolacustrine sediment records. *Holocene*, v. 11, p. 267-280.
- Riggs, S.R., York, L., Wehmiller, J., and Snyder, S.W., 1992. Depositional patterns resulting from high-frequency Quaternary sea-level fluctuations in northeastern North Carolina. In, *SEPM Spec. Pub. No. 48: Quaternary Coasts of the United States: Marine and Lacustrine Systems*. p. 141-153.
- Riggs, S.R. and Ames, D.V., 2003. Drowning the North Carolina coast: Sea-level rise and estuarine dynamics, North Carolina Sea Grant College Program, Raleigh, NC, Pub. No. UNC-SG-03-04, 152 p.
- Scott, T., 2006. Correlating late Pleistocene coastal deposits on the Coastal Plain of Virginia with the glacial-eustatic sea-level curve. Unpub. M.S. Thesis, Old Dominion University, 111 p.
- Shepard, F.P., and Young, R., 1961. Distinguishing between beach and dune sands. *Journal of Sedimentary Research*, v. 31, p. 196-214.
- Steele, G.A., 1980. Stratigraphy and Depositional History of Bogue Banks, North Carolina. Unpublished MS Thesis, Duke University, Durham, North Carolina, 201 p.



THE INFLUENCE OF DRAINAGE HIERARCHY ON PATHWAYS OF BARRIER RETREAT: AN EXAMPLE FROM CHINCOTEAGUE BIGHT, VIRGINIA, U.S.A.

G.F. OERTEL¹, T.R. ALLEN² AND A.M. FOYLE³

¹ Old Dominion University, Norfolk, VA 23528

² East Carolina University, Greenville, NC 27858

³ Pennsylvania University, Erie, PA 16563

ABSTRACT

A major offset in the Virginia coastline exists between Assateague Island and Wachapreague Island. The offset produces the broad Chincoteague Bight anchored by the cape-like southern tip of Assateague Island and the northern tip of Parramore Island.

A combination of factors has influenced the development of this part of the Virginia coast. In particular, the hierarchy of watersheds in the area has had a strong influence on the formation of Chincoteague Bight. Large watersheds on the Atlantic coast have shore-normal orientations conducive to the formation of coastal compartments. Intermediated-sized watersheds with nearly shore-parallel orientations intersect the coastline at very low angles. Smaller, moderate-sized watersheds that have shore-normal orientations are conducive to the formation of tide-dominated barrier islands. Chincoteague Bight may be a result of the oblique intersection of the intermediated-sized Chincoteague paleovalley and the Atlantic coastline. Projecting the coastline across Chincoteague Bay produces a "stretched" valley-section that is about 4-5 times the width of a perpendicular section. Since the width of Chincoteague Bight is comparable to the width of the stretched valley section, we interpret the Bight formed in response to the low-angle intersection of the coastline and the paleovalley.

Based on the characteristics of adjacent Coastal Plain watersheds, the present size of Chincoteague Bay may only represent a fraction of the entire Chincoteague watershed. Reconstruction of the entire system required

hindcasting the coastline seaward during lower stands of sea level. By doing this, the entrance to the Chincoteague watershed was projected 90 km farther to the south. Transgression of the sea from this point allowed us to see the effects of watershed hierarchy on coastal configuration. Interfluves of different size and orientation were major factors influencing pathways of inlet and barrier island retreat. In the Delmarva area, wave-dominated landforms were initially the dominant elements of the Delmarva coastal compartment; with continued transgression the tide-dominated elements became increasingly more important. The reverse is likely to occur under different stages of transgression.

INTRODUCTION

The Delmarva Peninsula is located on the Coastal Plain of the mid-Atlantic region of the United States (Fig. 1). The proximal end of the peninsula originates near Philadelphia, Pennsylvania and the axis extends south-southeast toward the coast of Delaware and Maryland. The distal end of the peninsula is the principal headland element of a major oceanic coastal compartment called the Delmarva Coastal Compartment (Oertel and Kraft, 1994). The Delmarva coastal compartment has six geomorphic elements (see Fig. 2; Oertel and Overman, 2004). Cape Henlopen forms a left-hand spit complex (Element 1). Eroding headlands (Element 2) and a right-hand spit (Element 3) occur between Cape Henlopen and Ocean City, MD and Assateague Island is the wave-dominated barrier island element (Element 4). Tide-dominated islands of antecedent origin (Element 5) occur between Assateague Island and the Ches-

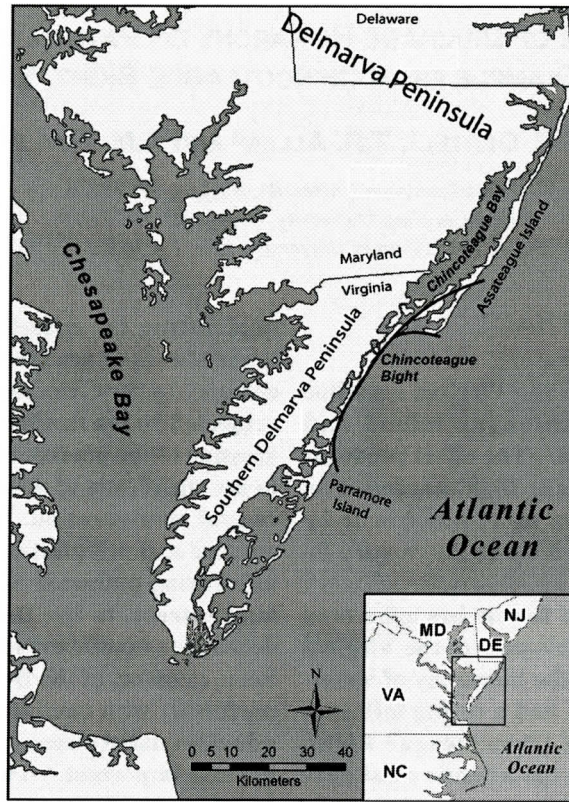


Figure 1. Location map of study area showing the relative locations of Chincoteague Bay, Assateague Island Parramore Island and Chincoteague Bight.

apeake Bay. Fisherman Island is an emergent barrier island (Element 6) at the southern end of the compartment.

The shoreline between the middle of Assateague Island and the tide-dominated islands has an orientation of about 35°-215°. However, at the distal end of Assateague Island the ocean shoreline is offset landward about 10 km (to Wallops Island). From Wallops Island to Parramore Island the shoreline is concave for about 40 km before returning to its more offshore orientation. The exposed, open-embayment between the distal end of Assateague Island and Parramore Island is designated here as the Chincoteague Bight (Fig. 1). Two intermediate-sized capes designated as Cape Assateague on the north and Cape Parramore on the south anchor the Bight. These capes are a size order smaller than the large capes described by Hoyt and Henry (1971) for the southern U.S. coast.

The linear distance between the capes is about 33 km (Circa 2007). However, about 150 years ago (Circa 1850, National Parks Service, 2005), the mouth of Chincoteague Bight was about 45 km wide.

Several different mechanisms have been offered to explain the origin of Chincoteague Bight. The embayment between Assateague Island and Parramore Island could be related to a former course of the Potomac or Susquehanna Rivers (see figure 9 in Mixon, 1985). Mixon (1985) illustrated that the Southern Delmarva Peninsula is relatively narrow in this region and top of the Tertiary was depressed (suggesting an ancient valley). Later, Oertel and Foyle (1995) suggested a Late Pliocene/Pleistocene path for the Susquehanna River in this area. However, since this Susquehanna Channel has not been active since Late Pliocene/Pleistocene, it is probable that numerous subsequent high-

stands would have filled and “smoothed over” the valley depression. Krantz (2007, personal communication) also thought there might be a connection between the Bight and mid-Pleistocene paths of the Susquehanna or Potomac Rivers. At depth beneath the Wallops Island shoreface he found a series of large seismic channels that were incised at depths between 15-45 m. However, smaller seismic valleys at 0-5 m were not coupled to the deeper valleys (Krantz, 2006). These shallow seismic valleys were abundant in the shoreface between Chincoteague Bight and the middle of Assateague Island (Krantz, 2006). Thus, although the deeper channels were filled during highstands and capped over by tabular marine deposits, some of the relief may still exist at gentler slopes. During subsequent lowstands, drainage was rejuvenated and topography was carved by a much greater density of low-order streams.

Dolan et al. (1979) hypothesized that wave refraction and edge-waves focused wave energy south of the Assateague Island spit causing an increase in shoreline retreat along the Chincoteague Bight. Dolan et al. (1979) and Dolan et al. (1980) believed that the accelerated rates of shoreline retreat were a function of shoreline orientation with respect to refracted wave approach. However, wave-refraction models of Goldsmith et al. (1975) illustrated a decrease in wave energy in the Chincoteague Bight. Dolan et al. (1980) also felt that relatively high erosion rates were related to the silty clay substrate immediately below the barrier islands.

Leatherman et al. (1982) and Demarest and Leatherman (1985), suggested the offset was caused by sediment starvation south of the Assateague Island spit. Demarest and Leatherman (1985) described the Chincoteague Bight as an “Arc of Erosion” extending from Wallops Island to the north end of Parramore Island. The Arc includes Wallops Island, Assawoman Island, Metompkin Island and Cedar Island and the curved shoreline actually continues in a northeast direction eventually crossing the Assateague Island coastline about 20 km north of Wallops Island.

In a 120-year survey of shoreline positions (Dolan et al. 1979; Leatherman et al. 1982)

found the shoreline recession rates of 4-5 m/yr at Assawoman, Metompkin and Cedar Islands were significantly greater than adjacent areas. Byrnes et al. (1989) reported an average recession rate at Metompkin Island of 6.7 m/yr. Leatherman et al. (1982) emphasized that islands in the arc illustrated a parallel shoreline retreat pattern, whereas south of the arc, islands appeared to be rotating during retreat, and moving landward at a much slower pace.

We feel the arc of islands on the landward side of the Bight once extended considerably north to the proximal end of Chincoteague spit. Halsey (1979) described ancient islands (Pirate Island, Pope Island and Chincoteague Island) in this northern part of the arc. She illustrated how these islands welded together forming one island from three (“Nexus” Halsey, 1979). Following nexus, Assateague Spit migrated on a more southerly direction and obliquely away from the intersection of the arc shoreline. Historical charts of the area (U.S. Department of Interior, 2007) show that today (Circa 2007) the spit is about 6 km longer than it was in 1852. If the Bight were 6 km wider just 150 years ago, then it is possible that it could have been 12 km wider earlier in the millennium.

The purpose of this research was to investigate the cause of the offset between the Assateague Island and Wallops Island shorelines. It was hypothesized that the offset was principally caused by the influence of an antecedent paleovalley on littoral sediment dispersion.

Dual Shoreline Concept

During the Holocene transgression, the rising sea progressively submerged greater portions of the gently sloping Coastal Plain of the Atlantic and Gulf Coasts of the United States. The middle Atlantic region of the United States has a typical dual-shoreline configuration formed by the Holocene transgression with leading and trailing shores. The subaerial leading edge of the transgression is located along an inner mainland shoreline in coastal barrier lagoons. Configuration of the shoreline is controlled by the complexity of the flooded antecedent surface. Recession rates along the

mainland shoreline are primarily determined by regional slope and the rate of sea-level rise. The subaerial trailing edge of the transgression is located at the outer coast formed by headlands, barrier islands and spits. Recession rates of these features are primarily governed the sediment redistribution by waves. Lagoons that separate the outer and inner shorelines illustrate a variety of shapes related to flooding of antecedent surfaces (Fig. 1).

At regional scales, the Coastal Plain appears to be planar. In section, the transgression is sometimes depicted as a shoreline receding up a relatively smooth inclined surface (Dolan et al., 1980; Leatherman, 1983b). However, the surface is neither planar nor smooth. During the previous regression and glacial lowstand, a hierarchical mosaic of streams and rivers sculptured the land surface. Thus, at local scales, Coastal Plain morphologies are considerably more complicated and quite variable in relief.

During post-glacial sea level rise, Coastal Plain flooding spread over irregular surfaces that were carved during highstands. The rising sea flooded higher-order valleys first, followed by progressively lower-order streams. Mainland lagoon-shorelines along the leading edge of the transgression became crenellated as water expanded into complicated networks of streams and interfluves. This highly crenellated feature of the "leading edge" shoreline is a typical characteristic of morphostatically-drowned coasts. Conversely, ocean shorelines are relatively linear because wave-dominated processes and shoreface erosion control their shape.

Between the mainland and ocean shorelines, the floors of coastal lagoons and estuaries inherit the topography of the antecedent surface. Seaward of the ocean shoreline, the conspicuous relief of the antecedent valleys has been "smoothed" by wave-dominated processes on the submerged shoreface. Cores and seismic records reveal evidence of numerous paleovalleys in the inner shelf, but attempts to map traces of valleys during the Holocene transgression are complicated because numerous transgressions and regressions have obscured earlier features.

Influence of sea-level change on coastal evolution

Although the boundary between the land and the sea (the shoreline) is one-dimensional, its orientation provides valuable information about the relationships between primary and secondary topography. In a fixed sea-level model, the character of the shoreline is solely dependent on remolding of terrestrial landforms by secondary marine processes. During transgression, coastal landforms evolve toward a state that represents a dynamic balance between antecedent topography and marine processes. However, natural fluctuations in sea level are ever introducing "disturbance" to coastal morphology. Rising sea level produces lateral shifts in the coastal position across terrestrial topography. Falling sea level produces coastal shifts toward and over shoreface topography.

The continental shelf along the mid-Atlantic region of North America has a relatively smooth surface with an average dip of 0.05° and an average width of about 100 km. The present coastline is located about midway between the landward limit of the Coastal Plain and the outer edge of the continental shelf (submerged part of the Coastal Plain). The present relatively high sea level is a result of global warming that began at end of the last glaciation (O isotope Stage 2) about 18,000 BP. Throughout the late Pleistocene and Holocene the rising sea has drown and remolded terrestrial topography.

Regional Setting and Coastal Compartments

Fisher (1968) noted that coastal areas could be logically subdivided into reaches of coastline separated by major rivers. Each reach is a headland of an interfluve that separates two adjacent drainage systems. When these reaches occur along substrates composed of friable material, sediments eroded from the headland move along the shoreline forming secondary coastal landforms. During transgression, barrier islands are prominent secondary landforms along these reaches of coast. Fisher (1967, 1968) described these reaches of coasts as "barrier-island chain

PATHWAYS OF BARRIER RETREAT

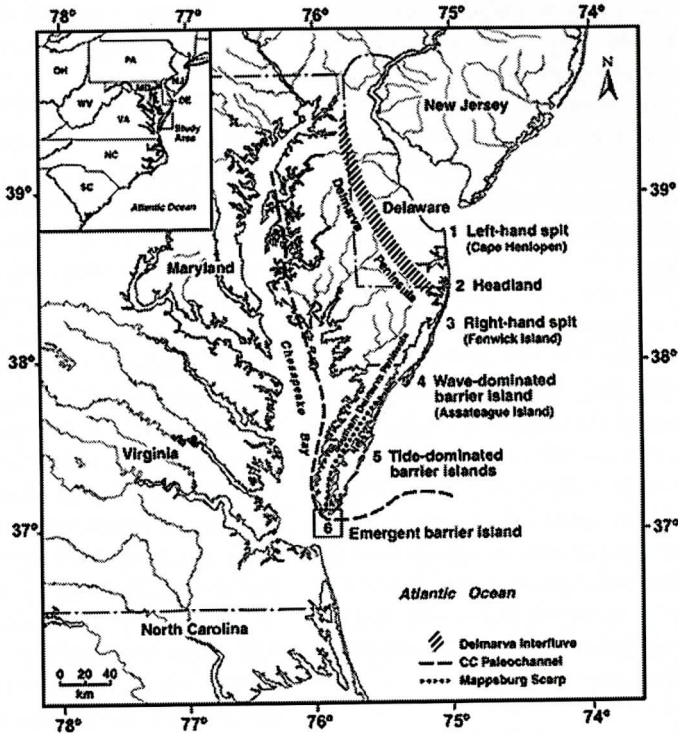


Figure 2. Map of the Delmarva Peninsula showing six elements of the coastal compartment located on the coastline of the Delmarva and Southern Delmarva Peninsulas.

shorelines". Fisher (1968) described the chains as having four elements (I-Spits, II-Baymouth barriers, III-Long Barrier Spits and Barrier Islands, IV-Short Barrier Islands and Barrier Beaches) that are logically arranged with respect to sediment dispersion from the headland. Swift (1969) referred to these "barrier-island chain shorelines" as "coastal compartments" and modified the description of the elements to: 1 northern spit, 2 eroding headland, 3 southern spit, and 4 barrier island chain. Hayden and Dolan (1979) developed a similar compartment (called a "barrier island ensemble") based on shoreface steepness and curvature.

Belknap and Kraft (1985) combined terminology from the Fisher (1968) and Swift (1969) models describing the elements as: (1) spit complex, (2) eroding headlands and baymouth barriers, (3) microtidal linear barriers, and (4) mesotidal sea island barriers. Although coastal compartments are common features between Massachusetts and North Carolina, they are rec-

ognized along many coastal areas of the world. Oertel and Kraft (1994) suggested coastal compartments could have up to five elements (left-hand spit, headland, right-hand spit, wave-dominated barrier islands and tide-dominated barrier islands). Tide-dominated barrier islands are associated with sediment-dispersion regimes that are uncoupled from the wave-dominated systems described by Fisher (1968). Tide-dominated barrier islands are associated with moderate-sized antecedent valleys with shore-normal orientations. The interfluvies between valleys become sites for tide-dominated barrier islands (Oertel et al, 1992). Oertel and Overman (2004) added an emergent barrier-island element to their coastal compartment (Fig. 2).

It is apparent that some sections of the coastal compartments described by (Fisher, 1968; Belknap and Kraft, 1985 and Oertel and Kraft, 1994) have distinct tide-dominated and wave-dominated reaches. Discrimination of the Delmarva coastal compartment into a wave-domi-

nated reach and a tide-dominated reach (Oertel and Kraft, 1994) suggests a transition from landforms predominantly sculptured by marine processes to landforms that adopt their shape predominantly from antecedent topography. The Chincoteague Bight is located between a wave-dominated barrier island (Assateague Island) and a tide-dominated barrier island (Parramore Island).

METHODS

In order to understand the processes that caused the offset between Assateague Island and Parramore Island, we looked both landward and seaward of the coastline for clues to coastal evolution. Our first objective was to determine if there were any patterns in topography and bathymetry that were associated with the "offset" coastline. A second objective was to determine if paleochannels influenced the formation of the offset coastline.

Pre-transgressed Coastal Plain

Since marine processes modify antecedent surfaces during transgression, our first task was to quantify the characteristics of the adjacent, pre-transgressed topography. The topographic investigation involved broad-scale spatial analysis of drainage basins and interfluves of the adjacent Coastal Plain. Drainage basins were clumped into hierarchal classes, and then each class was examined for size, orientation, relief and width. Analyses were conducted using Geospatial techniques available in ARC/INFO™. Drainage basins on the western side of the Delmarva Peninsula were identified as future sites of inundation that could provide information on the previous areas of the Coastal Plain that had already been transgressed. Areas, orientations and dimensions of these basins were estimated using standard geospatial techniques. It was anticipated that these characteristics could be hindcast to the adjacent continental shelf to determine previous locations of more seaward basins located on the mid-Atlantic shoreface.

Transgressed Coastal Plain (Bathymetry and Stratigraphy)

Shoreface Topography

At global and regional scales, the continental shelf appears have a relatively flat surface. However, locally the surface is often marked by topographic irregularities that may provide some understanding of its transgressive history. We believe that the shelf surface seaward of the shoreface is often too reworked (by wave and coastal currents) to provide viable information on the antecedent surface. However, since the upper shoreface is the "trailing" active edge of the transgression we look toward it to provide remnants of the antecedent topography.

Much of the shelf is covered with shore oblique linear ridges. Some of these features form, and are being maintained by active shelf processes (Swift, et al. 1986). Others may be relict spit ridges that continue to be maintained by waves and shelf currents. Smooth shoreface surfaces are frequently composed of muddy materials (relict estuaries and lagoons) too fine to retain ridge relief. Broad-scale rises and depressions on the shoreface may be respective indicators of antecedent highs and valleys on the underlying surface. Crescent patterns of sandbars and shoals that are associated with tidal inlets produce curved depth contours. Thus, when shoals are found along the margins of a section of smooth shoreface we interpret them as morphologic remnants left along the retreat paths of tidal inlets. Re-curved ridges along the edges of smooth areas are also used as indicators of relict spits on the margins of inlet systems.

A qualitative classification of the shoreface adjacent to the Chincoteague Bight was made based degree of topographic irregularity, and absence/presence of shoreface ridges. Topographic data were interpreted from USGS Quadrangles and USGS Digital Elevation Model of the region. Shadow relief projections of the DEMs were used to assist in visual analysis of topographic features.

Shoreface Stratigraphy

During the Holocene transgression, shoreface smoothing by waves often obliterates much of the relief on the pre-transgressed surface. However, bedding structures preserved below the shoreface can provide evidence of the surface forms. In the mid-Atlantic region, Kraft and his students (Halsey, 1979; Belknap and Kraft, 1977, 1981, 1985; Kraft, 1971; Kraft et al. 1987) have successfully used cores and seismic techniques to interpret the shape of the antecedent landforms. Belknap and Kraft (1985) illustrated the northeast drainage of pre-Holocene channels across the modern Delaware shoreline to an ancestral Delaware River paleochannel below the shoreface. The channels clearly flowed northeast and away from the major Delmarva interfluvium separating the Delaware and Susquehanna watersheds. The antecedent drainage of the coastal area south of the major Delmarva interfluvium (southern Delmarva Peninsula) and adjacent to the Chincoteague Bight is less well understood. Nevertheless, the base of the Holocene sequence in coastal lagoons (adjacent to the Chincoteague Bight) provides a foundation for extending this surface beyond the coastline. Numerous investigators have interpreted sediments in vibracores to speculate on the base of the Holocene in coastal lagoons of the Southern Delmarva Peninsula (Byrne, 1988; Finklestein, 1992; Finklestein and Ferland, 1987; Finklestein, and Kearney, 1988; Morton and Donaldson, 1973; Newman and Munsart, 1965; Newman and Rusnack, 1968; Shielder et al. 1984; Oertel et al., 1989; Oertel et al. 1992, Van de Plassche, 1990). Depths to the base of the Holocene reported by the above investigators vary significantly. Some authors have reported Holocene depths approaching 8 meters while other depths are less than a few meters. The differences indicate that there is no uniform depth through backbarrier sediments to the base of the Holocene. We interpret the differences in relief to be a response to sampling through "backbarrier fills" over multiple drainage basins and interfluviums. Oertel et al. (1989) and Newman and Rusnack (1968) reported that the pre-Holocene was closer to the surface in interfluvium parts of

the watersheds. Phytolith and age data behind Cedar and Metompkin Islands indicate that a considerable section of the fine-grained sediment accumulated within the last 4000 yrs BP was deposited under freshwater wetland and estuarine conditions (Van de Plassche, 1990).

Seaward of the coastline in Chincoteague Bight, there is a scarcity of published seismic data for detecting the base of the Holocene. Krantz (2006) has a web site with a rich set of seismic data from the shoreface between the Assateague Island and Wallops Island, VA. Between Parramore Island and the Chesapeake Bay entrance seismic reflection techniques were used to study transgressive systems and drainage patterns (Foyle and Oertel, 1992, Foyle, 1994, Oertel et al. 1994, Oertel and Foyle, 1995; Foyle and Oertel, 1997). Seismic data reveal a paleostream network adjacent to the Chincoteague Bight shoreface (Foyle, 1994; Oertel and Foyle, 1995). Seismic surveying was done using a modified Ferranti-ORE Geopulse System™. The boomer system was operated at the 175 J setting with a firing rate of one to four pulses per second. Acoustic returns were band-pass filtered between 1000 and 3000 Hz after detection with a twenty-hydrophone array. Reflector depth computations utilized acoustic velocities of 1500 m/s and 1600 m/s for water and sediment, respectively. ¹⁴Carbon dates from vibracores were provided chronologic markers along the tracklines.

Foyle and Oertel (1997) identified a seismic stratigraphic sequence composed of eleven seismic facies grouped into six sequences. Paleochannels occur in each sequence. Since our concern is to determine how the Holocene transgression influences the modern shoreline shape of the Chincoteague Bight, we are only interested in channels above the base of the Holocene. Foyle and Oertel (1997) labeled reflector SR-1 as the seafloor, R-2 as the Holocene ravinement surface and SR-3 as the base of the Holocene. In this study we confine our efforts to the pathways of channel facies that originate at or above the SR-3 reflector.

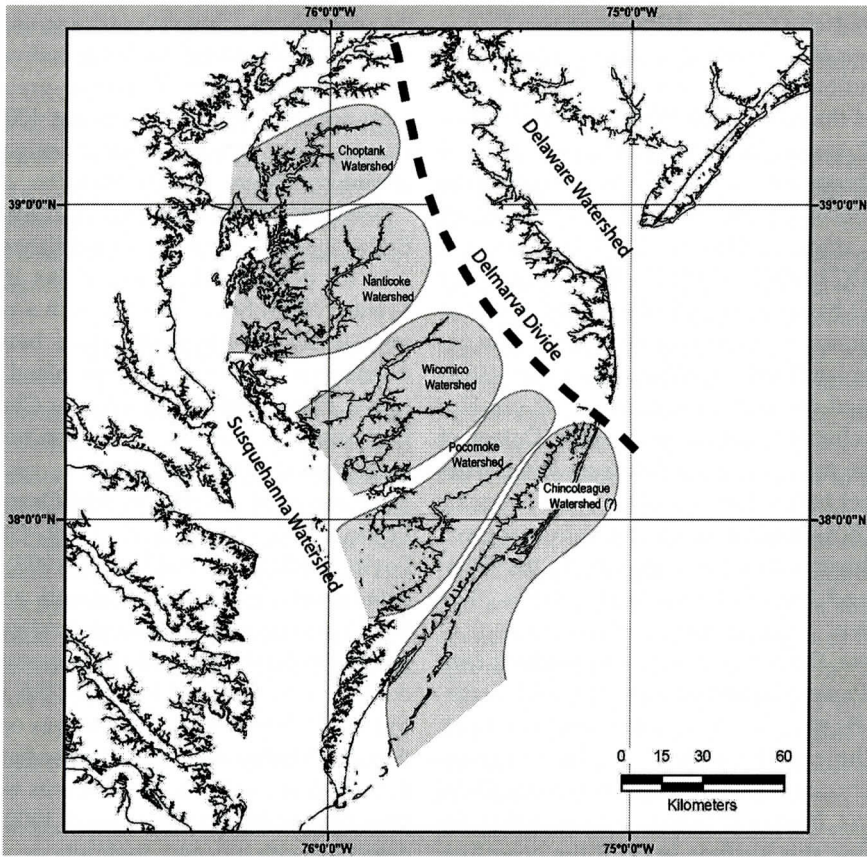


Figure 3. Map showing the location and orientation of “intermediate-sized” Coastal Plain watersheds on the west side of the Delmarva Peninsula. The Delmarva divide is the interfluvium between two “major” watersheds, the Delaware Watershed and the Susquehanna Watershed.

OBSERVATIONS/ INTERPRETATIONS

The Delmarva Topographic Setting

For the purposes of the research we have identified four watershed sizes that impact on coastal configuration. A four-tiered hierarchical classification of watersheds (major, intermediated, moderate and small) is used to evaluate the impact of each class on coastal configuration in the mid Atlantic region. “Major” watersheds are systems with drainage areas greater than 3×10^6 hectare. Intermediate-sized watersheds have areas between $1.0 - 3.0 \times 10^5$ hectare. Moderate-sized watersheds have areas between $1-2 \times 10^4$ hectare. Small watersheds ($<0.5 \times 10^4$ hectare) appear to be too small to

have impacted coastal configuration.

Major Watersheds

The Delaware River and Susquehanna River with areas about 3.5 million-hectare and 5.25 million-hectare, respectively are major watersheds in the middle Atlantic region of the United States. The Delmarva Peninsula is the major interfluvium separating Delaware Bay and Chesapeake Bay. North of the Delmarva Peninsula, the distal part of the Delaware River drainage basin has been inundated by rising sea level forming the Delaware Bay. To the south, the distal part of the Susquehanna River valley has submerged forming the Chesapeake Bay. The axis of the Peninsula is a meandering ridge with a north northwest to south southeast orientation. Elevations along the 150-kilometer long ridge

PATHWAYS OF BARRIER RETREAT

Table 1. Intermediate-sized, coast-parallel, drainage basins on south side of Delmarva Interfluve.

Watershed	Orientation (°)	Area (ha)	Interfluve Spacing (km)	Section Relief (m)
Choptank	232	260,000	31	22
Wicomico/Nanticoke	223	214,000	47	17
Pocomoke	220	176,000	38	16
Chincoteague	203	?	25*	15

exceed 15 meters. The southeast and distal end of the interfluve has a headland at the Atlantic Coastline.

The Delmarva headland region is a major sediment source for secondary landforms of the Delmarva Coastal Compartment. Cape Henlopen forms the left-hand spit of the compartment, Fenwick Island forms the right-hand spit, Assateague Island forms the wave-dominated barrier island element, and the Virginia islands are the tide-dominated barrier islands.

Intermediate-sized watersheds

The morphology of the Delmarva Peninsula has been sculptured by drainage basins of intermediate-sized watersheds (Fig. 3). The heads of these watersheds originate along the axis of the Delmarva interfluve and flow toward the Delaware and Chesapeake Bays (Oertel and Kraft, 1994). Interfluves between intermediate-sized watersheds are oriented approximately parallel to the Atlantic Ocean coastline. Intermediate interfluves are spaced about 20-30 km apart. On the north side of the Delmarva interfluve, the intermediate-sized basins (Murderkill River, Mispillion River, Cedar Creek, Primehook River, Broadkill River, and Love Creek) drain northward into the lower Delaware Bay. Several small rivers (Herring Creek, Indian River and Miller Creek) drain toward the Atlantic Ocean. Interfluves between these rivers have headlands on the Atlantic Ocean shoreline. Interfluves are slightly oblique (45-60 degrees) to the trend of the Atlantic Ocean shoreline.

There are five intermediate-sized watersheds on the south side of the Delmarva Peninsula. The Chester River watershed is located at the proximal end of the Delmarva Peninsula, and the Choptank River, Nanticoke-Wicomico River, and Pocomoke River systems are progres-

sively offset toward the distal end. The average size of the Choptank River, Nanticoke-Wicomico River, and Pocomoke River is about 2.15×10^5 hectare. Parts of each of these systems are submerged along the northern margin of the Chesapeake Bay. The terrestrial parts get progressively smaller in the southeast direction as the submerged parts of the basins get larger.

Intermediate-sized watersheds are considerably longer on the southeast end of the Delmarva Peninsula, than on the northwest end. The average watershed length of the Chester River, Choptank River, Nanticoke-Wicomico River, and Pocomoke River is about 45 kilometers. Submerged sections of the Nanticoke-Wicomico River, and Pocomoke River systems add an additional 20-30 kilometers to their length (Table 1). "Necks" adjacent to the submerged sections of the intermediate basins jut out into the Chesapeake Bay. Distal ends of the necks form headlands on the Chesapeake Bay. The mouths and lower parts of the stream valleys between these necks are broader than the average valley section drowning of the floors. The average width of river mouths for these systems is 20 km.

Interfluves between the intermediate-sized rivers (on the south side of the Delmarva divide) are spaced about 35-40 kilometers apart. The axes of these drainage systems have north northeast-south southwest orientations and have a relatively shore-normal orientation with the shoreline of the Chesapeake Bay. The Choptank, Wicomico, and Pocomoke watersheds have an average orientation of 45°-225°. The orientations have a slight counterclockwise rotation from the proximal to the distal end of the Delmarva Peninsula. The interfluve between the Pocomoke River drainage basin and the Chincoteague Bay is called the southern

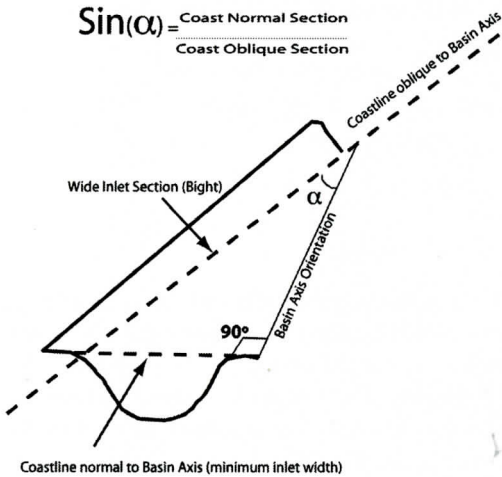


Figure 4. Sketch illustrating the sectional width produced by the relationship between coastline orientation and the axis of coastal basins. Large angles between coastlines and basin axes produce narrow sections. Near parallel, oblique angles between coastlines and basin axes produce very wide sections.

Delmarva Peninsula. The orientation of the Chincoteague watershed (and interfluvium) is about 25°-205°, and the present width of Chincoteague Bay is about 9.25 km. If Chincoteague Bay were draining into Chesapeake Bay with a shore-normal orientation (like the Choptank, Wicomico, and Pocomoke watersheds), then its maximum inlet section would be about 9.25 km. However, Chincoteague Bay intersects with the Atlantic coastline (35°-215°). The 5°-10° angle between the coastline and watershed produces a potentially very wide inlet section of greater than 50 km (Fig. 4). This is 12 km greater than the width of the Chincoteague Bight.

Moderate-sized watersheds

Moderate-sized watersheds occur along the flanks of each of the intermediated-sized basins. The watersheds have areas ranging from 1-2 x 10⁴ hectare, with orientations that trend approximately perpendicular to the coastline. The eastern side of the Southern Delmarva Peninsula has numerous moderate-sized watersheds that generally flow toward the east and are normal to the orientation of the coastline. Along the northern part of the Southern Delmarva

Peninsula these systems empty into Chincoteague Bay. Seven systems drain into the western side of Chincoteague Bay (Marshal Creek, Robins Creek, Scarboro Creek, Pawpaw Creek, Boxiron Creek, Rowley Creek and Mosquito Creek).

Halsey (1979) suggested that the necks between drainage basins once extended across the axis of Chincoteague Bay to the Atlantic Ocean. The headlands at the ends of these necks formed Chincoteague Island and Pope Islands. Through time, the littoral drift forming Assateague Island sealed the inlets between Chincoteague, Pope and Pirates Island. Halsey (1979) called this merger of small islands to form one large island the "nexus process". Oertel and Kraft (1994) noted that these islands were part of the arc of islands in the Chincoteague Bight. When included, the Bight may once have been about 50 km wide with the main exit to the Atlantic Ocean between Chincoteague and Pope Island. The present inlet between Chincoteague Bay and the Atlantic Ocean is located about 15 km south at Chincoteague Inlet.

Along the southern part of the Southern Delmarva Peninsula, these moderate-sized drainage basins empty into tide-dominated coastal lagoons that drain through tidal inlets. South of Chincoteague Inlet, Assawoman Creek, Gargathy Creek and Folly Creek drain into narrow coastal lagoons before entering the Chincoteague Bight. South of Chincoteague Bight, the Machipongo River, Cobb Mill Creek and Magothy Basin drain into broad coastal lagoons before exiting into the Atlantic Ocean.

Coastal Configuration

Assateague Island is located about 20 km east of the southern Delmarva Peninsula axis and is slightly oblique to the trend of the Atlantic Ocean shoreline. The location and orientation is consistent with the spacing for intermediate-sized interfluvium to the west. Although Assateague Island is a wave-dominated island that receives much of its sand from adjacent headlands (Leatherman, 1979, Halsey, 1979), we believe it may be perched on an intermediate-sized interfluvium along the outer margin of Chincoteague Bay. During lower sea levels,

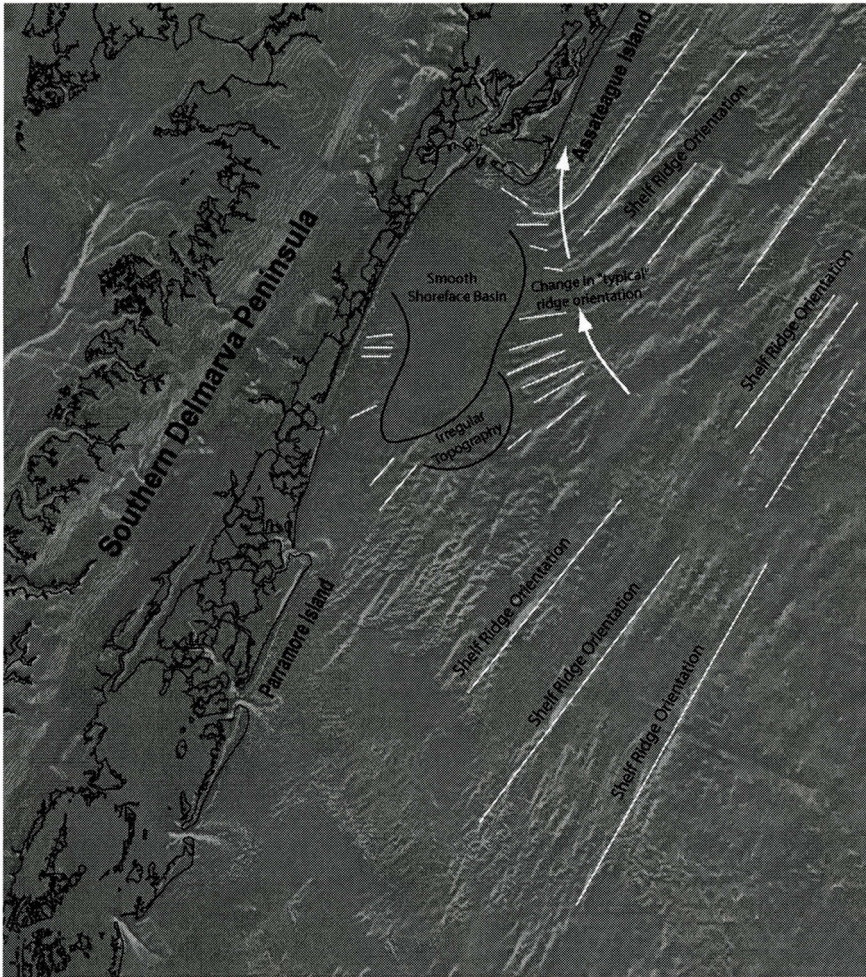


Figure 5. Shaded highlighted relief image of the middle Atlantic shoreface in and adjacent to the Chincoteague Bight. The image reveals the extensive coverage of the inner shelf by linear sand ridges that are slightly oblique to the coastline. Curved ridges and steeper ridge angle occur at the margin of a topographically smooth area of the shoreface.

Chincoteague Bay was once an intermediate-sized drainage basin similar to basins to the west (basins of the Pocomoke River, the Wicomico River, the Nanticoke River and the Choptank River).

Assateague Island is a wave-dominated dominated barrier island in the Delmarva Coastal Compartment. The island is about 60 km long and it is estimated that about 300,000 cubic meters of sand from the littoral systems are deposited at the distal end (Fishing Point) each year. The primary source of the littoral material comes from the headland region of the Delmar-

va coastal compartment. South of Fishing Point, the ocean shoreline is offset about 10 km landward of the ocean shoreline to Wallops Island. The trend of the Assateague Island shoreline extends across the Chincoteague Bight and is generally aligned with Parramore Island, Hog Island, Cobb Island. The bight between Fishing Point and Parramore Island is about 35 kilometers long. The barrier islands south of Fishing Point do not illustrate the long, narrow characteristics of Assateague Island or Chincoteague Bay. Instead, islands are relatively short and located at the headlands of moderate-

Pliocene/Pleistocene Lowstand

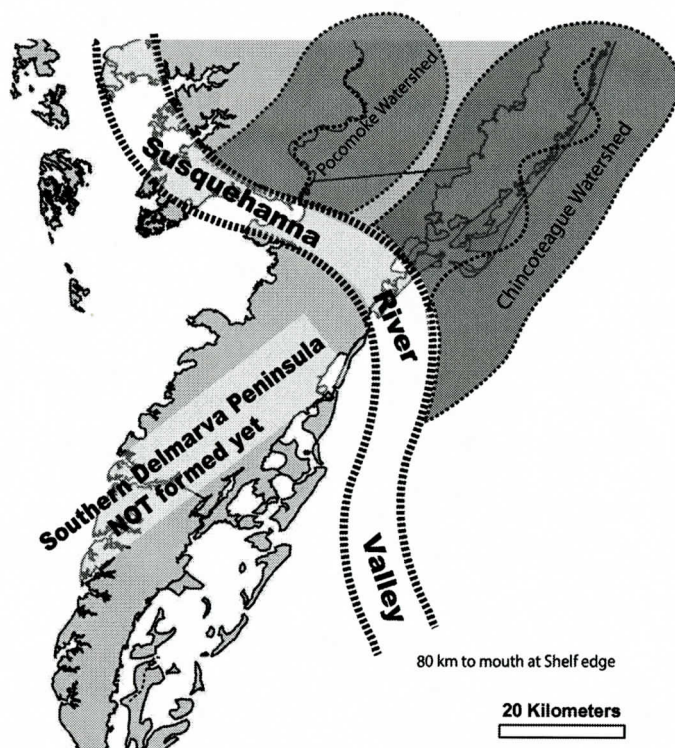


Figure 6. Hypothetical path of the Susquehanna River during a Late Pliocene/Pleistocene lowstand. Location is based on data from Mixon (1985), Foyle (1994) Oertel and Foyle 1995) and Krantz (2007).

sized interfluvies between shore-normal watersheds. These islands appear to receive very sand drift from the north.

Bathymetric Pattern

Three types of morphologic features are recognized in inner shelf bathymetry in and adjacent to the Chincoteague Bight. Chincoteague Bight is characterized by a smooth shoreface basin quite different from the usual pattern of sand ridges that prevails locally along the Delmarva shoreface. Similar features have been described on the continental shelves from New England to Florida (Hyne and Goodell, 1967; Moody 1964; Duane, Field, Meisburger, Swift and Williams, 1972). The relatively smooth surface of Chincoteague Bight extends 10-15 km beyond the bight onto the continental shelf where the surface is deeper than adjacent shore-

face areas to the north and south (Fig. 5). It is speculated that the absence of ridge topography may be related to the fine-grained surface texture in the Bight. Local fishermen know the Bight as "The Mud Hole". Krantz (2007) further noted difficulty in seismic profiling due to signal absorption into the soft muddy material. We believe the mud on the floor of Chincoteague Bight and the smooth-shoreface basin are exhumed fresh and estuarine wetlands that accumulated at the confluence of ancient Chincoteague and Susquehanna River (Fig. 6). Krantz (2006, 2007) believed the bathymetrically depressed Chincoteague Bight was related to pathways of ancient Susquehanna or Potomac Rivers. Although the Susquehanna paleochannel could have lowered the regional surface during the Late Pliocene/Pleistocene, these rivers were diverted over 90 km south

during three subsequent sea-level fluctuations. Smoothing and valley filling during subsequent highstands probably diminished the depth and relief of the ancient Susquehanna channel. It is probable that freshwater wetlands occupied the gently sloping remnants of the valley during lowstands and estuarine wetland occupied the depression during highstands. More recent sculpturing of the surface appears to be related to the intermediate-sized Chincoteague drainage basin that has re-occupied the abandoned section of the Susquehanna system. A freshwater wetland history of the region is supported by the findings of Groot et al. (1990) who found fossiliferous silicified mudstones exposed on the beaches of Assawoman, Metompkin and Cedar Islands, but not south of Parramore Island. Groot et al. (1990) believed the silicified mudstone was an early Pleistocene estuarine deposit. Oertel et al. (1989; 1992) use microfossil evidence to determine the presence of pre-Holocene "plastic" mud in barrier lagoons south of Parramore Island. However, those deposits were not silicified mudstones. The silicified mudstone petrology of the material on Assawoman, Metompkin and Cedar Islands suggests that the material is probably older than the Stage 5 highstand. However, we find it unlikely that it is as old as the Stage 11 or 13 highstands when the ancient Susquehanna may have crossed this area. More likely the mudstone formed as estuarine deposits of a Stage 7 or Stage 9 Chincoteague estuary. Lowery (2002) also reported silicified mudstone and Pleistocene findings of mineralized teeth of mammoth, giant beaver, horse, bison wolf and teeth, as well as fossilized walrus and whales bones.

A second group of important features on the inner shelf bathymetry is the oblique sand ridges. These ridges have a north-northeast orientation (NNE-SSW) and are slightly oblique to the coastline. They are prevalent features on the shelf north and south of the Chincoteague Bight. By projecting a line between the Assateague and Parramore Capes it can be seen that these feature do not occur on the shelf seaward of Chincoteague Bight for a distance of 10-15 km.

This indicates wave refraction and diffrac-

tion during spit development. Today, this process is occurring at the terminal end of Assateague Island where refraction causes sediment to drift around the island to Fishing Point. Remnants of earlier re-curved spits at the outer part of the smooth-shoreface basin indicate a transition from a shallow shoreface to a deeper bight environment. In this case, these features are located considerably south and seaward of their modern counterpart.

The third class of morphologic features is produced by sand ridges with northeast orientations (NE-SW). These ridges occur in a band between the smooth shoreface basin and the oblique sand ridges. Since wave refraction and diffraction is a response to changes in depth, we believe the change in orientation is a response to the edge of a paleovalley or basin. These ridges are also re-curved along the east and north side of the smooth-shoreface basin and form a series of en echelon steps that are offset west and north of seaward ridges. The en echelon pattern indicates the subsequent position of successive spits during sea-level rise and coastal retreat. By following the inner radius of each of these spits from the edge of the smooth-shoreface basin, the path of spit transgression can be traced to modern coastline.

Paleochannels in seismic lines

North of Assateague Island, Belknap and Kraft (1985) assembled seismic data from Sheridan et al. (1974) and Kraft et al. (1983) that showed valleys of Herring Creek, Indian Creek and Salt Pond Creek extended in an easterly direction and ultimately connected to an ancient Delaware shelf valley. Although the inner shelf and transgressive ravinement between Cape Henlopen and Fenwick Island (latitude 38° 20') is relatively smooth, the valleys of these intermediate-sized drainage basins could all be linked to the Delaware paleovalley offshore.

Foyle (1994) studied the shoreface south of Chincoteague Bight. He found the channels facies above the base of the Holocene (SR-3 unconformity) could be traced from moderate-sized streams, across coastal lagoons and onto the shoreface. Although the seabed and ravine-

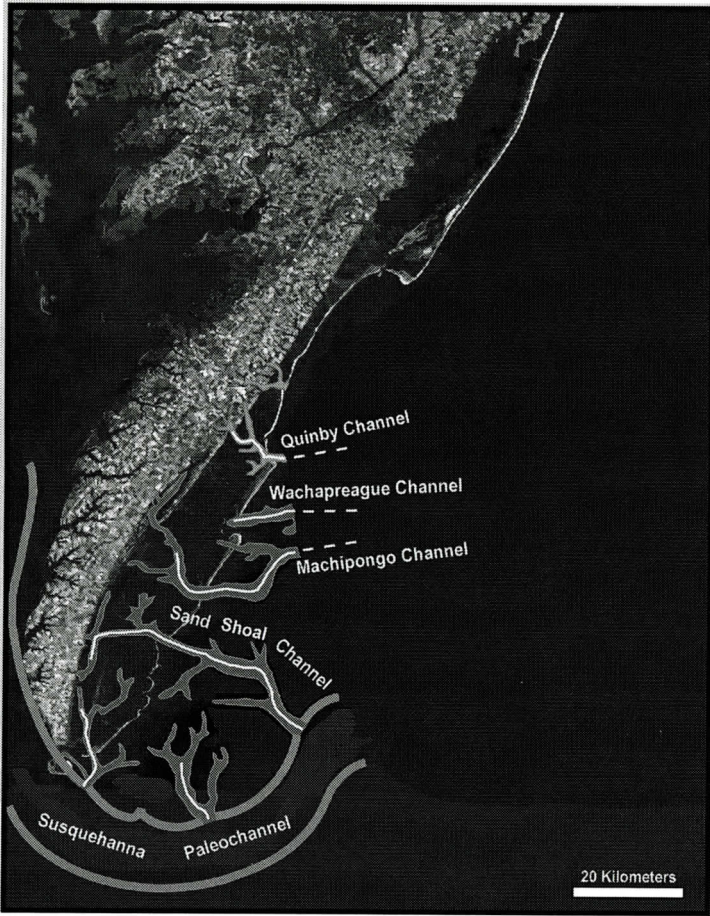


Figure 7. Seismic channels of coastal watersheds (modified after Foyle, 1994). Channels are at the base of the Holocene and represent the pre-Holocene transgressed surface. The large channel at the bottom of the image is the Cape Charles paleochannel of the Susquehanna River. Smaller channels were linked to intermediate-sized watersheds transecting coastal lagoons.

ment was relatively smooth, the pre-Holocene surface (SR-3 unconformity) illustrated paleovalley systems that crossed the shoreline and extended out beneath the continental shelf.

In the northern part of that study area, the Machipongo River watershed illustrates the fate of a moderate-sized drainage basin during transgression. The stream valley originates on the Coastal Plain surface and can be tracked across the floor of the coastal lagoon to the Great Machipongo Inlet. The trace of the channel from the head of the stream to the Great Machipongo Inlet is about 25 km. From the inlet, the filled channel can be traced east-northeast for another 25 km (Fig. 7). The path leads di-

rectly toward the southern edge of the smooth-shoreface basin of the Chincoteague Bight. We believe the moderate-sized Machipongo paleochannel is a tributary of an intermediate-sized paleochannel in the smooth-shoreface basin of the Chincoteague Bight.

Two other paleochannels designated as Quinby paleochannel and Wachapreague paleochannel also trended toward the east-northeast. These paleochannels were traced several kilometers landward of the present coastline to small and moderate-sized watersheds, respectively. Wachapreague paleochannel is believed to be a tributary of the Machipongo drainage basin and joins the Machipongo beneath the At-

PATHWAYS OF BARRIER RETREAT

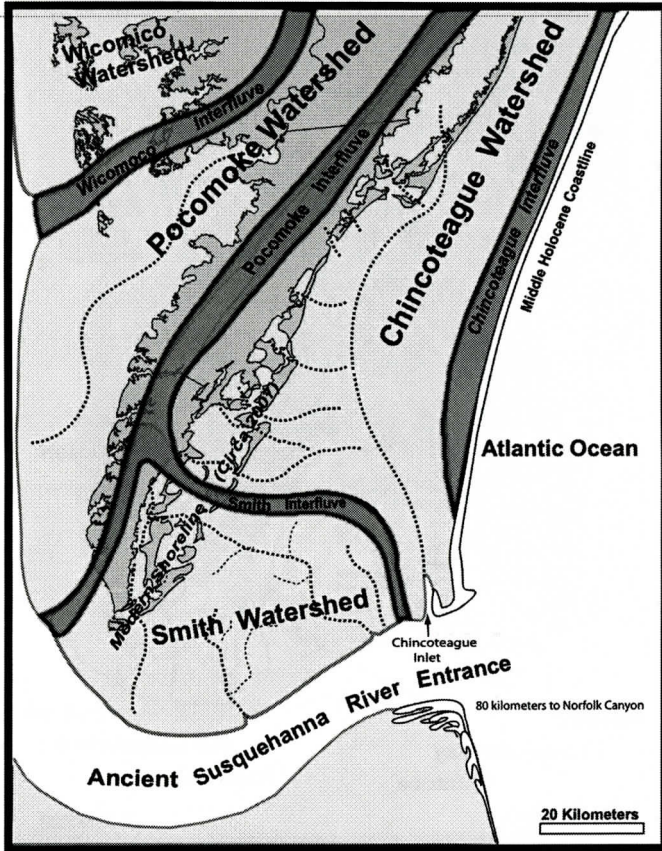


Figure 8. Chronosequence Stage 1 is a reconstruction of early Holocene paleogeography of the Delmarva Coastal Plain. The width and orientation of the Chincoteague Watershed is based on adjacent Coastal Plain watersheds, the seismic location the Cape Charles paleovalley and the hypothesized location of the Pliocene/Pleistocene Susquehanna valley (Fig. 6). Pathways of intermediate-sized streams are modified after seismic data of Foyle (1994), Krantz (2007) and Halsey (1969). Location of the Chincoteague River is based on base levels for intermediate-sized streams in the Chincoteague watershed.

Atlantic coastline. Quinby paleochannel can be followed for 15 km seaward of the coastline heading in a north-northeast direction toward the edge of the smooth-shoreface basin. These drainage directions support the above suggestion of a higher-order stream system just southeast of the Chincoteague Bight.

COASTAL EVOLUTION

Early Holocene Drainage

Evidence from Coastal Plain topography, shoreface bathymetry and seismic profiles sug-

gests the presence of an intermediate-sized Chincoteague watershed on the inner Delmarva shelf when sea was lower (Fig. 8). The watershed is believed to be similar in size and orientation to modern Coastal Plain counterparts. Chincoteague watershed has an average width of 25 km and an axis of 23°-203°. Since the average width of intermediate-sized watersheds on the Coastal Plain is 38 km, the eastern interfluvial of the watershed could have extended an additional 10-15 km offshore when the coastline was further to the east. Presently (Circa 2007), water depths 10-15 km offshore are 14 to 16 m. The intermediate-sized watershed

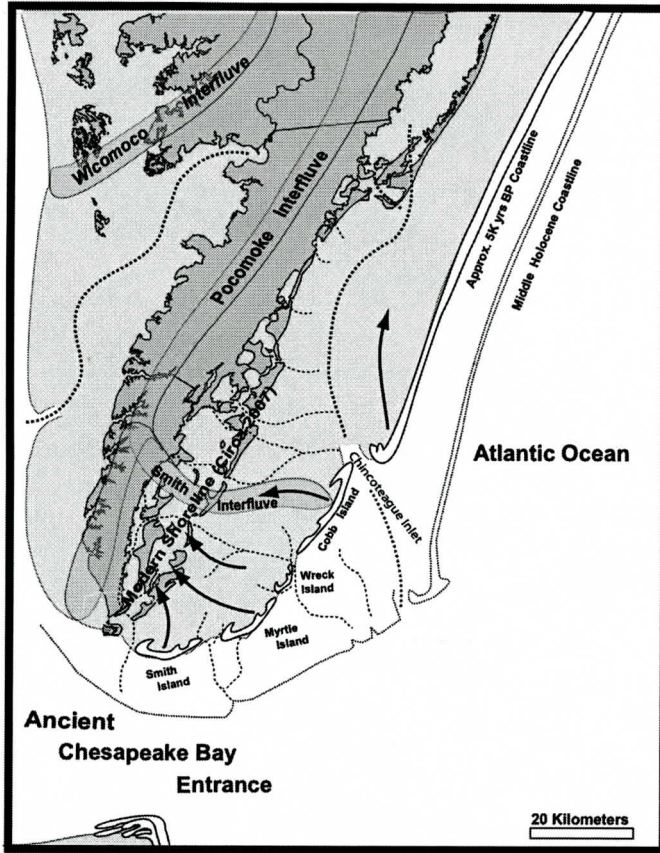


Figure 9. Chronosequence Stage 2 is a reconstruction of middle Holocene paleogeography of the Delmarva Coastal Plain based on hindcasting sea level and coastal position to 5,000 years before the present. The establishment of wave-dominated barrier island north of Chincoteague Inlet is based on the presence of a shore-parallel barrier platform composed of interfluvial sand. Tide-dominated barrier islands south of Chincoteague Inlet require the northward retreat of the wave-dominated island and the exposure of intermediate-sized headlands to ocean waves. During sea-level rise, the wave-dominated island retreats landward and northward and the tide-dominated islands retreat landward and to the northwest.

drained about 150 km south from its headwaters near the Delaware/Susquehanna interfluvium to a mouth at the confluence with an early Holocene Susquehanna River. Foyle (1994) called this the Cape Charles paleochannel of the Susquehanna River (labeled as "Ancient Susquehanna River Entrance" in Figure 8). The axis of the watershed and interfluvium is bimodal. The northern half of the watershed has a northeast-southwest orientation, whereas the southern half of the watershed bends east and has a northwest-southeast orientation. The southeast orientation may have been caused by the capture of stream

flow into an abandoned section of an early Pleistocene channel of the Susquehanna River. During a later Pleistocene highstand, progradation of Accomack Spit diverted the Susquehanna River farther south (Oertel and Foyle, 1997), and severed the connection between the Chincoteague and Susquehanna systems. The abandoned channel in the "confluence area" provided a depressed surface where fresh and estuarine wetlands developed during regressions of sea level. During transgression, the outer parts of the channel were filled at a relatively rapid rate by shoreface processes. The inner

PATHWAYS OF BARRIER RETREAT

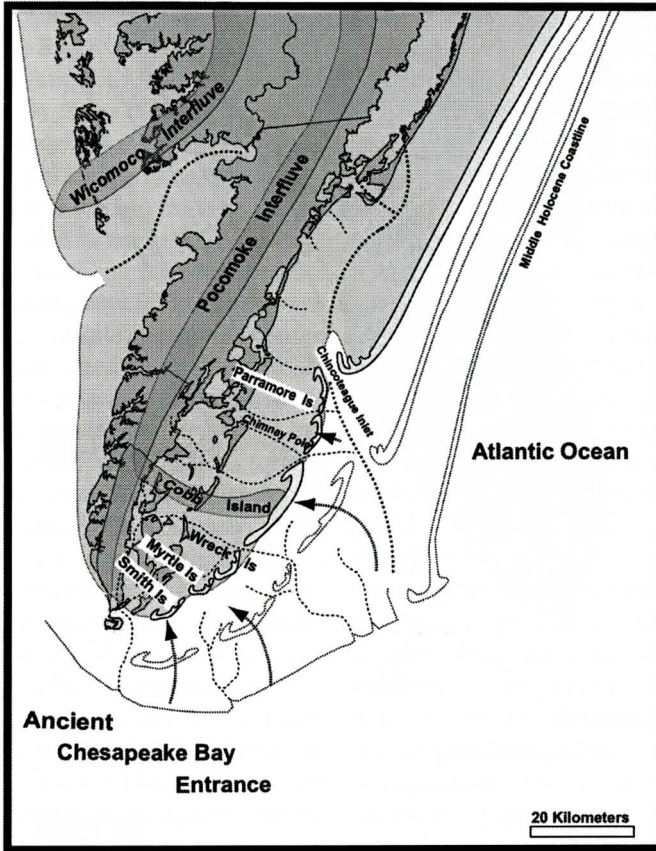


Figure 10. Chronosequence Stage 3 is a reconstruction of late Holocene paleogeography of the Delmarva Coastal Plain based on a 20 km northwest shift in the position of Chincoteague Inlet. The associated northward retreat of the wave-dominated island exposed more intermediate-sized headlands to ocean waves. Exposure caused the “birth” of two more barrier islands. During Stage 3, Chincoteague Inlet was at the edge of the smooth muddy surface of the Chincoteague Bight. The youngest barrier island to form was Parramore Island. Older barrier islands to the south continue to migrate landward along the axis of intermediate-sized interfluves.

confluence area remained as an emergent wetland in the depression left by the abandoned channel.

The ancient wetlands are recorded by a thick sequence of silicified mudstone. Archeological evidence has provided valuable information of the environmental conditions in this area. During the Late Archaic Period (6,000 to 3,000 BP) the mid-Atlantic area experienced warm, dry conditions with scrub/shrub forests and grasslands (Custer and Mellin, 1989 and Kellog and Custer, 1994). By Early to Middle Woodland Period (2,300 to 1000 BP) subsistence strategies of prehistoric communities appear to di-

verge between the northern and southern parts of the Delmarva Peninsula (Lowery, 2001). Shell middens throughout coastal areas of the northern Delmarva Peninsula produce materials indicative a hunter/gatherer community with a focus on coastal streams and estuaries. We believe these communities were taking advantage of the wetland resources along the axis of an ancient Chincoteague watershed. Coastal sites in the lower Southern Delmarva Peninsula did not produce large amounts of midden debris, and therefore Lowery (2001) believed communities in these areas took advantage of maize agriculture and other grassland resources. This sugges-

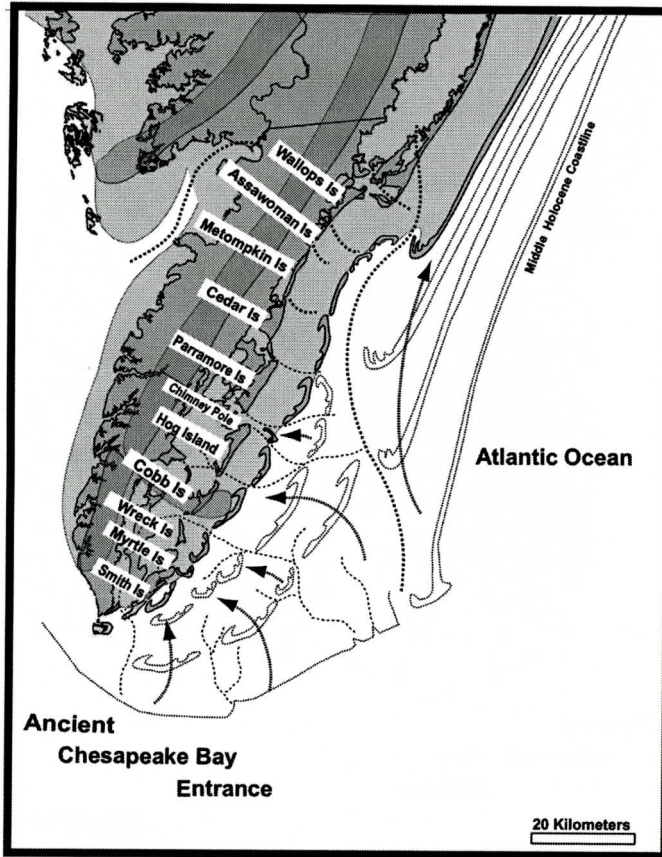


Figure 11. Chronosequence Stage 4 is a reconstruction of late Holocene paleogeography of the Delmarva Coastal Plain based on an additional 20 km shift in the position of Chincoteague Inlet. However, this shift was in a northeast direction along the axis of the stream channel. Northward retreat of the wave-dominated island exposed four more intermediate-sized headlands to ocean waves and the "birth" of new barrier islands. The youngest island to form in this way was Wallops Island. However, further south the divergence of channels produced a new interfluvial area between the Chimney Pole and Cobb Interfluvial areas. This led to the formation of Hog Island.

tion is supported by the bend in the Chincoteague River axis. Prehistoric communities south of the bend were too far inland to benefit from the wetland resources of the Chincoteague watershed.

Transgressive History

We have hindcast the position of middle Holocene coastline beyond the outer interfluvial area of the Chincoteague watershed (Fig. 8). We then migrated the coastline through three "relative" chronological stages en route to its present location. This allowed us to evaluate the effect of

sea-level rise and antecedent topography on coastal configuration. Seismic stratigraphy allowed us to map the moderate-sized drainage patterns that were part of an intermediate-sized Chincoteague watershed. During Stage 1 of the chronosequence, there were no tide-dominated barrier islands along the shoreline since the interfluvial area of the Chincoteague watershed extended all of the way to the Susquehanna River mouth. At Stage 1 time, moderate-sized watersheds within the Chincoteague and Smith Watersheds were shielded from the ocean. The Chincoteague River mouth was relatively narrow because of its shore-normal orientation

with respect to the Susquehanna River.

Chronosequence Stage 2 (about 5k yrs BP) followed a 10 km (approx.) landward shift in the coastline (Fig. 9). Then the Atlantic coastline was about at the edge of the Chincoteague watershed. The Cape Charles channel broadened transforming the Susquehanna River mouth into an entrance to an early Chesapeake Bay. Chincoteague Inlet and the shore-parallel interfluvial neck shifted about 25 km northwest. The northward shift in inlet position exposed the smaller, moderate-sized watersheds. Headlands of interfluvial areas between the watersheds evolved into tide-dominated barrier islands. Initially, Smith, Myrtle and Wreck islands formed on headlands of the Smith Watershed along the margins of the Chesapeake Bay entrance. Smith Island was about 20 km long and migrated north along a moderate-sized interfluvial area. Myrtle was initially 25 km long but waned to about 10 km as it migrated west northwest along an interfluvial area that was converging in width. Wreck Island did not exist when the Smith watershed was first exposed, but formed later from the headland of a small interfluvial area. Cobb Island formed on the intermediate-sized interfluvial area between the Smith and Chincoteague watersheds. Initially Cobb Island was very short (< 5 km), but then expanded to 25 km in length as it migrated northward along a diverging section of interfluvial area.

Between chronosequence Stage 2 and 3 (Fig. 10), there was only a modest shift in coastline location but the Chincoteague River bent toward the northwest maintaining a shore-normal inlet/coastline relationship. Chincoteague inlet migrated an additional 20 km to the northwest exposing two more moderate-sized headlands. This location placed it immediately adjacent to the muddy wetland bend in the stream axis. The two exposed headlands just south of the inlet evolved into Chimney Pole and Parramore Islands, each about 10 km long. There were no islands between Chimney Pole and Cobb Islands (still no Hog Island). However, Cobb Island remained 25 km in length as it migrated westward along the Smith interfluvial area. Wreck Island migrated westward varying in width from 5-10 km. Smith and Myrtle islands

narrowed considerably as they migrated toward each other along convergent interfluvial areas.

Between chronosequence Stage 3 and 4 (Fig. 11), there was only a modest shift in coastline location but the Chincoteague River bent sharply toward the northeast. At this time the axis of the Chincoteague watershed was almost parallel to the transgressing coastline. Chincoteague inlet migrated an additional 20 km to the northwest exposing four more interfluvial headlands. These headlands were in the shallow mudstone depression left by the abandoned Susquehanna paleochannel. The depression left by the abandoned river caused the islands to form further from the valley axis leaving a small offset in the coastline between Parramore and Assateague Island. Exposure of the mudstone headlands to the Atlantic Ocean produced primordial Wallops, Assawoman, Metompkin and Cedar Islands. Note that these islands formed quite recently after most of the southern islands had undergone a long history of landward migration. The recently formed islands between Cedar and Wallops Islands have a very short migration path from their initial formation to the present (Circa 2007) position. Initially, only a small part of the Wallops headland was exposed to the Atlantic Ocean, allowing a very small island to form. Chincoteague headland is still shielded from the Ocean by the northeast retreating, shore-parallel Assateague headland. Between the moderate-sized watersheds of Wallops and Cedar Islands, are relatively small inlets and interfluvial headlands that tend to be ephemeral. To the south, Parramore Island is rotating counterclockwise in order to stay normal to its interfluvial migration axis. Chimney Pole Island is shortening as it migrates into a convergent section of interfluvial area. Convergence is so severe that Chimney Pole Island will eventually weld to the north end of Hog Island. Hog Island has finally formed at an interfluvial area between two tributaries of an ancient Machipongo River system. Spits on the north end of Hog Island will eventually fill a small channel separating Chimney Pole and Hog Islands. Cobb Island is in a converging section of interfluvial area and has been reduced to about half its original length. Wreck, Myrtle and Smith Islands are all con-

verging on narrow, low-order interfluves.

As the spits and barriers on the east side of Chincoteague inlet migrated landward and northward during sea level rise, moderate-sized headlands on the west side of the watershed were exposed to the sea. Continued sea-level rise has flooded the Chincoteague valley forming Chincoteague Bay. The near parallel intersection of the Bay with the coastline produced a Bight in the shoreline between Parramore and Pope Islands. Although the initial Bight was about 50 km long, the southward migration of Assateague Spit reduced the width of the Bight to about 38 km.

Transgressive Summary

During sea-level rise and coastal inundation, drainage basins may be re-described as inundation basins. The alternating orientation and progressively smaller sizes of basins (and interfluves) has a considerable impact on the development of coastal landforms by inundation. Intermediate-sized watersheds that have shore-parallel orientations form the shore-parallel coastal bays (e.g. Chincoteague Bay) and shore parallel headlands. Wave-dominated barrier islands and spits are often perched on these sediment rich headlands (e.g. Assateague Island).

Approximately 5,000 BP the coastline coincided with the seaward side of Chincoteague watershed. The long-axis of the interfluve headland provided a prolific sediment supply for long, (wave-dominated) barrier islands and spits. During sea-level rise and coastal retreat, the intermediate-sized and shore-parallel Chincoteague Neck migrated northward and landward slowly exposing smaller tributary systems on the western margin of the Chincoteague watershed. In Chincoteague Bight, the distal parts of necks between Wachapreague Creek, Folly Creek, Parker Creek, Gargathy Creek, Assawoman Creek and Mosquito/Cockle Creek are composed of silicified mudstone that are exhumed at the modern barrier beaches. The paucity of coarse material may be a factor enhancing the retreat rate of tide-dominated barrier islands along the axes of the necks.

North of Chincoteague Bight, the main axis of the Chincoteague watershed flooded to form Chincoteague Bay.

As the shoreline transgressed across Chincoteague Neck, sand supply was diminished and spit migration and overwash deposits (Leatherman, 1979) transformed the shoreline into Assateague Spit. Continued transgression caused breaching at the northern end of Assateague Spit transforming the spit into Assateague Island. The island still receives sand from shoreface erosion and from the Delmarva headland at the northern end of the island.

CONCLUSIONS

Our investigation of the coastal offset at Chincoteague Bight has broader implications to coastal areas. Coastal configuration is a response to the balance between wave climate and terrestrial influences. If there were no wave processes to straighten a coastline, the coastline would have a "morphostatic" configuration produced by the drowning of coastal topography or the sculpturing by tidal currents. However, waves are present and have seasonal variability in strength and approach. This wave climate drives longshore flow (discharge) and littoral transport that tends to straighten the pre-existing coastal configuration. Shore-normal tidal forces interrupt longshore forces and enhance the formation of shore irregularities. The amount of interruption is related to the volume of tidal exchange. For example, a coastal inlet with a small tidal-discharge may be overwhelmed by the littoral-drift. However, larger systems may be able to flush their channels and remain open under the same conditions of longshore discharge.

Since the headlands are also important suppliers of sediment to the littoral system, the supply of sediment to fill inlets may also be limited by the size of an interfluve. We believe that our study indicates the effect of watershed size on coastal configuration, during coastal transgression.

One implication of our research is that antecedent topography related to drainage hierarchy plays a major role in determining coastal con-

PATHWAYS OF BARRIER RETREAT

figuration and the fate of barrier-island migration during sea level rise. The origin, expansion, migration and demise of barrier islands on the continental shelf are strongly influenced by antecedent interfluvial patterns.

Interfluve size and orientation appears to have an important influence of barrier island type (wave-dominated versus tide-dominated). In the mid-Atlantic area, watersheds (and their interfluves) are organized into four hierarchical classes (larger watersheds, intermediate-sized watersheds, moderate-sized watersheds and small watersheds). Small watersheds have discharges and headlands that are too small to have an effect on shore configuration. Longshore wave climate is sufficient to overwhelm shore-normal tidal flows and fill inlet channels with littoral sediment eroded from small headlands.

Large, intermediate and moderate-sized systems have different degrees of influence of coastal configuration. Drainage basins of large watersheds (Susquehanna and Delaware Rivers) produce large estuaries (Chesapeake and Delaware Bays) that produce large indentations in the ocean coastline. Large interfluves (Chesapeake/Delaware Interfluve) produce large headlands that provide large littoral sediment supplies for the formation of coastal compartments (Fisher, 1968).

Intermediate-size systems that are oriented parallel or nearly parallel to the coast have significant impacts on coastal configuration. In the mid-Atlantic region, the intermediate-sized and shore-parallel Chincoteague watershed can explain the offset in the coastline and origin of Chincoteague Bight. Coasts with similar low-angle relationships with interfluves might also produce bights in the coastline. When coastlines migrate to and across shore-parallel interfluves, large supplies of sediment to the littoral system result in wave-dominated spits and islands.

Tide-dominated barrier islands on the Virginia coast are associated with moderate-sized watersheds with shore-normal orientations. We feel this relationship may be found in other coastal areas because of the constrained relationship between tidal-drain capacity and littoral sediment supply. As sea level rises and

floods moderate-sized drainage basins the volume of water that must be exchanged on each tide also increases. Tidal discharges through the coastal inlets scour the channels and deposit material offshore in ebb tidal deltas. Maintenance of an "open" inlet is dependent on the ability of tidal currents to "sweep" littoral material out of the channel. Littoral material is primarily supplied from low-elevation headlands of moderate-sized interfluves between watersheds. The lateral redistribution of material from these headlands forms beach ridges and small spits. Enhanced ridge development on the left or right side of these low headlands produces the typical "drumstick" shape of tide-dominated barrier islands (Hayes, 1979). The distal ends of spits spill into the inlet margins partially constricting the pre-Holocene valleys (Hoyt and Henry, 1967). Throat narrowing tends to accelerate tidal flow through the inlets resulting in gorge deepening. As sea level rises, the inlets follow the path of the main antecedent channel and barrier islands retreat along the interfluves between watersheds. The length of barrier islands during transgression increases and decreases proportional to the size of the interfluve at given locations between watersheds.

ACKNOWLEDGEMENTS

This research is based upon work supported by the National Science Foundation under Grants No. BSR-8702333-06, DEB-9211772, DEB-9411974, DEB-0080381 and DEB-0621014. Any opinions, findings, and conclusions or recommendations expressed in this material are those of the authors and do not necessarily reflect the views of the National Science Foundation. The authors graciously thank Dr. David Krantz and Darrin Lowery for their discussions on shallow seismic data and archaeological data, respectively. Coast Reserve of the Nature Conservancy provided access to study sites.

REFERENCES

- Belknap, D.F. and Kraft, J.C. 1977. Holocene relative sea-level changes and coastal stratigraphic units on the northwest flank of the Baltimore Trough geosyncline.

- Jour. Sed. Petrol. 47: 610-629.
- Belknap, D.F. and Kraft, J.C. 1981. Preservation potential of transgressive coastal lithosomes on the U.S. Atlantic shelf. *Marine Geol.* 42: 429-442.
- Belknap, D.F. and Kraft, J.C. 1985. Influence of antecedent geology of stratigraphic preservation potential and evolution of Delaware's barrier islands. In: Oertel, G.F. and Leatherman, S.P. *Barrier Islands. Marine Geology*, 63: 235-262.
- Byrnes, M.R. 1988. Holocene geology and migration of a low-profile barrier island system, Metompkin Island, Virginia. Ph. D. Dissertation, Old Dominion University, Norfolk, Virginia. 302 p.
- Byrnes, M.R., Gingerich, K.J., Kimball, S. M. and Thomas, G.R., 1989. In: Stauble D.K. and Magoon, O.T., (Eds.), *Barrier Islands: Process and Management. American Society Civil Eng.*, New York, NY, p. 78-92.
- Custer, J.F. and Mellin, G.R., 1989. Archaeological survey in southwest Delaware, 1987-1988. *Bull. Archaeological Society of Delaware* 26: 1-68.
- Demarest, and Leatherman, 1985. Mainland influence on coastal transgression: Delaware Peninsula. In: Oertel, G.F. and Leatherman, S.P. *Barrier Islands. Marine Geology*, 63: 19-34.
- Dolan, R., Hayden, B. and Jones, C. 1979. Barrier island configuration. *Science* 204: 401-403.
- Dolan, R., Hayden, B. and Lins, H. 1980. *Barrier Islands. American Scientist*, 68: 16-25.
- Duane, D.B., Field, M.E., Meisburger, E.P., Swift, D.J.P., and Williams, S.J., 1972. Linear shoals on the Atlantic inner continental shelf, Florida to Long Island. In: Swift, D.J.P., Duane, D.B. and Pilkey, O.H. (Eds.) *Swift Sediment Transport: Process and Pattern*. Dowden, Hutchinson and Ross. Stroudsburg, PA.
- Finkelstein, K. and Kearney, M.S. 1988. Late Pleistocene barrier-island sequence along the southern Delmarva Peninsula; implications for middle Wisconsin sea levels. *Geology*; v. 16; no. 1; p. 41-45.
- Finkelstein, K. and Ferland, M.A. 1987. Back-barrier response to sea level rise, Eastern Shore of Virginia. In: Nummedal, D., Pilkey, O.H., and Howard, J.D. (eds.) *Sea-level fluctuations and coastal evolution: S.E.P.M. Special Publication* 41. 145-155.
- Finkelstein, K., 1992. Stratigraphy and preservation potential of sediments from adjacent Holocene and Pleistocene barrier-island systems, Cape Charles, Virginia. In Fletcher, C.H. and Wehmler, J.F. (Eds.). *SEPM Special Publication* 48. 129-140.
- Fisher, J.J. 1967. Origin of barrier island chain shorelines: Middle Atlantic States. *Geological Society of Am., Special Paper* 115: 66-67.
- Fisher, J.J. 1968. Barrier island formation: Discussion. *Geological Society of Am. Bull.*, 79: 1421-1426.
- Foyle, A.M., 1994. Quaternary seismic stratigraphy of the inner shelf and coastal zone, southern Delmarva Peninsula, Virginia. Ph. D. Dissertation, Old Dominion University, Norfolk, Virginia. 492 p.
- Foyle, A.M. and Oertel, G.F. 1997. Transgressive systems tract development in incised-valley fills within a Quaternary estuary-shelf system: Virginia inner shelf, U.S.A., *Marine Geol.* 137: 227-249.
- Goldsmith, V., Byrnes, R.B.J., Sallenger, A.H. and Drucker, D.M., 1975. The influence of waves on the origin and development of the offset coastal inlets of the southern Delmarva Peninsula. In: Cronin, L.U. (Ed.) *Estuarine Research II*, Academic Press New York, NY, p. 183-200.
- Halsey, S.D., 1979. Nexus: New model of barrier island development. In Leatherman (editor), *Barrier Islands*, Academic Press, New York, NY, p. 185-210.
- Hayden, B., and Dolan, R., 1979. Barrier islands, lagoons and marshes. *Journal of Sedimentary Petrology*, 49: 1061-1072.
- Hayes, M.O., 1979. Barrier island morphology as a function of tidal and wave regime. In: Leatherman, S.P. *Barrier Islands. Academic Press. New York, NY*, p. 1-28.
- Hoyt, J.H. and Henry, V.J., 1967. Influence of island migration on barrier island sedimentation. *Geol. Soc. Am. Bull.* V78; 77-86.
- Hoyt, J.H. and Henry, V.J., 1971. Origin of capes and shoals along the southeastern coast of the United States, *GSA Bulletin*; v. 82; no. 1; p. 59-66
- Hyne, N.J. and Goodell, H.G. 1967. Origin of sediments and submarine geology of the inner continental shelf off Choctawhatchee Bay, Florida. *Mar. geol.*: 1125-1136.
- Kellog, D.C. and Custer, J.F., 1994. Paleoenvironmental studies of the Statte Route 1 corridor: Contexts for prehistoric settlement, New Castle and Kent Counties, Delaware. Delaware Department of Transportation *Archaeological Series No. 114*. Dover, Delaware.
- Kraft, J.C., 1971. Sedimentary facies patterns and geologic history of a Holocene marine transgression. *Geol. Soc. Am. Bull.*, 82: 2131-2158.
- Kraft, J.C., Chrastowski, M.J., Belknap, D.F., Toscano, M.A., and Fletcher, C.H., 1987. The transgressive barrier-lagoon coast of Delaware: Morphology, Sedimentary sequences and responses to relative sea level. In: Nummedal, D., Pilkey, O.H., and Howard, J.D. (eds.) *Sea-level fluctuations and coastal evolution: S.E.P.M. Special Publication* 41, p. 129-143.
- Krantz, D.E., 2006. Interpretation of seismic data in the Wallops Island shoreface. *Maryland Coastal Bays Figures*. <http://www.eescience.utoledo.edu/Faculty/Krantz/>.
- Krantz, D.E., 2007. Personal Communication.
- Leatherman, S.P., Rice, T.E. and Goldsmith, V. 1982. Virginia barrier island configuration: A reappraisal. *Science*, 215: 285-287.
- Leatherman, S.P., 1983a. Barrier island dynamics and landward migration with Holocene sea-level rise. *Nature*, 301: 415-418.
- Leatherman, S.P., 1983b. *Barrier Island Handbook*. University of Maryland, College Park, MD. 109 p.
- Leatherman, S.P., 1979. Migration of Assateague Island, Maryland, by inlet and overwash processes. *Geology*: 104-107.

PATHWAYS OF BARRIER RETREAT

- Lowery, D., 2001. Archaeological survey of the Atlantic coast shorelines associated with Accomack County and North Hampton County, Virginia. Chesapeake Bay Archaeological Research Foundation. Tighman, MD.
- Lowery, D., 2002. Personal communication in a letter dated September 11, 2002. Findings of silicified mud, and mineralized vertebrate remains at Assawoman, Metompkin and Cedar Islands, Virginia.
- Mixon, R.B. Stratigraphic and geographic framework of upper Cenozoic deposits in the Southern Delmarva Peninsula, Virginia and Maryland. U.S. Geological Survey Professional Paper 1067-G, 53 p.
- Moody, D.W., 1964. Coastal morphology and processes in relation to development of submarine sand ridges off Bethany Beach, Delaware. 160 pp. Ph. D dissertation, The Johns Hopkins University, Baltimore, MD.
- Morton, R.A. and Donaldson, A.C., 1973. Sediment distribution and evolution of tidal deltas along a tide-dominated shoreline, Wachpreague, Virginia. *Sedimentary Geology* 10: 285-299.
- Newman, W.S. and Rusnack, G.N. 1965. Holocene submergence of the Eastern Shore of Virginia. *Science* 148: 1464-1466.
- Newman, W.S. and Munsart, C.A. 1968. Holocene geology of the Wachpreague lagoon, Eastern Shore Peninsular, Virginia. *Marine Geology*, 6: 81-105.
- Oertel, G.F., Kearney, M.S., Leatherman, S.P. and Woo, H.J. 1989. Anatomy of a barrier platform: outer barrier lagoon, southern Delmarva Peninsula, Virginia. in: Ward, L.G. and Ashley, G.M. (Eds.) *Physical Processes and Sedimentology of Siliciclastic Dominated Lagoonal Systems*. *Marine Geology*, 88: 303-318.
- Oertel, G.F., Kearney, M.S., Leatherman, S.P. and Woo, H.J. 1992. Rational theory for barrier lagoon evolution. In: Fletcher, C.H. and Wehmiller, J.F. *Quaternary coasts of the United States: Marine and Lacustrine Systems*. SEPM Special Publication 48: 77-87.
- Oertel, G.F., and Kraft, J.C. 1994. New Jersey and Delmarva barrier islands. In Davis, R.A. (Editor), *Geology of Barrier Islands*, Springer-Verlag, New York, p. 207-232.
- Oertel, G.F., and Foyle, A.M. 1995. Drainage displacement by sea-level fluctuation at the outer margin of the Chesapeake seaway. *Journal of Coastal Research*, 11: 583-604.
- Oertel, G.F. and Overman, K., 2004. Sequence morphodynamics at an emergent barrier island, middle Atlantic coast of North America. *Geomorphology* 58: 67-83.
- Sheridan, R.E., Dill, Jr., C.E. and Kraft, J.C. 1974. Holocene sedimentary environments of the Atlantic inner shelf off Delaware. *Geological Soc. American Bull.*, 85: 1319-1328.
- Shiedler, G.L., Ludwick, J.C., Oertel, G. F. and Finkelstein, K. 1984. Quaternary stratigraphic evolution of the southern Delmarva Peninsula coastal zone, Cape Charles, Virginia. *Bull. Geol. Soc. Am.* V. 95: 489-502.
- Swift, D.J.P., 1969. Inner shelf sedimentation: Processes and products. In D.J. Stanley (editor), *The new concepts in continental margin sedimentation*. Am. Geol. Institute, Washington, D.C., p. DS-4: 1-46.
- Swift, D.J.P., 1975. Barrier Island genesis: evidence from the central Atlantic shelf, eastern U.S.A. *Sedimentary Geology*, 14: 1-43.
- Swift, D.J.P., Thorne, J.A. Vincent, C.E. and Oertel, G. F. 1986. Fluid processes and seafloor response on a modern storm dominated shelf: middle Atlantic shelf of North America. Part II Response of the seafloor. In: Knight, R.J. and Mclean, J.R. (Eds.), *Shelf sands and sandstones*. Canadian Soc. of Petrol. Geol. Memoir II, P. 191-211.
- Swift, D.J.P., Niedoroda, A.W., Vincent, C.E. and Hopkins, T.S., 1985. Barrier island evolution, middle Atlantic shelf., U.S.A. Part I: Shelf Dynamics. *Marine Geol.*, 63:308-331.
- U.S. Department of the Interior, National Park Service, 2007. Historic Shorelines – Tom’s Cove Virginia. <http://www.nps.gov/asis/naturescience/index.htm>
- Van de Plassche, O., 1990. Mid-Holocene sea-level change on the Eastern Shore of Virginia. *Marine Geol.* 91: 149-154.